# Lovastatin Sensitizes the Trail-induced Apoptosis in Human Glioblastoma – How does it work?

**LIU, Pi-chu**

A Thesis Submitted in Partial Fulfillment

of the Requirement for the Degree of

Doctor of Philosophy

in

Surgery

The Chinese University of Hong Kong

August 2011





ProQuest LLC.
789 East Eisenhower Parkway
P.O. Box 1346
Ann Arbor, MI 48106 - 1346

Thesis/ Assessment Committe

Professor CHEN Gong George (Chair)

Professor POON Wai Sang (Thesis Supervisor)

Professor WONG Kwok Chu (Committee Member)

Professor WHITTLE Ian (External Examiner)

論文評審委員會

陳功 教授 (主席)

潘偉生 教授 (論文導師)

黃國柱 教授 (委員)

WHITTLE Ian 教授 (校外委員)

# Abstract

Glioblastoma is a common malignant brain tumour. The incidence of glioblastoma is significantly lower in Asian populations, but the prognosis remains poor. It has a high resistance to conventional cancer therapy that may be due to its diffuse and infiltrative nature. Recently, the tumour necrosis factor-related apoptosis inducing ligand (TRAIL) has been shown to be responsive in experimental solid cancers such as colon, lung, and breast cancer. This thesis examines its potential in for use in treating glioblastoma.

We have previously shown that two out of three human glioblastoma cell lines are resistant to TRAIL-induced apoptosis. Lovastatin, which is a 3-hydroxy-3-methylglutaryl coenzyme A (HMG CoA) reductase inhibitor, has been shown to sensitize glioblastoma cells to TRAIL-induced cell death in the G0/G1 phase. To investigate the possible mechanisms of sensitization of TRAIL-induced apoptosis in human glioblastoma by lovastatin, the protein expression of TRAIL receptors/death receptors (TRAIL-R/DR) were observed by western blotting. A significant increase in DR5 (TRAIL-R2) expression was found when cells were treated with lovastatin. According to recent studies in the literature, the up-regulation of DR5 might relate to the NF-κB pathway. We have demonstrated that the active NF-κB p65, which is one of the components of the NF-κB subunit, was down-regulated by lovastatin. Bay (Bay 11-7082), which is an inhibitor of cytokine-induced IκBα phosphorylation, was used to confirm the role of NF-κB signaling in TRAIL-induced apoptosis sensitized by

lovastatin in glioblastoma. DR5 expression in glioblastoma cells treated with Bay showed a similar trend to those treated with lovastatin. This indicates that lovastatin may sensitize human glioblastoma cells to TRAIL-induced apoptosis by NF-κB p65 inactivation.

In addition, mitogen-activated protein kinase (MAPK) signaling was also significantly dysregulated after lovastatin treatment in human glioblastoma cells. This result was confirmed by western blotting, which showed that ERK/MAPK expression was down-regulated and JNK/p38 expression up-regulated in cells treated with lovastatin. It suggests that lovastatin not only sensitize TRAIL-induced apoptosis by up-regulation of DR5 level via NF-κB inactivation but also directly induce apoptosis by dysregulation of MAPK pathway.

To confirm the effect of lovastatin and TRAIL *in vivo*, U87 MG, a grade IV human glioblastoma cell line, was transduced with luciferase and EGFP. Consequently, the transduced cells were used to establish subcutaneous brain tumour model and the tumour-bearing mice were received lovastatin or TRAIL treatment. Although the tumour growth rate was significantly reduced when the mice treated with lovastatin intraperitoneally, the DR5 expression in tumour tissue was not increased. However, the DR5 expression of tumour tissue was markedly up-regulated in tumour-bearing mice with local peri-tumoural administration of lovastatin. Our further study also confirmed that local peri-tumoral injection of lovastatin and TRAIL significantly decreased tumour volume in subcutaneous nude mice model.

In conclusion, this study demonstrates the efficacy of lovastatin and TRAIL in combination. A synergistic antitumour effect of lovastatin and TRAIL was found in grade IV human glioblastoma cell line, U87 MG. The major mode of cell death was apoptosis. This study examined the mechanism by which lovastatin sensitizes TRAIL-induced apoptosis. TRAIL-induced apoptosis was found to be sensitized by lovastatin through an increase in DR5 expression. Furthermore, the up-regulation of DR5 may be related to the NF-κB pathway and the down-regulation of active NF-κB p65 raised the DR5 expression. Moreover, preclinical animal study confirmed that DR5 expression in tumour tissue was significantly increased with peri-tumoural administration of lovastatin. A synergistic anti-tumour effect was also found by combination therapy of lovastatin and TRAIL. These data suggest that combination of lovastatin and TRAIL is a feasible treatment strategy for TRAIL-resistant glioblastoma and DR5 is a potential biomarker for screening glioma patients who are sensitive to TRAIL therapy.

# 摘　要

神經膠質瘤是最常見的惡性腦瘤。雖然亞洲人的發病率明顯低於西方人種，但是患者的預後一樣很差。其對傳統治療的高度耐受可能是由於該種癌細胞的瀰漫性和浸潤性的生物學行爲特點。近期，腫瘤壞死因子相關凋亡誘導配體 (TRAIL)成爲癌症研究領域的熱點。已有研究證實，TRAIL 對許多不同的腫瘤均有明顯的抗腫瘤作用，例如：結腸癌、肺癌和乳癌。本課題主要研究 TRAIL 治療神經膠質瘤的可行性。

我們既往的研究已經表明三種人神經膠質瘤細胞株中，有兩種都對 TRAIL 誘導的凋亡呈現耐受作用。洛伐他汀(3 羥-3-甲基戊二醯輔酶 A 還原酶抑制劑)可以促使神經膠質瘤細胞停留在 G0/G1 期，從而增加對 TRAIL 誘導細胞凋亡的敏感性。根據 Western Blotting 的結果發現，當細胞受到洛伐他汀處理後，DR5（TRAIL-R2）表達顯著增加。證實 TRAIL 誘導凋亡的敏感性增加可能是通過 TRAIL 受體/死亡受體的表達升高而達成。而既往的研究表明，DR5 的表達可能是與 NF-κB 通路的調控有關。此項推論在本研究中也經 Western Blotting 的結果證實，洛伐他汀明顯下調 NF-κB 家族中的一個亞型--Rel A (p65)。我們進一步利用 IκBα 磷酸化抑制劑--Bay 來證實 NF-κB 通路在洛伐他汀對 TRAIL 誘導的細胞凋亡中起到的作用。結果是肯定的，Bay 治療組和洛伐他汀組的 DR5 表達趨勢十分相似。這足以證實洛伐他汀

DR5 表達來增強 TRAIL 誘導的細胞凋亡。(b) DR5 上調可能與 NF-κB 路徑有關。通過降低 IKKα/β 及 IκBα 的磷酸化而減少 NF-κB p65 的活化，最終增加 DR5 的表達。(c) 洛伐他汀同時能對 MAPK 通路進行調控，主要通過降低 ERK/MAPK 表達和增加 JNK/p38 水平，從而促進人神經膠質瘤細胞的細胞凋亡。(3) 洛伐他汀和 TRAIL 的臨床前期研究：(a) 成功利用慢病毒基因載體系統(lentivirus system)將發光酵素(luciferase)和綠色螢光蛋白(EGFP)轉入 U87 細胞，並用轉導后的細胞成功建立動物皮下腫瘤模型。(b) 腫瘤旁注射洛伐他汀可以明顯升高腫瘤組織內的 DR5 表達。(c) 瘤旁注射洛伐他汀和 TRAIL 可以顯著抑制裸鼠皮下腫瘤的生長。綜上所述，利用洛伐他汀和 TRAIL 的綜合療法治療對 TRAIL 耐受的神經膠質瘤是可行的，而 DR5 可作爲一個生物指標用於篩查對 TRAIL 治療敏感的神經膠質瘤患者。

# Publications

## Journal Articles

- David YL, Chen GG, Poon WS, **Liu PC**. Lovastatin sensitized human glioblastoma cells to TRAIL-induced apoptosis. Journal of Neurooncology. 2008; 86(3): 273-83.

- Liu PC, Li J, Lu G, Chen GG, Poon WS. Inhibition of NF-kB pathway and activation of JNK/p38 in glioblastoma and implications for Lovastatin and Tumor necrosis factor -Related Apoptosis Inducing Ligand (TRAIL) combination therapy. (submitted)

- Lu G, **Liu PC**, Poon WS, Deng M, King AD, Leung KC, Wang YX. Magnetic targeted transcatheter SPIO labeled stem cell delivery: preliminary results in a rat intracerebral hemorrhage model. (submitted)

## Poster Presentation

- **Liu PC**, Chen GG, Poon WS. Effect of TRAIL and lovastatin on human glioblastoma cells. 14$^{th}$ Annual Scientific Meeting, Hong Kong Neurosurgical Society, Hong Kong, 2007: No.OP101.

- Lu G, **Liu PC**, Poon WS, Deng M, King AD, Leung KC, Wang YX. Magnetic targeted transcatheter SPIO labeled stem cell delivery: preliminary results in a rat intracerebral hemorrhage model. Proceedings of the European Society for Magnetic Resonance in Medicine and Biology, Antalya, 2009: No. 299

- **Liu PC**, Li J, Chen GG, Lu G, Poon WS. Lovastatin sensitizes tumour necrosis factor-related apoptosis-inducing ligand-mediated apoptosis through inactivation of NF-κB pathway and activation of JNK/p38 pathway in human glioblastoma cells. American Association for Cancer Research 101th Annual Meeting, Washington DC, 2010: No.1539.

# Acknowledgements

I would like to express my gratitude to all those who helped me during my research period.

My deepest gratitude goes first and foremost to Professor Poon Waiseng, my supervisor, and Professor George Gong Chen and Professor George Kwok Chu Wong, my co-supervisors, for their valuable guidance, innovative suggestions, and constant encouragement. I am deeply grateful for their help with completing this thesis.

Second, I would like to express my heartfelt gratitude to my colleagues in the Department of Surgery for their assistance in every aspect of my study. I would like to thank Professor Gang Lu, Dr. Jun Li, Mrs. Tian Jiu, Mr. Jonathan Ip, Ms. Xiaoxu Lu, and Ms. Guifang Zeng for their comments and support. I would also like to thank Mr. Billy Leung, Ms. S.Y. Chun, Mr. Rocky Ho, and Mr. Ernest Chak for their technical assistance. I am grateful to my colleagues in the Department of Surgery and the Sir YK Pao Cancer Centre laboratories, who made my time in the laboratory enjoyable.

Finally, I am indebted to my family for their continuous support and encouragement. They are the most valuable treasures in my life.

# Abbreviations

| | |
|---|---|
| **5-ALA** | 5-aminolevuleic acid |
| **5-FU** | fluorouracil |
| **%** | percentage |
| **Aβ** | β-amyloid |
| **㎕** | micro-liter |
| **㎛** | micro-molar per liter |
| **AD** | Alzheimer's disease |
| **ATCC** | American Type Culture Collection |
| **ATP** | adenosine-5'-triphosphate |
| **BBB** | blood-brain barrier |
| **Bcl-2 family** | B-cell leukemia/lymphoma-2 protein family |
| **BCNU** | *N,N'*-bis(2-chloroethyl)-*N*-nitrosourea |
| **Bid** | Bcl-2 inhibitory BH-2-domain-containing protein |
| **BLI** | bioluminescent imaging |
| **BNCT** | boron neutron capture therapy |
| **bp** | base pair |
| **BSA** | bovine serum albumin |
| **℃** | degrees Celsius |
| **Caspase** | cysteinyl aspartic acid-protease |

| | |
|---|---|
| **ERK** | extracellular signal-regulated kinase |
| **FADD** | Fas-associated death domain |
| **FBS** | fetal bovine serum |
| **FDA** | Food and Drug Administration |
| **FLICE** | Fas-associated death domain-like interleukin-1 converting enzyme |
| **FPP** | farnesyl pyrophosphate |
| **GBM** | glioblastoma multiforme |
| **GFP** | green fluorescence protein |
| **GGPP** | geranylgeranylpyrophosphate |
| **h** | hour |
| **HBS** | HEPES-buffered saline |
| **HMG-CoA** | 3-hydroxy-3-methylglutaryl-CoA |
| **HRP** | horseradish peroxidase |
| **IAP** | inhibitors of apoptosis protein |
| **IHC** | immunohistochemistry |
| **i.p.** | intraperitoneal |
| **JNK** | c-Jun N-terminal kinase |
| **kDa** | kilodalton |
| **LDL** | low density lipoprotein |
| **Luc** | luciferase |
| **mAb** | monoclonal antibody |

| | |
|---|---|
| **MADD** | mitogen-activated kinase-activating death domain protein |
| **MAP** | mitogen-activated protein |
| **MAPKs** | mitogen-activated protein kinase |
| **MEM** | minimum essential medium |
| **mg** | milli-gram |
| **MGMT** | methylated O(6)-methylguanine-DNA-methyltransferase |
| **min** | minutes |
| **ml** | milli-liter |
| **MRI** | magnetic resonance imaging |
| **mRNA** | messenger RNA |
| **MS** | multiple sclerosis |
| **MtS** | metabolic syndrome |
| **MTT** | 3-[4,5-dimethylthiazol-2-yl-]-2,5-diphenyltetrezolium bromide |
| **NF-κB** | nuclear factor-kappa B |
| **NHL** | non-Hodgkin lymphoma |
| **nM** | nano-meter |
| **nm** | nano-molar per liter |
| **NP-40** | Nonidet P-40 |
| **OPG** | osteoprotegerin |
| **PBS** | phosphate buffer saline |
| **PCR** | polymerase chain reaction |

| | |
|---|---|
| **PD** | Parkinson's disease |
| **PDGF** | platelet-derived growth factor |
| **PET** | positron emission tomography |
| **PI** | propidium iodide |
| **PKB** | protrin kinase B |
| **PMSF** | phenylmethysulfonyfluorid |
| **PS** | phosphatidylserine |
| **RA** | rheumatoid arthritis |
| **rhTRAIL** | recombinant human TRAIL |
| **RNA** | ribonucleic acid |
| **RT-PCR** | reverse transcription PCR |
| **SD** | standard deviation |
| **SDS** | sodium dodecyl sulfate |
| **sec** | seconds |
| **TNF** | tumour necrosis factor |
| **TRAIL** | tumour necrosis factor – related apoptosis – inducing ligand |
| **TRAIL-R** | TRAIL-receptor |
| **VEGF** | vascular endothelial growth factor |
| **WBRT** | whole-brain radiotherapy |
| **WHO** | World Health Organization |

# List of figures


**Figure 1-1** CNS tumour incidence in Hong Kong

**Figure 1-2** CNS tumour mortality in Hong Kong

**Figure 1-3** Development of primary and secondary GBM

**Figure 1-4** Intrinsic and extrinsic pathways of apoptosis

**Figure 1-5** Mevalonate pathway and mechanism of HMG-Co A reductase inhibitors (statins)

**Figure 1-6** Mechanism of the NF-κB pathway

**Figure 2-1** Principle of the MTT assay

**Figure 2-2** Cell morphology after treatment with lovastatin or TRAIL

**Figure 2-3** Effect of TRAIL on cell proliferation

**Figure 2-4** Effect of lovastatin on cell proliferation

**Figure 2-5** Effect of lovastatin and TRAIL on cell proliferation

**Figure 2-6** Cell viability of U87 MG incubated with different concentrations of lovastatin with and without TRAIL for 48 hours.

**Figure 2-7** Anti-proliferation effect of lovastatin alone versus lovastatin plus TRAIL for 48 hours

**Figure 2-8** Cell cycle determination on U87 MG cells

**Figure 2-9** Apoptosis detected by Annexin V/PI staining of U87 MG cells

**Figure 2-10** Apoptosis detected by Annexin V/PI staining of T98G cells

**Figure 3-1** Bioluminescent reactions catalyzed by firefly and *Renilla* luciferases

**Figure 3-2** Map of NF-κB-luciferase plasmid

**Figure 3-3** Map of *Renilla*-luciferase vector

**Figure 3-4** Decoy receptor 1 expression in human glioblastoma cells

**Figure 3-5** DR4 expression in human glioblastoma cells

**Figure 3-6** DR5 expression in human glioblastoma cells

**Figure 3-7** mRNA level of DR5 in human glioblastoma cells

**Figure 3-8** DR5 expression in human stromal cells

**Figure 3-9** NF-κB activity in human glioblastoma cells

**Figure 3-10** Effect of lovastatin on NF-κB pathway in M059K at different time points

**Figure 3-11** Decrease in expression of active NF-κB in human glioblastoma cells due to lovastatin

**Figure 3-12** DR5 expression sensitized by an NF-κB inhibitor

**Figure 3-13** Lovastatin affected both the intrinsic and extrinsic apoptotic pathways

**Figure 3-14** Regulation of the MAPK signal by lovastatin in human glioblastoma cells

**Figure 4-1** Map of the transfer vector (lenti-GFP-Luc)

**Figure 4-2** Principle of bioluminescence assay

**Figure 4-3** Morphology of the transduced U87 MG

**Figure 4-4** Intensity of the luciferin signal in U87 MG and U87-GFP-Luc

**Figure 4-5** Growth curves of transduced and untransduced U87 MG

**Figure 4-6** Growth curve of transduced U87 MG in nude mice

**Figure 4-7** IVIS imaging of the U87-GFP-Luc subcutaneous tumour model

**Figure 4-8** Body weight change in the subcutaneous mouse model after treatment

**Figure 4-9** Tumour volume in the subcutaneous mouse model after intraperitoneal administration of lovastatin

**Figure 4-10** Nude mice bearing subcutaneous brain tumours receiving lovastatin treatment by intraperitoneal injection

**Figure 4-11** IVIS imaging of the subcutaneous brain tumour mouse model

**Figure 4-12** The bioluminescent density of the tumour in the subcutaneous mouse model after intraperitoneal administration of lovastatin

**Figure 4-13** The expression of Ki-67 in tumour tissue was detected by immunohistochemical staining

**Figure 4-14** The DR5 protein expression in tumour tissues harvested from nude mice receiving intraperitoneal administration of lovastatin

**Figure 4-15** The DR5 protein expression in tumour tissues harvested from nude mice receiving peri-tumoral administration of lovastatin

**Figure 4-16** The expression of DR5 in tumour tissue was detected by immunohistochemical staining

**Figure 4-17** Tumour volume in the subcutaneous mouse model after local peri-tumoral administration of lovastatin

**Figure 4-18** Nude mice bearing subcutaneous brain tumours receiving peri-tumoral administration of lovastatin with/ without TRAIL

**Figure 4-19** IVIS imaging of the subcutaneous brain tumour mice receiving local peritumoral administration of lovastatin plus TRAIL

**Figure 4-20** The bioluminescent density of the tumour in the subcutaneous mouse model after local peri-tumoral administration of lovastatin with/ without TRAIL

**Figure 5** Schematic representation of the mechanism of TRAIL-induced apoptosis sensitized by lovastatin in human glioblastoma cells

# Contents


**Abstract** ..... I

**摘　要** ... IV

**Publications** . VII

**Acknowledgements** ... IX

**Abbreviations** X

**List of figures** XV

**Contents** . XIX

**Chapter One General ntroduction** 1

**1.1 Glioblastoma multiforme (GBM)** .. 2
*1.1.1 Epidemiology* ... 2
*1.1.2 Classification* ... 4
*1.1.3 Treatment* . . 7
**1.2 Tumour necrosis factor (TNF) related apoptosis-inducing ligand (TRAIL)** . ... 11
*1.2.1 TRAIL and TRAIL receptors* 11
*1.2.2 Distribution of TRAIL and its receptors in normal and cancer tissue* ... 12
*1.2.3 Toxicity of TRAIL* ... . 14
*1.2.4 Pathway of TRAIL-induced apoptosis* .... 15
*1.2.5 Mechanism of TRAIL resistance* .. ... . 18
*1.2.6 Clinical application of TRAIL* . ..... 22
**1.3 3-hydroxy-3-methylglutaryl-CoA (HMG-CoA) reductase inhibitors** . .. 25
*1.3.1 Biosynthesis of statins* .. ..... 26
*1.3.2 Pharmacology of lovastatin* .... ..... 27
*1.3.3 Clinical uses of statins* ..... ..... 28
*1.3.4 Potential anticancer mechanisms of statins* .. 31
**1.4 Nuclear factor-kappa B (NF-κB) pathway** .. 32
*1.4.1 Structure of NF-κB* . ... 33
*1.4.2 NF-κB and cancers* . 35
*1.4.3 NF-κB and glioma* .. . 37
**1.5 Perspective** .. .. .. 38

**Chapter Two Establishment of cellular assessment platform for lovastatin-sensitized TRAIL-sensitization in GBM** .. .. .. 40

**2.1 Introduction** . .. 41

**2.2 Materials and Methods** . 42
*2.2.1 Cell lines and cell culture* ... 42
*2.2.2 Cell viability as measured by MTT assay* 43
*2.2.3 Cell proliferation as measured by BrdU cell proliferation assay.* 44
*2.2.4 Cell cycle as measured by propidium iodide staining* 45
*2.2.5 Apoptosis as measured by annexin V and propidium iodide (PI) staining* 46
*2.2.6 Statistical analysis* 47
**2.3 Results** ... . . 47
*2.3.1 Cell morphology after treatment with lovastatin or TRAIL* 47
*2.3.2 Cell viability as measured by MTT assay* 49
*2.3.3 Cell anti-proliferation effect as measured by BrdU cell proliferation assay* ... 54
*2.3.4 Cell cycle analysis by PI staining* .... 57
*2.3.5 Apoptosis detected by Annexin V/PI staining* 59
**2.4 Discussion** . ... . .. 64

**Chapter Three How does lovastatin sensitize TRAIL-induced apoptosis in TRAIL-resistant GBM cells** . **67**

**3.1 Introduction** . .. 68
**3.2 Materials and Methods** . ..... 69
*3.2.1 Cell lines and cell culture* ... 69
*3.2.2 Western blotting* ... ... 70
*3.2.3 mRNA level of DR5 as detected by real-time PCR* ... 72
*3.2.4 NF-κB activity as measured by dual-luciferase reporter assay* ... 75
*3.2.5 Statistical analysis* 78
**3.3 Results** ... . . 79
*3.3.1 Expression of TRAIL receptors in human glioblastoma cells* 79
*3.3.2 mRNA level of DR5 in human glioblastoma cells* . 83
*3.3.3 DR5 expression in human stromal cells after treated with lovastatin* 84
*3.3.4 Change of NF-κB activity in human glioblastoma cells as detected by dual-luciferase reporter assay* .... 85
*3.3.5 Change in the NF-κB pathway in human glioblastoma cells induced by lovastatin* ... 86
*3.3.6 Expression of death receptors in human glioblastoma cells following the inhibition of NF-κB* 92
*3.3.7 Lovastatin affects the regulation of downstream molecules in the apoptotic pathway* .. 94
*3.3.8 Regulation of the MAPK pathway induced by lovastatin treatment in human glioblastoma cells* . 97
**3.4 Discussion** . ... . .. 100

**Chapter Four Preclinical animal studies in nude mice model of GBM . 105**
**4.1 Introduction . .. 106**
**4.2 Materials and Methods . ..... 107**
*4.2.1 Cell lines and cell cultures ...* . 107
*4.2.2 Lentivirus production and transduction* . 108
*4.2.3 Confirmation of the transduced cell line* 113
*4.2.4 Growth curve assay of the transduced cell line* 114
*4.2.5 Establishment of the subcutaneous brain tumour model and treatment* 114
*4.2.6 In vivo imaging system . .. . ..* 116
*4.2.7 Immunohistochemical staining .. .* 116
*4.2.8 Expression of DR5 in tumour tissues as determined by western blotting .. . .. . ..* 118
*4.2.9 Statistical analysis* 119
**4.3 Results ... .** 119
*4.3.1 Transduction rate observed by fluorescence microscopy* 119
*4.3.2 Bioluminescent assay of U87-GFP-Luc* 121
*4.3.3 Cell proliferation of transduced and untransduced cells ....* 122
*4.3.4 Subcutaneous brain tumour model and IVIS image* . 123
*4.3.5 Anti-tumour effect of lovastatin on glioblastoma animal model by intraperitoneal injection* . 126
*4.3.6 The Ki-67 expression of tumour tissue collected from nude mice receiving intraperitoneal administration of lovastatin as detected by immunohistochemical staining* . 132
*4.3.7 The DR5 protein expression of tumour tissue collected from nude mice receiving intraperitoneal administration of lovastatin as determined by western blotting* . 134
*4.3.8 The DR5 protein expression of tumour tissue collected from nude mice receiving local peri-tumoral administration of lovastatin as investigated by western blotting and immunohistochemical staining* 136
*4.3.9 Synergistic effect of lovastatin and TRAIL on subcutaneous brain tumour model in vivo* 139
**4.4 Discussion . ... . .. 144**
**Chapter Five Conclusion and Future Prospects . 150**
**5.1 Summary of results . ... 151**
**5.2 Conclusion . . ..... 152**
**5.3 Future prospects ... . ..... 154**
**References . . . . ... 155**

# Chapter One

# General Introduction

## 1.1 Glioblastoma multiforme (GBM)

### 1.1.1 Epidemiology

A brain tumour is an abnormal cell growth that can occur both inside the cranium and in the central spinal canal. In the United States, there were 22,020 estimated new cases of malignant neoplasm of the central nervous system (CNS) in 2010 (Society 2010), with 1.4% of cancer patients being diagnosed with a brain tumour. Based on the latest data from the Central Brain Tumour Registry of the United States, the incidence rate of primary malignant brain tumour is 7.32 cases per 100,000 person years (CBTRUS 2002-2006). Many studies have reported that the incidence and mortality of brain tumours in developed countries has risen significantly over the past three decades (Wrensch, Bondy et al. 1993; Davis, Malinski et al. 1996; Mark Bernstein 2008). This may be related to improved diagnostic procedures. However, the prevalence in the Asian population is much lower than that in the United States. From 1998 to 2007, the incidence rate of malignant tumours in the CNS was 2.9 per 100,000 person years in Hong Kong (Hong Kong Cancer Registry 2010). This lower prevalence is positively associated with age, and shows a peak incidence at around 70 years old. However, although the incidence is quite low in Hong Kong, the mortality rate is relatively high, at 1.4 cases per 100,000 person years. The incidence and mortality of CNS tumours in Hong Kong are shown in Figures 1-1 and 1-2 (Hong Kong Cancer Registry 2010).

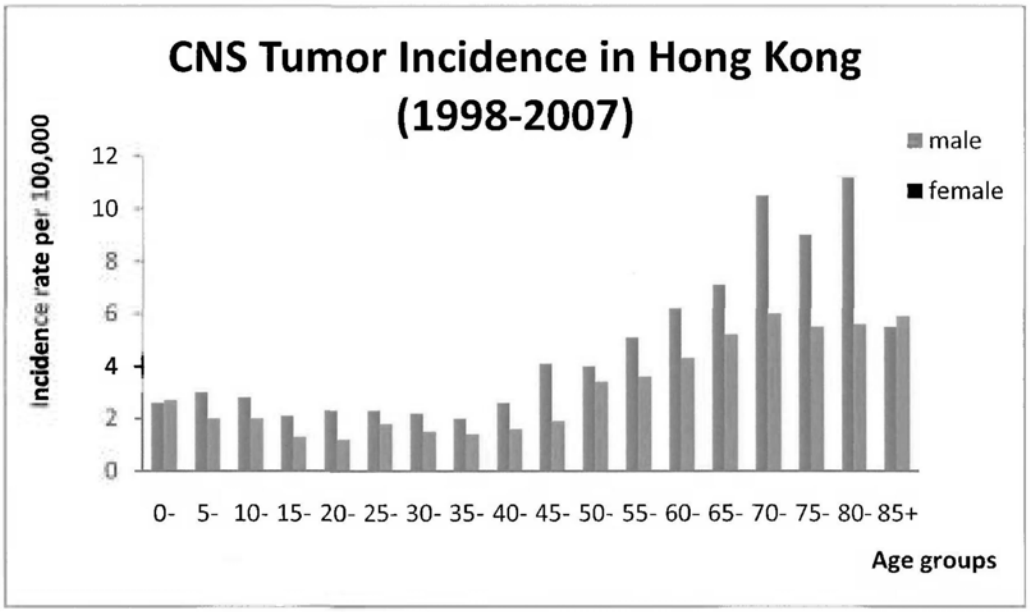


**Figure 1-1 CNS Tumour Incidence in Hong Kong**

CNS tumour incidence rate per 100,000 in Hong Kong from 1998 to 2007, with the peak incidence occurring at around 70 years old (data from the Hong Kong Cancer Registry, Hospital Authority).

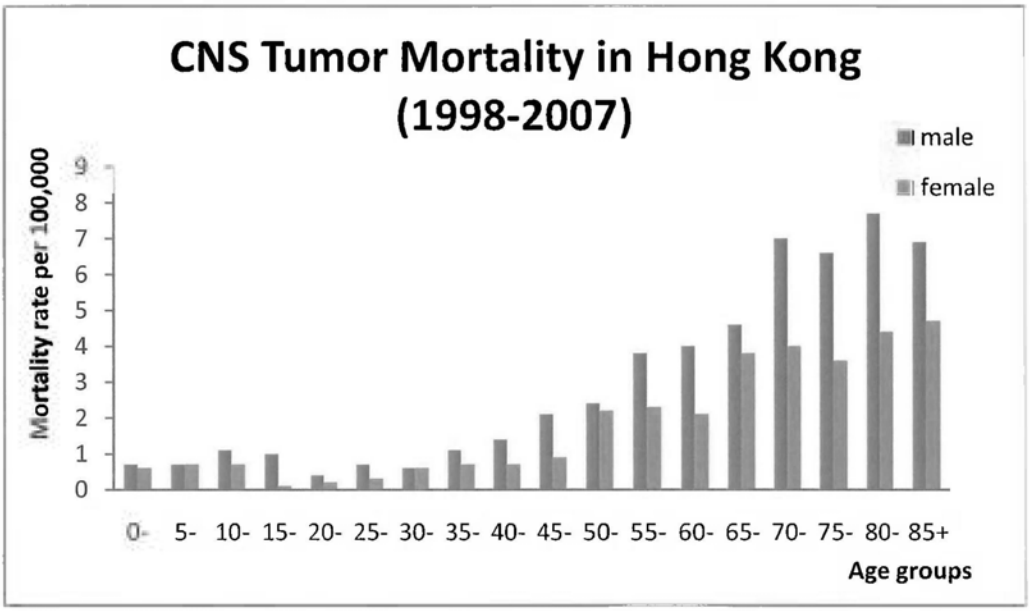


**Figure 1-2 CNS Tumour Mortality in Hong Kong**

CNS tumour mortality rate per 100,000 in Hong Kong from 1998 to 2007 (data from the Hong Kong Cancer Registry, Hospital Authority).

### 1.1.2 Classification

Gliomas are the most common type of malignant brain tumour, and are derived from glial cells. At present, the most widely accepted grading system of CNS tumours used in clinic is the World Health Organization (WHO) system, which was first published in 1979 (KJ 1979). According to the latest version published in 2007 (Louis, Ohgaki et al. 2007), gliomas can be divided into astrocytomas,

oligodendrogliomas, and ependymomas according to cell type. Of these three subtypes, astrocytomas are the most frequent type, and can be further divided into four grades, which include WHO grade 1 (benign), WHO grade 2 (low-grade astrocytoma), WHO grade 3 (anaplastic astrocytomas), and WHO grade 4 (glioblastoma multiforme, GBM). The latter two are considered to be malignant or high-grade gliomas (Jorg-Christian Tonn 2010).

Up to 80 percent of patients with malignant glioma are diagnosed as having a glioblastoma mutilforme (GBM). The histological characteristics of the GBM include increased cellularity and pleomorphism, a higher mitotic rate, and the presence of vascular proliferation and necrosis. Most primary GBMs develop *de novo*, and secondary GBMs progress only gradually. The ways in which GBMs develop are illustrated in Figure 1-3 (Jorg-Christian Tonn 2010). Some studies have reported that changes in molecular factors and chromosomes accompany GBM development, such as epidermal growth factor receptor (EGFR), platelet-derived growth factor receptor (PDGF), and p53 (Mark Bernstein 2008). These can be used as prognostic factors to predict the survival of GBM patients. For example, the deletion of 1p and 19q has been found in GBM patients who survive longer (Senger, Cairncross et al. 2003).

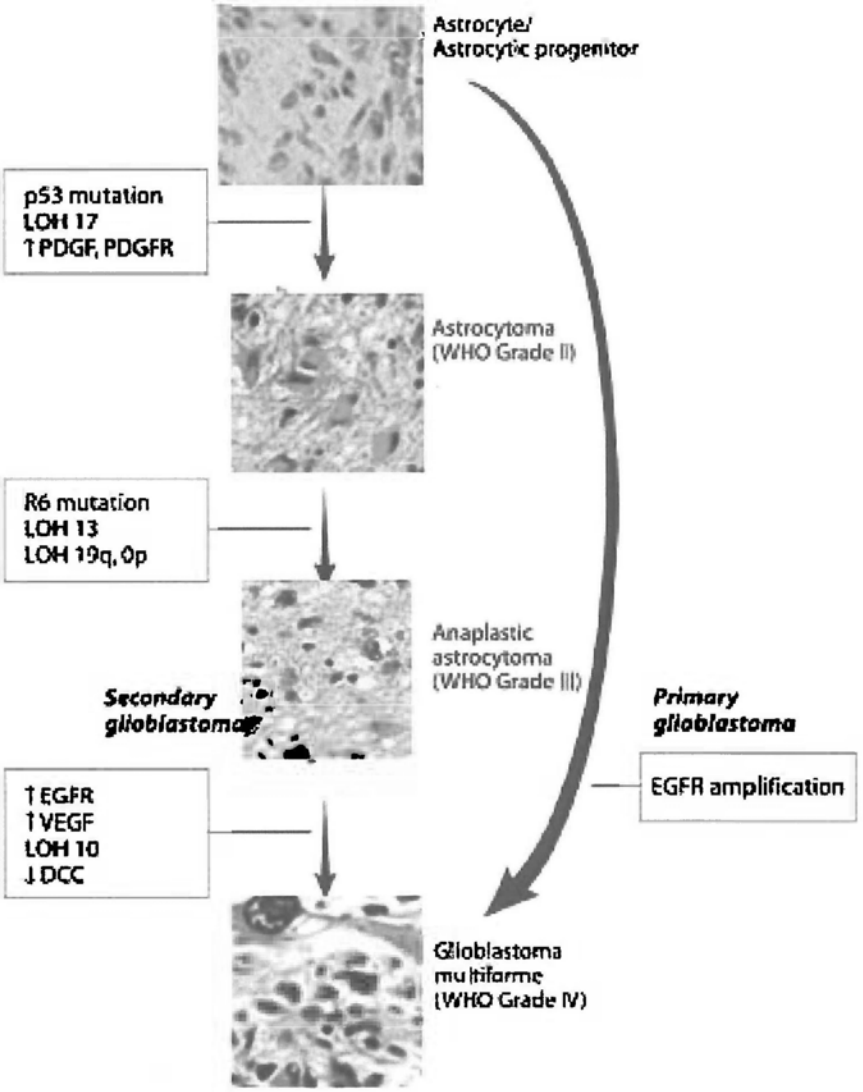


**Figure 1-3 Development of primary and secondary GBM**

During GBM development, several receptors dysregulate and chromosomal abnormalities occur. (Modified from: Neuro-oncology of CNS tumours)

### 1.1.3 Treatment

Surgery, radiotherapy, and chemotherapy are still the main treatments for GBM. Among the treatments, surgical resection is the first choice for patients. The current goals of surgery for GBM patients are not only histological diagnosis and mass resection, but also the improvement of life quality and the delivery of adjunctive therapy (Lemke 2004). Recently, the surgical procedure for GBM becomes safer than before because of the improvement of imaging technology, such as electrophysilogical mapping, intraoperative imaging, intraoperative navigation systems, and intraoperative functional mapping (Duffau, Capelle et al. 2003; Albayrak, Samdani et al. 2004). It has been reported that GBM patients treated with gross-total resection have a longer survival and a better quality of life than those receiving near-total or subtotal resection (Berger 1994; Laws, Parney et al. 2003). However, fast growth and spread into the surrounding brain tissues limits the efficacy of all of these procedures. In order to locate the residual effectively, the intraoperative fluorescence was introduced for guidance of tumor resection (Stummer, Stocker et al. 1998; Stummer, Stocker et al. 1998). 5-aminolevuleic acid (5-ALA) is a typical photosensitiser and makes the fluorescent porphyrin accumulate in high-grade glioma cells. Some clinical trials also confirmed that application of introaperative fluorescence may improve glioma progression-free survival (Kremer, Fardanesh et al. 2009; Widhalm, Wolfsberger et al. 2010). However, the fluorescence signal induced by 5-ALA is only detected in high-grade gliomas (Hefti, von Campe et al. 2008).

In addition to surgery, radiotherapy is a very important treatment for GBM patients. Three decades ago, whole-brain radiotherapy (WBRT) was applied, especially for patients with brain metastasis (Order, Hellman et al. 1968). However, the high morbidity and severe side effects were also observed after receiving whole-brain radiotherapy (Packer, Sutton et al. 1989). The comparison study also confirmed that the similar outcome could be found in whole-brain radiotherapy group and local radiotherapy (Kita, Okawa et al. 1989).

Although previous data has shown that radiotherapy can improve the long-term survival of GBM patients, especially those aged below 65 years old (Leibel and Sheline 1987), the prolonged survival is not satisfied. To enhance the effect of radiotherapy for GBM patients, the dosing schemes, fractionation, and deliver vector are considered to adjust. However, there is no survival advantage in hyperfractionated radiotherapy, accelerated hyperfractionated radiotherapy and hypofractionated radiotherapy compared with conventionally fractionated irradiation (Horiot, van den Bogaert et al. 1988; Nelson, Diener-West et al. 1988; Nieder, Andratschke et al. 2004). Moreover, brachytherapy, stereotactic radiosurgery, and boron neutron capture therapy (BNCT) are also investigated. The escalation of local dose can be achieved by these techniques and finally prevents the surrounding normal tissues from radiotherapy. Unfortunately, these methods are difficult to be widely used in clinic because of complex procedure, high expense, and limited effect (Laperriere, Leung et al. 1998; Capala, Stenstam et al. 2003; Maranzano, Anselmo et al. 2011). Furthermore,

radiosensitizing agent is another study area for improving the efficacy of radiotherapy, such as temozolamide and 5-FU (Goffman, Dachowski et al. 1992; Roullin, Mege et al. 2004; Stupp, Mason et al. 2005).

Chemotherapy for GBM patients involves many challenges. The major problem is the blood-brain barrier (BBB), which limits the transport of drugs to the brain and leads to a drug concentration that is below the effective level in patients receiving systemic chemotherapy (Muldoon, Pagel et al. 1999). Clinical data has also demonstrated that there is no difference in the survival of GBM patients undergoing radiotherapy only and radiotherapy combined with chemotherapy (2001). Therefore, chemotherapy is thus only prescribed after surgery or radiotherapy.

Up to date, alkylating agents are the most common used chemotherapeutic agent for GBM, like carmustine (BCNU) (Figueiredo, Faria et al. 2010; Reithmeier, Graf et al. 2010). In 2005, temozolomide, a new introduced oral anti-tumour drug, was approved by the Food and Drug Administration (FDA), and has been confirmed in its ability to improve the median survival and two-year survival of GBM patients receiving postoperative radiotherapy and daily temozolomide, especially those with methylated O(6)-methylguanine-DNA-methyltransferase (MGMT) (Hegi, Diserens et al. 2005; Stupp, Mason et al. 2005; Minniti, Salvati et al. 2011).

At the same time, researchers also try to improve the chemosensitivity of GBM patients via regulation of potential pathways that related to the resistance of chemotherapy for GBM patients, such as loss of p53 (Park, Park et al. 2006), up-regulation of epidermal growth factor receptor (EGFR) (Chakravarti, Loeffler et al. 2002) , BCL-2 (Zhu, Li et al. 2003) , and inhibitor-of-apoptosis-proteins (IAPs) (Ziegler, Keating et al. 2011). But most of these results are limited in experimental level. Except to develop new anti-tumour drugs continuously, the drug local delivery method which may elevate the drug concentration in tumour tissue and minimize neurotoxicity induced by chemotherapy has also established, including carmustine (BCNU) wafers (Westphal, Hilt et al. 2003; Bock, Puchner et al. 2010; Salvati, D'Elia et al. 2011), convection-enhanced delivery (Rainov, Gorbatyuk et al. 2008) , slow-releases biopolymer (Chandy, Das et al. 2000; Kim, Gaber et al. 2009) , and nanoparticle vehicle (Hua, Liu et al. 2011).

Recently, other novel applications have also been explored, including stem cell therapy (Yong, Shinojima et al. 2009; Kim 2011) , virus-mediated gene therapy (Grandi, Fernandez et al. 2010) , oncolytic virus therapy (Geletneky, Hartkopf et al. 2010), immunotherapy (Waldron, Yang et al. 2010; Weller 2010), and small-molecule-based therapy(Hatanpaa, Burma et al. 2010) . However, the efficacy of these treatments remains unconfirmed, and random clinical trials are needed. Another new strategy highlighted in recent cancer research is death receptor therapy (Weller, Kleihues et al. 1998) . Among the several death ligand,

tumour necrosis factor-related apoptosis-inducing ligand receptors (TRAIL) is the most promising candidate and usually combining used with radiotherapy or chemotherapy (Tsurushima, Yuan et al. 2007; Fiveash, Gillespie et al. 2008; Chen, Sun et al. 2010).

## 1.2 Tumour Necrosis Factor (TNF) Related Apoptosis-inducing Ligand (TRAIL)

### 1.2.1 TRAIL and TRAIL receptors

The tumour necrosis factor related apoptosis-inducing ligand (Apo2L/TRAIL), which belongs the TNF superfamily, was first introduced by Wiley in 1995 (Wiley, Schooley et al. 1995; Pitti, Marsters et al. 1996). It is a type II transmembrane protein with homology with other members of the TNF family. TRAIL thus possesses the common characteristics of a member of the TNF superfamily. For example, the active soluble form is produced by metalloproteases, and the homotrimer is formatted with other receptors (Mariani and Krammer 1998). In humans, it consists of 281 amino acid proteins and encodes the gene at chromosome 3q26. Unlike the other TNF superfamily members, there is a unique insertion loop of about 12 to 16 amino acids in soluble TRAIL near its amino-terminal end. In addition, an internal zinc ion binds to a cystein residue (Cys 230) at the trimer's interface (Bodmer, Meier et al. 2000) . This special structure is critical to the stability and activity of the

trimer. It has been reported that the deletion of the zinc ion may significantly down-regulate apoptotic activity (Hymowitz, Christinger et al. 1999) , and that a zinc ion feeding strategy may improve the expression and bioactivity of TRAIL (Sun, Shen et al. 2006).

In humans, TRAIL has five receptor molecules, including TRAIL receptor 1 (death receptor 4) (Pan, O'Rourke et al. 1997), TRAIL receptor 2 (death receptor 5, TRICK2, KILLER) (Walczak, Degli-Esposti et al. 1997) , TRAIL receptor 3 (decoy receptor 1, TRID, LIT) (Degli-Esposti, Smolak et al. 1997) , TRAIL receptor 4 (decoy receptor 2, TRUNDD) (Marsters, Sheridan et al. 1997) , and osteoprotegerin (OPG, decoy receptor 3) (Emery, McDonnell et al. 1998). The first two receptors contain a special death domain (DD) and transfer an apoptotic signal when engaged with TRAIL. Decoy receptor 1 and decoy receptor 2, which have either no death domain or a truncated death domain, bind competitively and inhibit apoptosis (Almasan and Ashkenazi 2003). OPG, which has a much weaker affinity with TRAIL, is a soluble receptor and also protects cells from apoptosis.

### 1.2.2 Distribution of TRAIL and its receptors in normal and cancer tissue

Data on the distribution of TRAIL and TRAIL receptors in human tissue are limited. Nevertheless, previous studies have shown that TRAIL and its receptors are widely detected in normal human tissue. According to

immunohistochemistry (IHC), western blot, and reverse transcription polymerase chain reaction (RT-PCR) results, TRAIL can be found in the liver, bile duct, convoluted tubule of the kidney, cardiomytocyte, lung epithelia, Leydig cells, normal odontogenic epithelium, megakaryocytic cells, and erythroid cells (Secchiero, Melloni et al. 2004; Spierings, de Vries et al. 2004; Kumamoto and Ooya 2005; Melloni, Secchiero et al. 2005). However, it is very difficult to detect the expression of TRAIL in the colon, glomeruli, Henle's loop, germ and Sertoli cells, heart endothelium, smooth muscle cells of the lung and spleen, and follicular cells in the thyroid gland (Strater, Hinz et al. 2002; Daniels, Turley et al. 2005). Like the TRAIL, death receptors are observed in the liver, lung, and colon (Arts, de Jong et al. 2004), whereas decoy receptors are expressed in the liver, thyroid, and testis (Daniels, Turley et al. 2005).

In humans, TRAIL mRNA has been observed in both primary and metastasizing brain tumours and normal tissue (Frank, Kohler et al. 1999; Rieger, Ohgaki et al. 1999). A low level of TRAIL expression has also been detected in the glial cells of the cerebellum (Daniels, Turley et al. 2005). However, other studies have demonstrated the opposite result, finding only a low TRAIL expression in the human brain (Dorr, Bechmann et al. 2002).

The data on TRAIL receptor expression, in contrast, are consistent across studies. The death receptors and decoy receptors are co-expressed in normal and tumour tissues localized on the neurons, astrocytes, and oligodendrocytes

(Frank, Kohler et al. 1999; Dorr, Bechmann et al. 2002). However, the expression levels in the four receptors in each brain region are quite different. Although the expression of death receptors is much greater than that of decoy receptors in tumour tissues, the sensitivity of TRAIL does not accord with this pattern in many glioblastoma cells (Knight, Riffkin et al. 2001; Hetschko, Voss et al. 2008; Kuijlen, Bremer et al. 2010).

### 1.2.3 Toxicity of TRAIL

It is widely known that TRAIL only selectively attacks tumour cells and protects normal cells from apoptosis. However, not all forms of TRAIL have this property. In the last decade, many researchers have debated the toxicity of TRAIL to human normal tissues. Several research centers have found that recombinant human TRAIL (rhTRAIL) with a tag, such as leucine zipper-fused, polyhistidine-tagged, or flag-tagged TRAIL, may induce apoptosis in normal cells (Walczak, Miller et al. 1999; Jo, Kim et al. 2000; Nitsch, Bechmann et al. 2000). In 2001, Hao and Lawrence demonstrated that soluble rhTRAIL without a tag did not induce the death of human astrocytes and hepatocytes (Hao, Beguinot et al. 2001; Lawrence, Shahrokh et al. 2001). Other studies have also revealed tolerance to rhTRAIL in mice, cynomolgus monkeys, and chimpanzees without any side effects (Ashkenazi, Pai et al. 1999; Walczak, Miller et al. 1999). These important discoveries facilitated further studies and pushed TRIAL into clinic application. The results of the phase I trial of the clinical use of TRAIL confirming the safety of rhTRAIL for human normal tissues were

published at the 42nd Annual Meeting of the American Society of Clinical Oncology (Anita C. Bellail 2009).

### 1.2.4 Pathway of TRAIL-induced apoptosis

TRAIL mainly induces apoptosis through a combination of death receptor 4 (DR4) and death receptor 5 (DR5), the so-called extrinsic pathway that is one of the major mechanisms of cell death. When TRAIL binds to DR4 or DR5, the intracellular adaptor, Fas-associated death domain (FADD), which comprises a carboxy-terminal death domain and an amino-terminal death effector domain (DED), is stimulated (Chinnaiyan, O'Rourke et al. 1995; Walczak, Degli-Esposti et al. 1997). DED is a very important part of the process, and recruits the downstream molecules caspase-8 and caspase-10 to generate a death-inducing signaling complex (DISC). Apoptosis is then achieved through a cleaved caspase cascade (Fox, Humphreys et al. 2010).

An intrinsic pathway is needed on addition to the extrinsic pathway for TRAIL-induced apoptosis. The active caspase-8 recruited by FADD may induce the Bcl-2 inhibitory BH-2-domain-containing protein (Bid) cleave to a truncated Bid (tBid) (Li, Zhu et al. 1998; Youle and Strasser 2008). The latter subsequently translocates to the mitochondria and interacts with Bax and Bak. Finally, cytochrome c is released from the mitochondria and initiates a downstream apoptotic mechanism. Figure 1-4 illustrates the intrinsic and

extrinsic apoptotic signaling pathways. In only a small number of cells, named type I cells, is apoptosis induced through the DR-initiated extrinsic pathway alone. In type 2 cells, an amplified signal must be generated by cross-talk between the intrinsic and extrinsic pathways (Wiezorek, Holland et al. 2010).

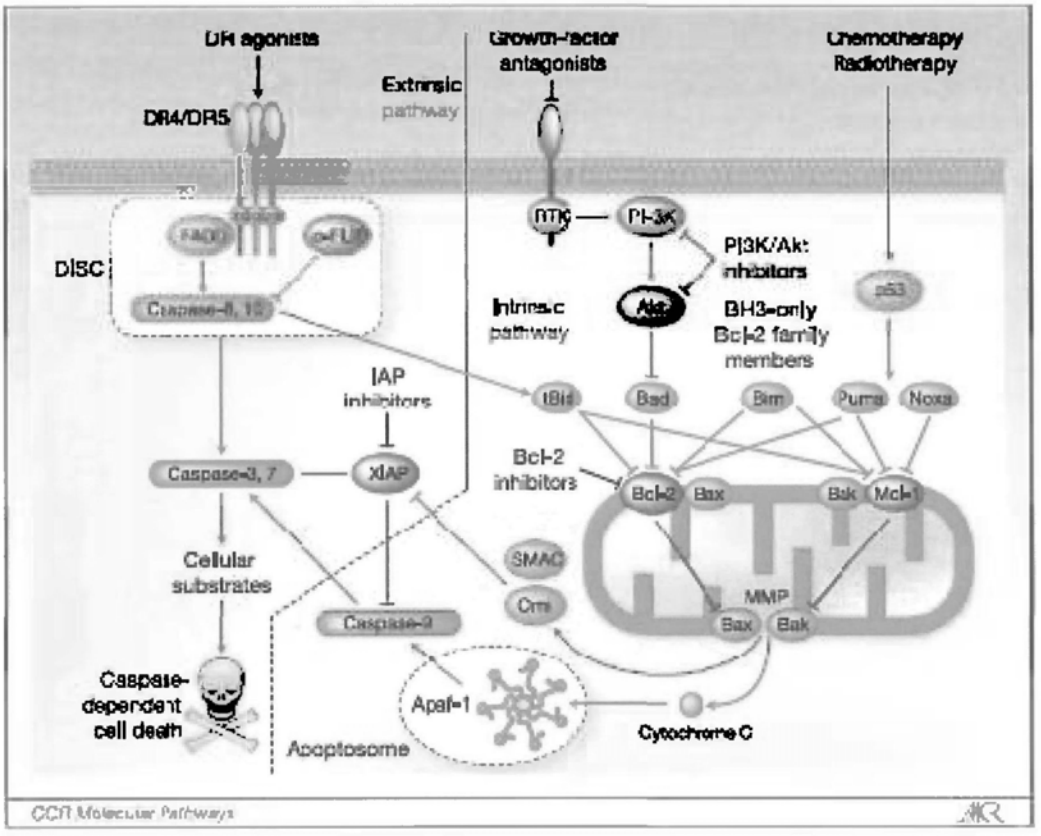


**Figure 1-4 Intrinsic and extrinsic pathways of apoptosis**

The apoptotic signal is mainly transmitted through two pathways: the intrinsic pathway and the extrinsic pathway. Bid plays an important role in the crosstalk between the two pathways (Ashkenazi 2002; Wu 2009; Wiezorek, Holland et al. 2010) (reproduced with the permission of the publisher).

### 1.2.5 Mechanism of TRAIL resistance

TRAIL receives more attention than the other TNF superfamily members because of its selective antitumour ability. However, there are still many tumour cells that can resist TRAIL attack, and the mechanism of TRAIL resistance remains unclear. Because TRAIL performs a dual function through binding to death receptors or decoy receptors, the differential expression level of the two types of receptors is regarded as the main reason for the differential sensitivity to TRAIL in different tissues. It also explains the low sensitivity to TRAIL of normal tissues, as a higher expression of decoy receptors is observed in normal tissues than in tumour tissues (Ashkenazi and Dixit 1998; Chinnaiyan, Prasad et al. 2000; Leverkus, Neumann et al. 2000). However, the opposite has also been proposed, with some studies demonstrating no correlation between the expression of DR5, DcR1, and DcR2 and sensitivity to TRAIL (Griffith and Lynch 1998; Griffith, Wiley et al. 1999; Kim and Gupta 2000). It may be that resistance to TRAIL is controlled by multiple mechanisms.

An anti-apoptotic protein, cellular Fas-associated death domain-like interleukin-1 converting enzyme (FLICE) inhibitory protein (c-FLIP), is regarded as crucial to TRAIL resistance (French and Tschopp 2002; Zong, Yin et al. 2009). c-FLIP is an analog of caspase-8, and can interact with FADD to inhibit downstream caspase molecular activation (Irmler, Thome et al. 1997). Caspase-3 is responsible for c-FLIP cleavage, which is one of facilitating factors of TRAIL-induced apoptosis. This indicates that there is a vicious circle between the

overexpression of c-FLIP and caspase-3 down-regulation (Shankar and Srivastava 2004). Other research has also confirmed the role of c-FLIP. A higher expression of c-FLIP has been found in certain tumours that are resistant to TRAIL, such as colorectal carcinomas (Ryu, Lee et al. 2001), gastric carcinomas (Lee, Kim et al. 2003), pancreatic carcinomas (Mori, Doi et al. 2005), and melanoma (Griffith, Chin et al. 1998). The RNAi-based knockdown of c-FLIP also sensitises cells to TRAIL-induced apoptosis.

In addition to c-FLIP, mutations in the caspase-8 and caspase-10 genes also affect the sensitivity of cells to TRAIL. Resistance to TRAIL can also be detected in dendritic cells with mutant caspase-10 (Wang, Zheng et al. 1999). Alternatively, the catalytically inactive caspase-10 mutant may compete with caspase-8 to inactivate the downstream caspase cascade.

As mentioned, most cells need an intrinsic pathway to amplify the apoptotic signal from the extrinsic pathway. This indicates that the anti-apoptotic molecule in the intrinsic pathway, Bcl-2, is also involved in TRAIL resistance (Hinz, Trauzold et al. 2000; Munshi, Pappas et al. 2001). When the activated caspase-8 cleaves Bid, which is a BH3-only protein, the truncated Bid interacts with Bcl-2 and further inhibits Bax/Bak activation to maintain the mitochondrial membrane potential (LeBlanc, Lawrence et al. 2002). However, the other members of the Bcl-2 family, Bax and Bak, may induce the opposite effect (Youle and Strasser 2008). tBid interacts with Bax/Bak to induce the

oligomerization of Bax and Bak at the mitochondrial membrane. This modification changes the mitochondrial membrane potential and promotes TRAIL-induced apoptosis (Gross, Jockel et al. 1998; Wei, Lindsten et al. 2000).

The inhibitors apoptosis protein (IAP) family, which includes XIAP, cellular IAP1 (cIAP1), cIAP2, survivin and livin, are also reported to be responsible for TRAIL resistance. IAP may block the cleavage of caspase-3 and caspase-7 and enzymatic activation (Salvesen and Duckett 2002). It has been proven that the down-regulation of XIAP and survivin enhances TRAIL-induced apoptosis (Chawla-Sarkar, Bae et al. 2004; Cummins, Kohli et al. 2004).

In addition to these possible mechanisms, the protein kinase B (PKB, Akt), nuclear factor (NF)-κB and mitogen-activated protein (MAP) kinases are related to the inhibition of TRAIL-induced apoptosis (Tran, Holmstrom et al. 2001; Kavurma, Schoppet et al. 2008; Goncharenko-Khaider, Lane et al. 2010). It has been shown that the expression of Akt, which improves cellular survival and resistance to chemotherapy and radiotherapy, is significantly elevated in many cancers, such as prostate cancer, ovarian cancer, and gastric cancer (Chen, Thakkar et al. 2001; Martelli, Tazzari et al. 2003; Nam, Jung et al. 2003; Lane, Goncharenko-Khaider et al. 2010). It enhances resistance to TRAIL through the up-regulation of c-FLIP and the phosphorylation of mitogen-activated kinase-activating death domain protein (MADD). Akt-phosphorylated MADD competitively interacts with DR4 (Nam, Jung et al. 2003; Lane, Goncharenko-

Khaider et al. 2010; Li, Jayarama et al. 2010). Some studies have obtained similar results using the PI-3 kinase inhibitor to reduce Akt activity and improve TRAIL-induced apoptosis.

The nuclear factor (NF)-κB pathway is another widely observed pathway in cancer research. Both DR4 and DR5 are believed to initiate NF-κB activity (Jeremias and Debatin 1998; Hu, Johnson et al. 1999). However, NF-κB has a dual effect in TRAIL-induced apoptosis. One subunit of NF-κB, RelA/p65, not only up-regulates anti-apoptotic genes, such as c-FLIP, Mcl-1, and cIAP2, but also down-regulates the expression of DR4/DR5 and caspase-8 (Hall and Cleveland 2007). Another NF-κB subunit, c-Rel, improves the expression of TRAIL, DR4, DR5, and Bcl-X, and blocks IAP and survivin after TRAIL treatment (Chen, Kandasamy et al. 2003).

Many researchers have investigated the relationship between the MAPK pathway and TRAIL. Nevertheless, the role of the MAPK pathway in TRAIL-induced apoptosis remains controversial. Some results have shown the activation of the extracellular signal-regulated kinase (ERK) to be a critical factor in conferring TRAIL resistance by the inhibition of caspase-8 and Bid (Soderstrom, Poukkula et al. 2002). This finding has also been confirmed in human breast cancer, in which TRAIL-induced apoptosis is increased when ERK is down-regulated (Lee, Lee et al. 2006). Other factors in the MAPK pathway, JNK and p38, were found not to be correlated with TRAIL-induced

apoptosis in HeLa cells and human colon cancer cells (Muhlenbeck, Haas et al. 1998; Zhang, Zhu et al. 2004). However, active ERK shows a proapoptotic property in lung cancer cells (Frese, Pirnia et al. 2003). At the same time, the conflicting result also reveals that TRAIL-induced apoptosis can be detected in malignant mesothelioma through JNK phosphorylation (Abayasiriwardana, Barbone et al. 2007).

The final factor that should be mentioned is physiological temperature. According to the results of an *in vitro* study, the affinity of TRAIL receptors to TRAIL is similar at 4 ℃, whereas a differential affinity is detected at 37 ℃(Srivastava 2001).

### 1.2.6 Clinical application of TRAIL

TRAIL was first introduced in 1995, and has been studied continuously ever since. Its abilities to make targeted attacks on tumour cells and its lack of toxicity to normal cells are very attractive properties, and as a result most researchers regard TRAIL as a potential candidate for anti-cancer therapy. To date, at least 50 primary human tumour specimens treated with TRAIL have been investigated, including colon cancer (Sung, Ravindran et al. 2010), breast cancer (Yin, Sethi et al. 2010), glioma (Chen, Sun et al. 2010), prostate cancer (He, Shi et al. 2010), ovarian cancer (Lane, Goncharenko-Khaider et al. 2010), and myeloma (Lee, Yagita et al. 2010).

However, researchers have found that poor efficacy and TRAIL resistance can be detected in most cells. Thus, TRAIL is currently regarded as an adjuvant drug that is only suitable for use in combination with other therapies. Both *in vitro* and *in vivo* studies have shown TRAIL to have an effective synergetic effect when applied with γ-radiation (Chinnaiyan, Prasad et al. 2000), IFN-γ (Shigeno, Nakao et al. 2003) and genotoxic agents (such as doxorubicin, cisplatin, etopsoside, paclitaxel, and irinotecan) (Naka, Sugamura et al. 2002; Hotta, Suzuki et al. 2003; Dorsey, Mintz et al. 2009). Other drugs, such as cyclooxygenase-2 (Cox-2) inhibitors (Gaiser, Becker et al. 2008), daidzein (Siegelin, Gaiser et al. 2009), myricetin (Siegelin, Gaiser et al. 2009), and troglitazone (Grund, Ahmadi et al. 2008), have also been applied in various research centers. The underlying mechanism of these synergistic treatments is the targeting of hypothesized TRAIL resistance in different cancers.

Because the half-life of rhTRAIL is short (approximately 30 min), DR4 and DR5 agonistic monoclonal antibodies (mAb) have been developed as a targeted therapy for cancer (Lawrence, Shahrokh et al. 2001; Wiezorek, Holland et al. 2010). At present, one DR4 agonist (Mapatumumab, HGS-ETR1) and six DR5 agonists (Lexatumumab (HGS-ETR2), Apomab, conatumumab (AMG655), Tigatuzumab (CS1008), LBY135, and HGS-TR2J (KMTR2)) are available (Fox, Humphreys et al. 2010). All of these drugs have undergone clinical phase I or II trials. The preliminary data confirms that the DR4/DR5 agonists are safe and well tolerated by humans. The half-life of HGS-ETR1 and HGS-ETR2 is

significantly longer than that of rh-TRAIL, at around 17 days (Gajewski 2007; Anita C. Bellail 2009). These agonists have been investigated both as single agents and synergistic therapy with other treatments in non-Hodgkin lymphoma (NHL) and advanced solid cancer (Leong, Cohen et al. 2009; Zhang, Frank et al. 2009; Trarbach, Moehler et al. 2010).

New carriers and delivery systems for TRAIL have been investigated, including neural stem cells (Ehtesham, Kabos et al. 2002), adenovirus vectors (Wohlfahrt, Beard et al. 2007), and cationic albumin-conjugated pegylated nanoparticles (CBSA-NP) (Lu, Sun et al. 2006). These reagents may be delivered by local convection-enhanced delivery, intratumoral injection, intraperitoneal injection, and intravenous injection. These improved modalities overcome the limits of the blood brain barrier (BBB) and increase the accumulation of TRAIL in brain tumours.

In addition to its application in cancer research, TRAIL is also a hot topic in the neuroscience field. Due to its ability to induce apoptosis and its immunoregulatory capacity, TRAIL is regarded as a double-edged sword in central nervous system inflammatory diseases such as multiple sclerosis (Aktas, Schulze-Topphoff et al. 2007), Alzheimer's disease (Genc, Egrilmez et al. 2009), and bacterial meningitis (Hoffmann, Zipp et al. 2009). More research of the application of TRAIL in these areas is needed in the future.

## 1.3 3-hydroxy-3-methylglutaryl-CoA (HMG-CoA) reductase inhibitors

HMG-CoA reductase inhibitors, also called statins, were first introduced by a Japanese scientist. The first statin was isolated from *Penicillium citrinum* and named mevastatin (Endo, Kuroda et al. 1976). Subsequently, another natural type statin, lovastatin, was isolated from *Monacus ruber*. In 1987, lovastatin was approved by the Food and Drug Administration (FDA) for clinical trials, which confirmed its ability to significantly decrease low density lipoprotein (LDL) (Barrios-Gonzalez and Miranda 2010). Due to this dramatic clinical effect, more statins were developed, such as semi-synthetic statin (simvastatin and pravastatin) and synthetic statin (fluvastatin, atorvastatin, rosuvastatin, and pitavastatin), and the use of statin in patients with cardiovascular disease has since been widely promoted. This has made statins the most prescribed therapeutic drug, except for analgesics, in the world. According to data from multicenter trials, statins not only decrease the level of total cholesterol and LDL, but also improve the survival rate of patients with hypercholesterolemia (1994; Downs, Clearfield et al. 1998).

### 1.3.1 Biosynthesis of statins

Statins reduce cholesterol levels mainly through blocking the rate-limiting step of the mevalonate pathway. This indicates that statins inhibit HMG-Co A reductase, which catalyzes HMG-Co A to mevalonate. However, the mevalonate pathway involves not only cholesterol synthesis, but also isoprenylated proteins, dolichol, and ubiquinone. These play important roles in several cellular functions, such as maintaining the cellular membrane structure and integrity; the synthesis of glycoproteins, steroid hormones, and bile acid; cell signaling; and mitochondrial respiration (Goldstein and Brown 1990; Edwards and Ericsson 1999). Thus, statins may influence all of the downstream products of the mevalonate pathway and their functions. Figure 1-5 shows the mevalonate pathway and its downstream products.

**Figure 1-5 Mevalonate pathway and mechanism of HMG-Co A reductase inhibitors (statins) (Chan, Oza et al. 2003)** (reproduced with the permission of the publisher)

### 1.3.2 Pharmacology of lovastatin

Lovastatin is a natural type of statin that is derived from a fungus. It is activated in the liver to become β-hydroxy acid. Compared with other statins, the concentration of lovastatin is relatively higher in the liver than in peripheral tissues (Germershausen, Hunt et al. 1989). This may be related to its lipophilic

property, which allows it to cross the blood-brain barrier and the placental barrier (Chan, Oza et al. 2003). The clearance route of lovastatin differs across species. β-oxidation is the major pathway for lovastatin metabolism in rodents, whereas the oxidation of CYP3A4, a member of the cytochrome P-450 (CYP-450) superfamily, is the primary route in humans and dogs (Halpin, Ulm et al. 1993). In the latter, the increased serum level of lovastatin may be due to the inhibition of isozymes of CYP.

### 1.3.3 Clinical uses of statins

As mentioned, statins can inhibit all of the downstream products of the mevalonate pathway, such as isoprenoids (farnesyl pyrophosphate (FPP) and geranylgeranylpyrophosphate (GGPP)). These isoprenylated proteins play crucial roles in the post-translational modification and isoprenylation of small GTP-binding proteins (such as Ras, Rho, Rac and Rap) (Jackson, Ericsson et al. 1997). Thus, statins may decrease the serum cholesterol level, and at the same time may regulate the balance between proliferation and apoptosis, inflammatory chemokines, and cytogenic messages. These findings indicate that statins may be effective for both cholesterol-mediated and non-cholesterol-mediated diseases, and may have pleiotropic effects (Wang, Liu et al. 2008).

The main application of statins is in the treatment of cardiovascular disease. Several multicenter studies have confirmed the efficacy of statins in both the

primary and secondary prevention of coronary artery disease. This is due to the ability of statins to directly down-regulate the serum LDL level, stabilize atheromatous plaque, improve endothelial function, reduce the inflammatory response, and decrease thrombogenicity (Wang, Liu et al. 2008). In addition, statin therapy may be used to treat metabolic syndrome (MtS) and diabetes mellitus (DM) by lowering the blood pressure, improving coronary collateral circulation, modulating glucose metabolism, and enhancing insulin sensitivity (Massy and Guijarro 2001). At the same time, statins may reduce the incidence of cardiovascular disease in the DM population (Nash 2005).

In addition to being used to treat cholesterol-mediated diseases, statins are also a possible medicine for other chronic diseases, such as osteoporosis and rheumatoid arthritis (RA). It has also been reported that lovastatin may stimulate bone formation and improve bone mineral density. However, the mechanism of statin-modulated bone formation is not clear (Edwards and Spector 2002). The properties of statins, including their immunomodulatory and anti-inflammatory effects, may render them an effective treatment for RA. Preliminary clinical data have suggested the efficacy of statins for RA patients, but larger and multicenter clinical studies are needed for confirmation (Turesson, Jacobsson et al. 2008)

Recent epidemiological studies suggest that statins may also benefit patients with neurological diseases (Willey and Elkind 2010). In addition to

cerebrovascular disease, statins also show potential beneficial effects for Alzheimer's disease (AD), Parkinson's disease (PD), and multiple sclerosis (MS). It has been reported that lovastatin decreases the incidence of AD through the down-regulation of the neuron toxicant β-amyloid (Aβ) in the blood (Wolozin 2002). Statins may be suitable for the treatment of PD and MS due to their anti-inflammatory and immunomodulatory properties (Wahner, Bronstein et al. 2008). However, the long-term clinical efficacy and exact mechanisms still needed to be investigated.

Statins have attracted renewed attention recently for their anti-tumour properties. Patients treated with statins have a lower incidence of tumour (Blais, Desgagne et al. 2000), and many retrospective studies have shown that statin therapy may be useful in preventing several kinds of cancers, such as glioblastoma, colorectal cancer, prostate cancer, breast cancer, lung cancer, and pancreatic cancer (Gauthaman, Fong et al. 2009). In addition to investigating the individual effects of statins in cancer therapy, scientists are trying to determine the joint effects of statins when used with other drugs. Thiazolidinediones, gefitinib, BCNU (*N,N'*-bis(2-chloroethyl)-*N*-nitrosourea), and β-interferon have all been tested for their ability to enhance the anti-tumour effect of statins in glioma (Tapia-Perez, Sanchez-Aguilar et al. 2010). However, the findings are contradictory, with some studies indicating that there is no association between statin treatment and cancer development (Hebert, Gaziano et al. 1997).

### 1.3.4 Potential anticancer mechanisms of statins

Both *in vitro* and *in vivo* studies show that statins have anti-proliferation and apoptosis-regulating properties. It is also known that statins inhibit the synthesis of cholesterol and FPP, GPP, and dolichol. The down-regulation of dolichol by statins inhibits cell growth and DNA synthesis (Wejde, Hjertman et al. 1998). At the same time, the decrease in FPP and GPP makes the small GTP-binding proteins, such as Rho, Rac, and Ras, inactive. These G proteins are crucial factors in cell proliferation, differentiation, and apoptosis prevention, and are always more highly expressed in cancer tissues (Hindler, Cleeland et al. 2006). Statins also arrest cells in the S phase through the down-modulation of cyclin-dependent kinases or the up-modulation of the cyclin-dependent kinase inhibitors p21 and p27 (Lee, Ha et al. 1998). In addition, statins induce apoptosis not only by reducing G proteins, but also by up-regulating proapoptotic proteins (such as Bax and Bim) and down-regulating antiapoptotic proteins (such as Bcl-2) (Cafforio, Dammacco et al. 2005). The changes in these molecules indicate that statins induce apoptosis mainly via the mitochondria.

New blood vessels can always be found in tumour tissues to provide oxygen and nutrients. Thus, antiangiogenesis is an important mechanism for inhibiting tumour growth. The efficacy of antiangiogenesis by the application of statins differs depending on the type and concentration of statin used (Weis, Heeschen et al. 2002). Low doses of statins raise angiogenesis via the sensitization of endothelial nitric oxide synthase (eNOS). High-dose statins achieve

antiangiogenesis by blocking the vascular endothelial growth factor (VEGF), decreasing endothelial cell growth, and inhibiting the connection with the extracellular matrix (Frick, Dulak et al. 2003).

The final potential mechanism by which statins may depress cancer development is through the inhibition of tumour metastasis. Increasing numbers of studies confirm that statins affect this process via the down-regulation of E-selectin and matrix metallo-proteinase-9, which are important for endothelial adhesion (Wang, Lin-Shiau et al. 2000; Nubel, Dippold et al. 2004). Furthermore, statins may also mediate epithelial growth factor-induced invasion and restrain tumour migration (Kusama, Mukai et al. 2001).

## 1.4 Nuclear factor-kappa B (NF-κB) pathway

NF-κB (nuclear factor kappa-light-chain-enhancer of activated B cells) is a protein complex that controls the transcription of DNA. It was identified in 1986 (Sen and Baltimore 1986) as a nuclear factor that binds the light chain enhancer in B-cells and plays a role in immune responses. Originally, it was thought that NF-κB was required mainly for B-cell development and maturation, but recently it has been found to play a role in many other cellular processes. It is involved in cellular responses to stimuli such as stress, cytokines, free radicals, and bacterial or viral antigens. It is also persistently active in many disease states, such as arthritis, asthma, neurodegenerative diseases, heart disease, and

cancer. Its signaling transduction pathway in apoptosis is a hot topic in cancer research.

### 1.4.1 Structures of NF-κB

Five DNA binding members of the NF-κB family have been identified in humans. These include p65 (also called RelA), c-Rel, RelB, p50, and p52. They can be divided into two classes based on the sequences C-terminal to the RH domain. All of them share a Rel homology domain in their N-terminus. The members of the first class have long C-terminal domains that act to inhibit such molecules as p105 and p100. p50 is derived from p105, and p52 comes from p100. Both lack the trans-activation domain. Generally, members of this class are not activators of transcription. The second class (the Rel proteins) includes RelA, RelB, and c-Rel, which have a transactivation domain in their C-termini and are often not conserved at the sequence level across species, although they can activate transcription in a variety of species. Transcription by NF-κB is carried out upon DNA binding of the dimers of these five DNA binding subunits of the family (Ghosh and Karin 2002). Each dimer has a distinct DNA binding site specificity.

NF-κB activity is chiefly regulated by interaction with a second family of proteins called IκB proteins, which act as inhibitors. Like the NF-κB proteins, there are several kinds of IκB proteins, all of which have different affinities for the corresponding NF-κB family members, and are expressed in a tissue-specific manner and regulated individually (Perkins 1997; Totzke, Essmann et

al. 2006). The IκB proteins include p105, p100, IκB $\alpha$, IκB $\beta$, IκB $\gamma$, IκB $\varepsilon$, IκB $\zeta$, Bcl-3, and the Drosophila Cactus protein. The interaction of an IκB protein with NF-κB has two results: it either blocks DNA binding or causes the complex to be localized primarily in the cytoplasm. Many signals, such as cytokines, growth factors, and viral infections, can activate NF-κB complexes by targeting IκB for degradation. This pathway enables NF-κB to enter the nucleus, bind to DNA, and regulate gene transcription (Jacobs and Harrison 1998). The most commonly used molecular inhibitor of NF-κB activation is the IκBα super-repressor, and kinase-dead IKKα and β mutants can act as dominant-negative blockers of NF-κB activation (Muenchen, Lin et al. 2000; Massa, Li et al. 2005). Various chemicals, natural products, and small molecules, which appear to act as anti-tumour agents by inhibiting the activation of IKK or DNA binding by NF-κB, have been the focus of recent research (Harikumar, Sung et al. 2010).

The importance of NF-κBs in regulating cellular responses lies in their membership of the category of "rapid-acting" primary transcription factors. This makes NF-κB act as "first responder" to harmful cellular stimuli. The stimulation of a wide variety of cell-surface receptors, such as RANK and TNFR, leads directly to NF-κB activation and fairly rapid changes in gene expression (Theill, Boyle et al. 2002).

### 1.4.2 NF-κB and cancers

It has been found that NF-κB plays a key role in regulating the immune response to infection, and increasing attention is thus being paid to the role of NF-κB in cancer (Dolcet, Llobet et al. 2005).

Genetic alterations in NF-κB genes have been identified in several human cancers. Clinical studies have shown that NF-κB overexpression is associated with the progression of several cancers, such as breast cancer, colon cancer, and lymphoid cancers (Aranha, Borralho et al. 2007). Thus, the inhibition of NF-κB may be a novel therapeutic approach for cancer treatment, in the same way as has been for inflammatory bowel disease (Egan and Toruner 2006).

In some normal cells, NF-κB is constitutively located in the nucleus. In many cancer cells (including breast cancer, colon cancer, prostate cancer, and lymphoid cancers), NF-κB is constitutively active and is also located in the nucleus. In some cancers, this is due to the chronic stimulation of the IKK pathway, whereas in others the gene encoding IκB may mutate and become defective. Many multiple myelomas have mutations in the genes encoding NF-κB signaling regulatory proteins that cause the constitutive activation of NF-κB. Some researchers believe that continuous nuclear NF-κB activity protects cancer cells from apoptosis, and in some cases stimulates their growth. The resistance of cancer cells to chemotherapy and radiotherapy has already been

attributed to NF-κB. For example, resistance to CPT-11 can be overcome by the inhibition of NF-κB in colorectal cancer cells *in vitro* and *in vivo* (Cusack, Liu et al. 2000). It has also been found that radiation induces NF-κB activation, and that the inhibition of this radiation-induced NF-κB activation is sufficient to increase apoptosis (Russo, Tepper et al. 2001). Many proteins, such as Bcl-2, TRAF, and JNK, are known to play a role in the NF-κB signaling pathway in its anti-apoptotic function. The exact mechanism remains unclear, yet the indications are that inhibitors of NF-κB signaling may have uses in both the prevention and treatment of cancer. For cancer prevention, such inhibitors may exert effects as anti-inflammatory agents. For treatment, current anti-tumour therapies seek to block NF-κB activity as a means of inhibiting tumour growth or sensitizing the tumour cells to chemotherapy or radiotherapy. In cancer treatment, NF-κB inhibitors may have a use either as primary treatment agents or as adjuvant therapeutics. Anti-NF-κB inhibitors may act as adjuvant therapeutics for cancers in which constitutive NF-κB activity has an anti-apoptotic (survival) function in tumour cells.

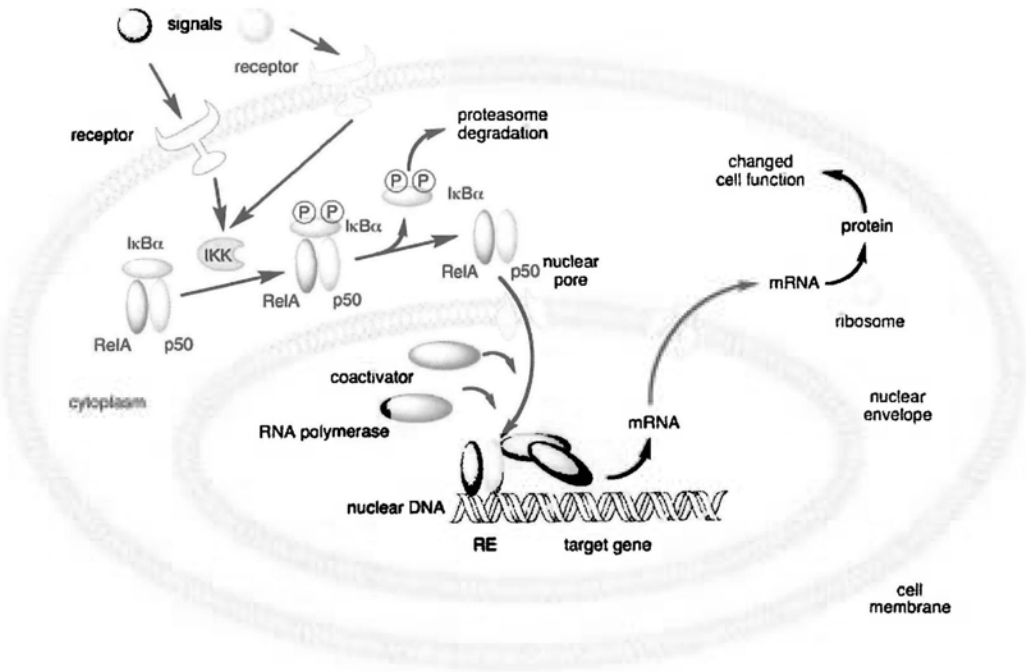


**Figure 1-6 Mechanism of the NF-κB pathway**

### 1.4.3 NF-κB and glioma

The NF-κB family has been implicated in the development of many human cancers, and more recently has been a target for molecular intervention for several cancers, including glioma. The NF-κB signaling pathway is activated in a large proportion of GBMs (Nagai, Washiyama et al. 2002), which enables GBMs and other cancer cell types to resist cytotoxic insults (Aggarwal 2004).

It has been demonstrated that invasive malignant glioma cells show a decrease in proliferation rate and a relative resistance to apoptosis, which may contribute to their resistance to chemotherapy and radiotherapy. As mentioned, the NF-κB signaling cascades play a critical role in the regulation of gene expression and prevention of apoptosis. Components of these pathways mutate or are aberrantly expressed in glioblastomas. One study (Weaver, Yeyeodu et al. 2003) found that after inserting a mutant inhibitor of NF-κB into GBM cells, the cells were more susceptible to death by chemotherapy through increased apoptosis. Another study (Otsuka, Nagaya et al. 1999) found that the inhibition of NF-κB activation confers sensitivity to TNF alpha via the impairment of the cell cycle progression in human glioma cells. The inactivation of chemotherapy-induced NF-κB activation by drugs not only restores the sensitivity of GMB cells to apoptosis, but also interferes with their migratory processes (Lefranc, Brotchi et al. 2005).

## 1.5 Perspective

Glioblastoma multiforme (GBM), or glioblastoma, is the most common type of primary brain tumour in adults. It is characterized by rapid growth, aggressive infiltration, and resistance to treatment. The therapeutic regime for glioblastoma is constantly being modified. However, the efficacy of the various treatments is not satisfactory, and leads to a low survival rate. A more effective therapy is thus urgently needed. The past decade has seen the introduction of TRAIL and extensive interest in its application due to its targeted toxicity to cancer cells. However, several cancer cells, including glioblastoma cells, are resistant to

TRAIL attack. Researchers are thus trying to find a substance that will sensitise cells to TRAIL. At present, chemotherapy and radiotherapy are the most common used strategy to sensitise tumour cells to TRAIL attack (Kim, Oh et al. 2010; El Fajoui, Toscano et al. 2011). However, chemotherapy and radiotherapy still showed marked harm to normal tissues. Therefore, the other sensitisers which are safe to normal tissue are being sought.

Lovastatin is a safe drug that is widely used in clinic for lowering cholesterol. It can cross the brain blood barrier, and has been studied for the treatment of several neurological diseases. It has been proven that lovastatin has anti-tumour properties by inducing apoptosis (Tapia-Perez, Sanchez-Aguilar et al. 2010). In this project, we investigated lovastatin-induced apoptosis in different human GBM cell lines.

It is known that TRAIL-induced apoptosis occurs mainly via the extrinsic pathway, whereas lovastatin-induced apoptosis occurs through the intrinsic pathway. We hypothesize that the combination of TRAIL and lovastatin may have a synergistic apoptotic effect on GBM cells, and discuss how this might work and whether it might be a potential treatment strategy for GBM patients. Finally, we investigate the antitumour effect of lovastatin and TRAIL on subcutaneous brain tumour model.

# Chapter Two Establishment of cellular assessment platform for lovastatin-sensitised TRAIL-sensitization in GBM

## 2.1 Introduction

Glioblastoma is the most common malignant brain tumour, but has a poor prognosis. The median survival of patients with glioblastoma is only 14 months. Researchers are thus making a continuous effort to seek novel treatments. However, the outcomes of present therapies for glioblastoma are not satisfactory. The main barriers in the traditional treatment of glioblastoma are the diffuse infiltration of the brain and a high resistance to conventional cancer therapies (Laws, Parney et al. 2003).

Recently, the tumour necrosis factor-related apoptosis inducing ligand (TRAIL) and lovastatin were introduced as separate antitumour agents. Neither is a traditional antineoplastic drug, but both have been widely studied in several cancers. However, the antitumour efficacy of each drug by itself is unsatisfactory, and they are usually combined with other therapies, such as chemotherapy and radiotherapy, to amplify its own effect. But the serious side effects are accompanied. A new regime that comprises a combination of TRAIL and lovastatin was first reported by our laboratory (Chan, Chen et al. 2008). Our previous study demonstrated that three human glioblastoma cell lines (M059J, M059K, and A172) show moderate to severe resistance to TRAIL, but that TRAIL-induced apoptosis in these cells is sensitised by lovastatin, which may arrest the cells in the G0/G1 phase.

In this project, the grade IV glioblastoma cell lines U87 MG and T98G were newly enrolled. We determined the effect of a combination of TRAIL and lovastatin on grade IV human glioblastoma cell lines.

## 2.2 Materials and Methods

### 2.2.1 Cell lines and cell cultures

A172, M059J, M059K, U87 MG, and T98G were purchased from the American Tissue Culture Collection (ATCC). They were all malignant glioblastoma cells that belong to different pathological stages. A172 was isolated from the tumour of a 53-year-old male and cultured in Dulbecco's modified Eagle's Medium (DMEM) (Gilbo, Grand Island, NY). Both the M059J and M059K cell lines were derived from the same male patient, who was 33 years old and had not received treatment. M059J cells lack DNA-dependent protein kinase activity, whereas M059K express normal levels of this enzyme. These two cell lines were cultured in Dulbecco's modified Eagle's Medium (DMEM)/F12 medium (Gibco, Grand Island, NY).

U87 MG and T98G are GBM, and are classified as grade IV glioblastoma cells. The former were isolated from a 44-year-old female patient, and the latter from a 61-year-old male. Both cell lines were maintained in Eagle's Minimum

Essential Medium (MEM) (Gibco, Grand Island, NY). All of the media were supplemented with 10% fetal bovine serum (FBS) (HyClone, Logan, UT), 100U/mL of penicillin, and 100g/mL of streptomycin (Gibco, Grand Island, NY) and the cells were cultured at 37°C with 5% $CO_2$/95% air. The media were changed every two to three days. When the confluence reached around 90%, cells was passaged using 0.05% Trypsin-EDTA (Gibco, Grand Island, NY).

### 2.2.2 Cell viability as measured by MTT assay

MTT (3-(4,5-dimethylthiazol-2-yl)-2,5-diphenyltetrazolium bromide) is a tetrazolium salt that can be converted into a formazan product by living cells. The absorbance of formazan is thus used as a measure of cell viability.

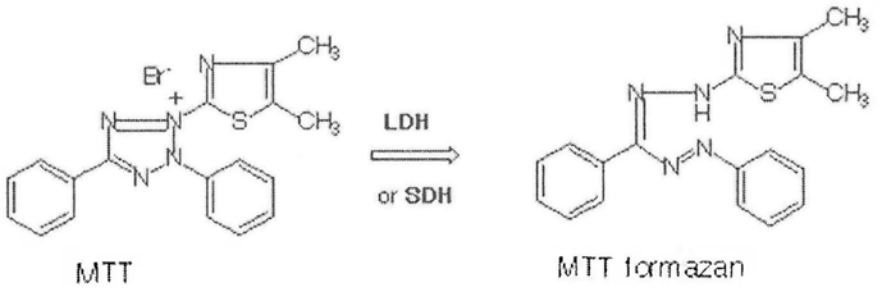


**Figure 2-1 Principle of the MTT assay**

Five thousand cells were seeded into 96-well plates with appropriate complete medium. After cell attachment, the cells were treated with different

concentrations of lovastatin (TRC Inc., Ontario, Canada) (0 μM, 0.625 μM, 1.25 μM, 2.5 μM, 5 μM, 10 μM, and 20 μM) with and without 100 ng/ml TRAIL (PeproTech, Rocky Hill, NJ) for 24, 48, and 72 hours.

After the incubation period, the medium was discarded and 100 μl of working MTT solution (Promega, USA) was added into each well. The cells were then incubated at 37°C in 5% $CO_2$ for three hours. After the three hours, the MTT solution was changed and an equal volume of DMSO (Sigma-Aldrich, St. Louis, MO) was used to dissolve the formazan crystals. The plate was shaken gently and the absorbance was measured at 570 nm with a reference of 630 nm using a microplate (ELISA) reader (Spectra Rainbow, TECAN).

Calculation of cell viability

= (Absorbance of the treatment / Absorbance of the control) ? 100%

### 2.2.3 Cell proliferation as measured by BrdU cell proliferation assay

The BrdU cell proliferation assay is another traditional method of detecting cell proliferation. BrdU, which is a thymidine analog, is used to alternate [3]thymidine, and is incorporated into newly synthesized DNA strands of S phase cells. The amount of BrdU thus indicates the number of live cells. A

CHEMICON®'s BrdU Cell Proliferation Assay Kit (CHEMICON, Temecular, CA) was used in this experiment.

Briefly, 5000 cells were seeded into 96-well plates and treated with different concentrations of Lovastatin (0 μM, 0.625 μM, 1.25 μM, 2.5 μM, 5 μM, 10 μM, and 20 μM) with and without 100 ng/ml of TRAIL for 48 hours. At four hours before the end of the treatment, BrdU solution was added to each sample. The plate was then incubated at 37°C until the treatment was complete. At the end of the treatment, the medium was discarded and Fix Solution was added to fix the cells for 30 minutes at room temperature. Subsequently, anti-BrdU mouse monoclonal antibody was used to detect the BrdU in the cells. Goat anti-mouse IgG-peroxidase conjugated secondary antibody, substrate, and stop solution were then added gradually. Finally, the plate was measured at 450 nm with a reference of 595 nm.

### 2.2.4 Cell cycle measured by propidium iodide staining

The total nuclear DNA content and the fraction of cells in each phase of the cell cycle can be detected from the binding of PI and DNA. 2? $0^5$ cells were seeded into a 60mm dish for 24 hours. The cells were treated with different concentrations of Lovastatin (0 μM, 1.25 μM, 5 μM, and 20 μM) for 48 hours. At the end of the treatment, the cells were collected by trypsin, washed in PBS, and fixed in 70% cold ethanol. The samples were kept at -20°C overnight. On the second day, the samples were centrifuged and washed in PBS. Cell pellets were mixed with PI and RNase A in the dark for 30 minutes. After incubation,

the cell cycle distribution was determined and 20,000 cells were counted for each group.

### 2.2.5 Apoptosis as measured by annexin V and propidium iodide (PI) staining

Annexin V/PI staining is a widely used method for distinguishing live cells, apoptotic cells, and dead cells according to their characteristic morphological and biochemical changes. A green fluorescence can be detected in apoptotic cells, indicating that phosphatidylserine (PS) has been translocated from the inner to the outer leaflet of the plasma membrane and the cell membrane is intact. Conversely, the disruption of the cell membrane in dead cells leads the PI to bind tightly to nucleic acids. Dead cells show a red and green fluorescence.

2? $0^5$ cells were seeded into a 60-mm dish 24 hours in advance of the experiments. The cells were treated with vehicle-DMSO, 100 ng/ml of TRAIL, 20 μM of lovastatin, and 100 ng/ml of TRAIL plus 20 μM of lovastatin. The collected cell pellets were washed in PBS and stained with annexin V fluorescence dye (Molecular Probe, Eugene, OR) and PI (Molecular Probe, Eugene, OR) in the dark at room temperature for 30 minutes. The cells were then mixed with binding buffer (10 mM of HEPES/NaOH, 140 mM of NaCl, 2.5 mM of $CaCl_2$, pH 7.4) and analyzed by flow cytometry.

### 2.2.6 Statistical analysis

The data were presented as the mean ? one standard deviation (SD) for at least three separate determinations for each group. Differences between the groups were examined for statistical significance using a Student's *t*-test or one-way ANOVA followed by a Student's *t*-test. $P<0.05$ was used to indicate a statistically significant difference.

## 2.3 Results

### 2.3.1 Cell morphology after treatment with lovastatin or TRAIL

Different morphologies of the U87 MG cells were found after treatment with lovastatin or TRAIL for 48 hours (Figure 2-2A-D). Compared with the normal U87 MG cells, the morphology was not significantly altered when the cells were treated with 100 ng/ml of TRAIL. However, obvious shrinkage, condensation, and a spherical shape were found in the cells in the 20μM lovastatin group. When the cells were treated with 20 μM of lovastatin and 100 ng/ml of TRAIL in concert, a large number of cells were dead and had detached from the culture dish.

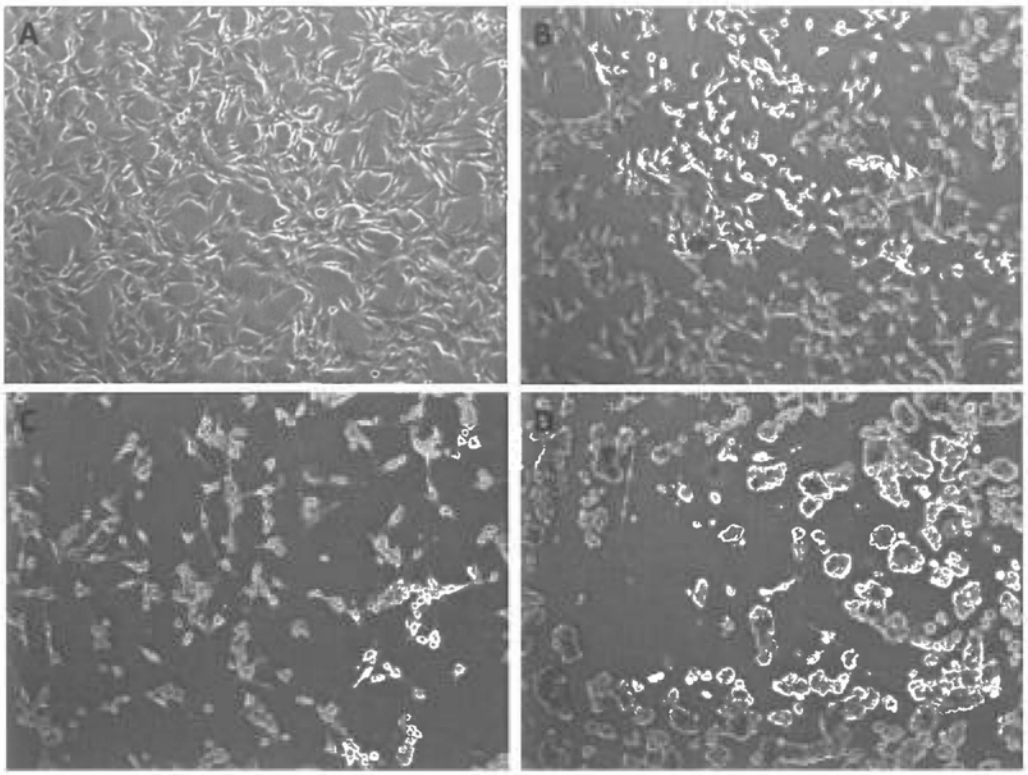


**Figure 2-2 Cell morphology after treatment with lovastatin or TRAIL**

The morphologies of the U87 MG cells were significantly changed by treatment with lovastatin with and without TRAIL. U87 MG control, 100 ng/ml of TRAIL, 20 μM of lovastatin, and 100 ng/ml of TRAIL plus 20 μM of lovastatin (A, B, C, and D respectively)

### 2.3.2 Cell viability as measured by MTT assay

MTT assay is a widely used method of determining the anti-proliferation effect of the various treatments. In this project, newly recruited human glioblastoma cell lines U87 MG and T98G were tested. The cell viability after culturing with TRAIL is shown in Figure 2-3. Compared with the control group, the cell viability was not significantly decreased by treatment with 100 or 200 ng/ml of TRAIL at 24 or 48 hours. Although the cell proliferation was inhibited by 200 ng/ ml of TRAIL at 72 hours, the difference was not statistically significant. The effect of TRAIL on T98G was also investigated. T98G was highly sensitive to TRAIL attack. Around 60% of the T98G cells were dead after treatment with 10 ng/ ml of TRAIL, and almost all of the T98G cells were dead after treatment with 100 ng/ ml of TRAIL.

A.

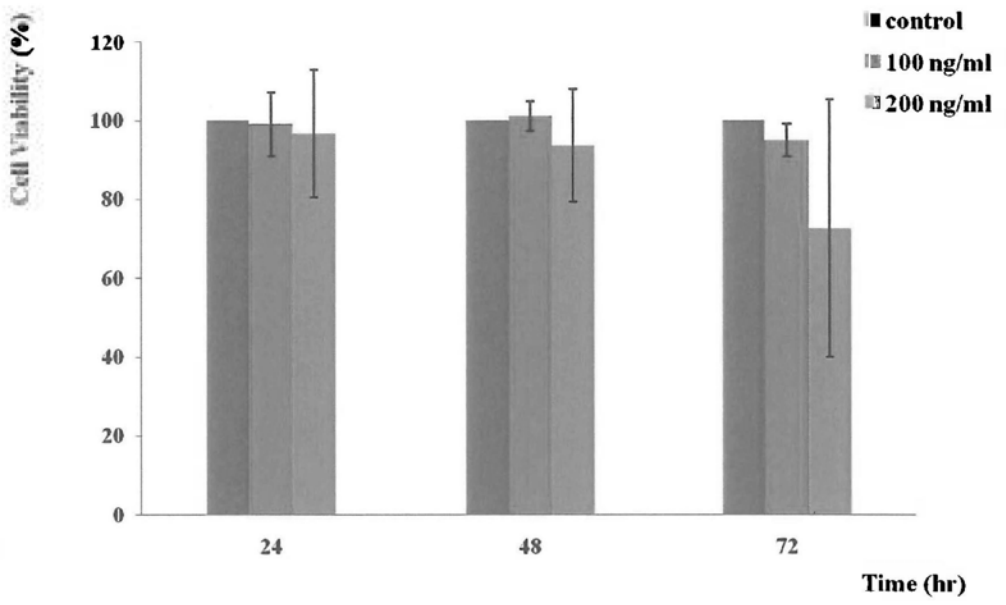

**B.**

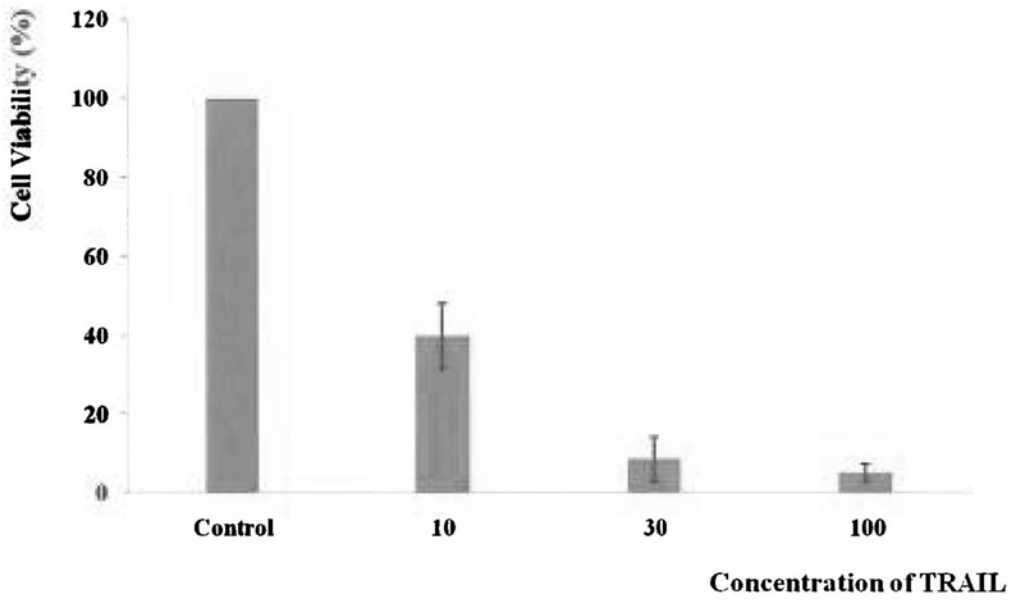


**Figure 2-3 Effect of TRAIL on cell proliferation**

U87 MG (A) was resistant to TRAIL attack, whereas T98G (B) was sensitive to TRAIL attack. Data are the mean ± one S.D. of three separate experiments.

The lovastatin-induced anti-proliferation effect was also observed in the U87 MG cells (Figure 2-4). There was no significant difference when the cells were treated with different concentrations of lovastatin at 24, 48, or 72 hours. However, the combined treatment (lovastatin with 100 ng/ml of TRAIL) significantly inhibited the proliferation of U87 MG, especially at 48 and 72

hours. The anti-proliferation trends at these two time points were similar, indicating that the cell death rate was not significantly increased after combined incubation for 48 hours. The data also show that TRAIL combined with higher concentrations of lovastatin triggered a faster rate of cell death than combination with lower concentrations of lovastatin (Figure 2-5). Figure 2-6 shows the synergistic effect of TRAIL and lovastatin on anti-proliferation compared with lovastatin alone at 48 hours.

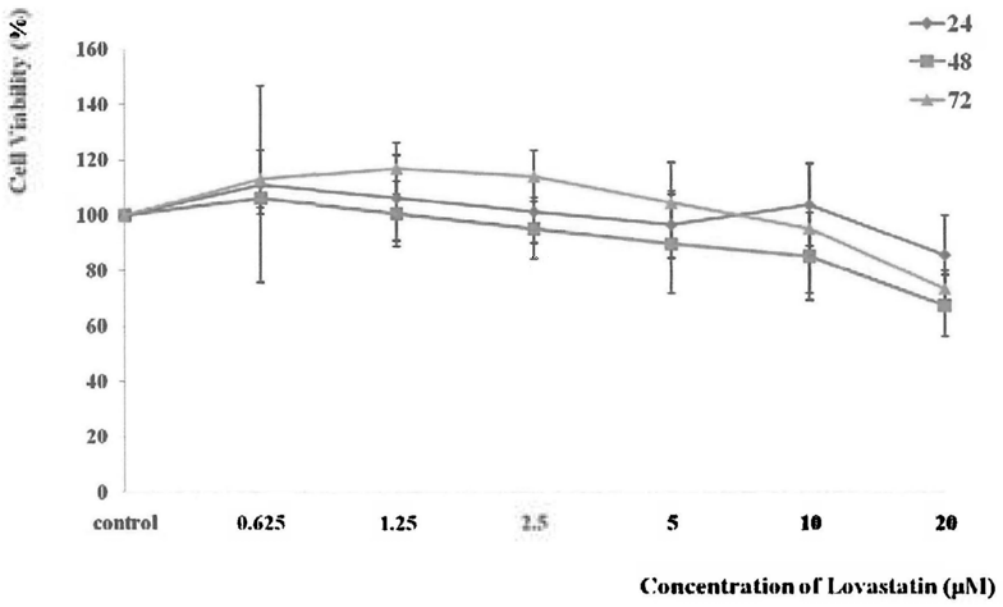


**Figure 2-4 Effect of lovastatin on cell proliferation**

After incubation with different concentrations of lovastatin, the cell proliferation did not change significantly at different time intervals (24, 48, and 72 hours). Data are the mean ± S.D. of three separate experiments.

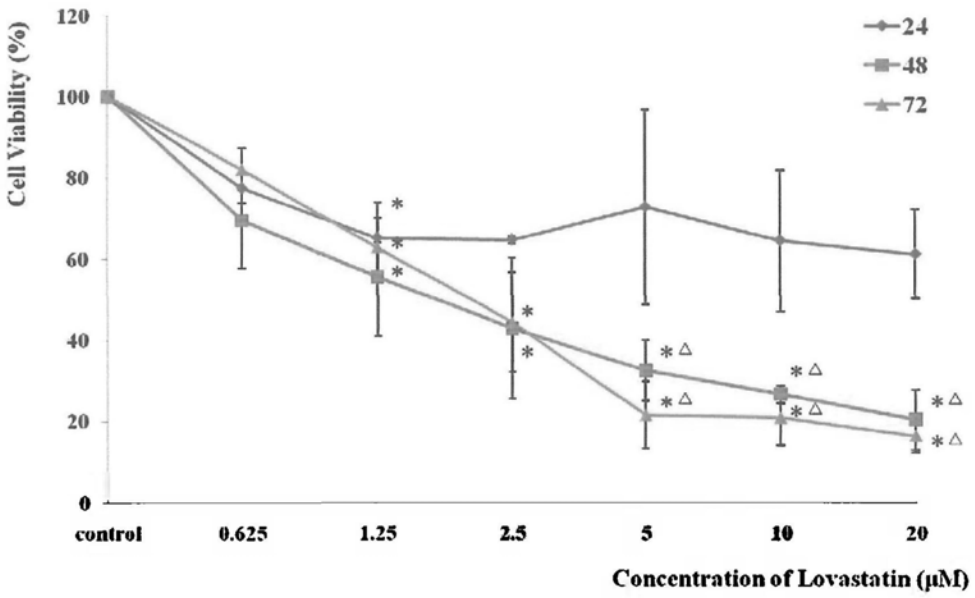


**Figure 2-5 Effect of lovastatin and TRAIL on cell proliferation**

Cell viability was detected by MTT assay at different time intervals (24, 48, and 72 hours). When cells were treated with lovastatin and TRAIL together, the number of live cells significantly decreased after incubation for 48 hours. In addition, TRAIL combined with higher concentrations of lovastatin induced a faster rate of cell death. Data are the mean ± S.D. of three separate experiments. * $p < 0.05$ when compared with the control group at each time point; $^{\triangle}$ $p < 0.05$ when compared with the data at 24 hours for each dose group.

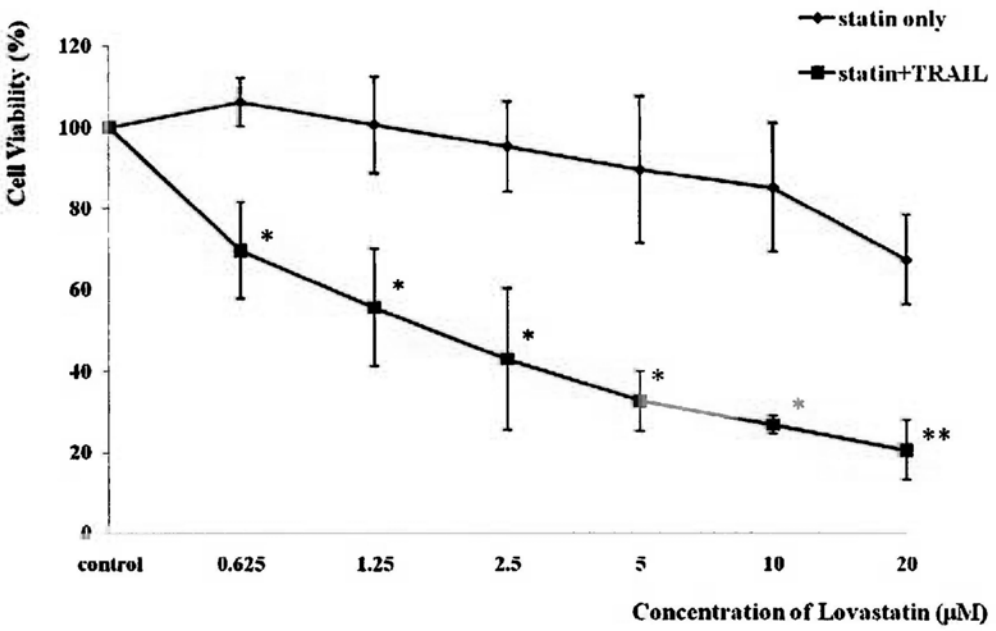


**Figure 2-6 Cell viability of U87 MG incubated with different concentrations of lovastatin with and without TRAIL for 48 hours.**

Compared with treatment with a single agent, cell viability was significantly decreased after treatment with lovastatin and TRAIL for 48 hours. Data are the mean ± S.D. of three separate experiments. * $p < 0.05$ when compared with the lovastatin only group.

### 2.3.3 Cell anti-proliferation effect as measured by BrdU cell proliferation assay

The cell cycle is the series of events that occurs in a cell that induces its division and duplication. In this cycle, the S phase is responsible for DNA synthesis and replication. BrdU assay can be used to determine the number of live cells by labeling newly synthesized DNA strands of the S phase cells. In this study, four human glioblastoma cell lines, A172, M059J, M059K, and U87 MG, were used to confirm the MTT results. All of the cells were treated with different concentrations of lovastatin (Vehicle-DMSO, 1.25 μM, 2.5 μM, 5 μM, 10 μM, and 20 μM) with and without 100 ng/ml of TRAIL for 48 hours. Compared with the lovastatin group, cell proliferation was significantly decreased by the combination of TRAIL and lovastatin in the four human glioblastoma cell lines, especially at medium to high doses of lovastatin (5 μM, 10 μM, and 20 μM). The results also revealed that TRAIL (100 ng/ml) induced around 20% cell death in the A172 cells, whereas the other cell lines were resistant to TRAIL treatment alone (Figure 2-7).

**A.**

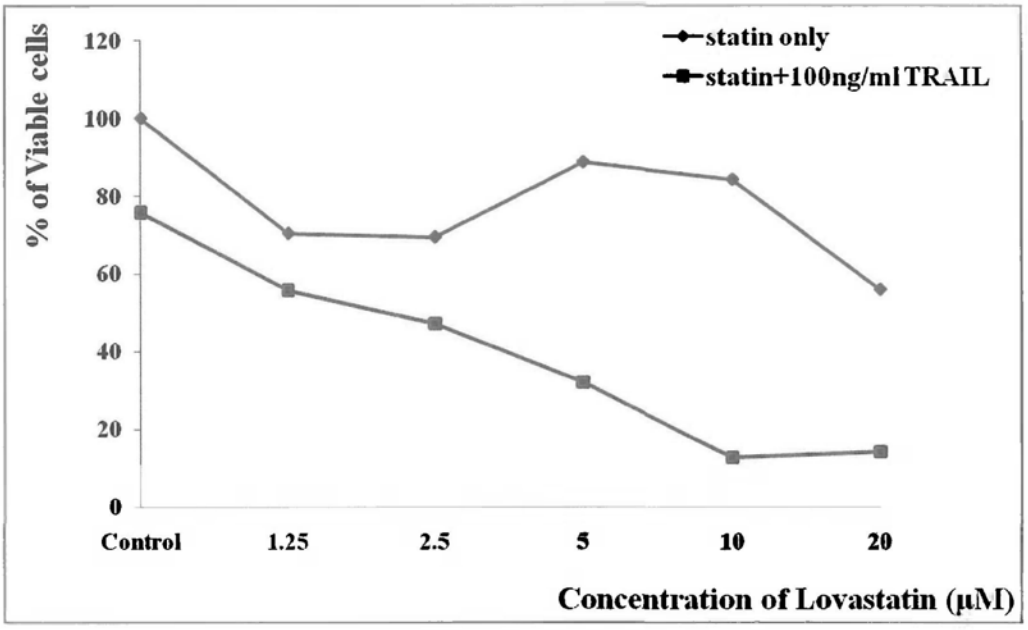
% of Viable cells
120
100
80
60
40
20
0
Control
1.25
2.5
5
10
20
Concentration of Lovastatin (µM)
statin only
statin+100ng/ml TRAIL

**B.**

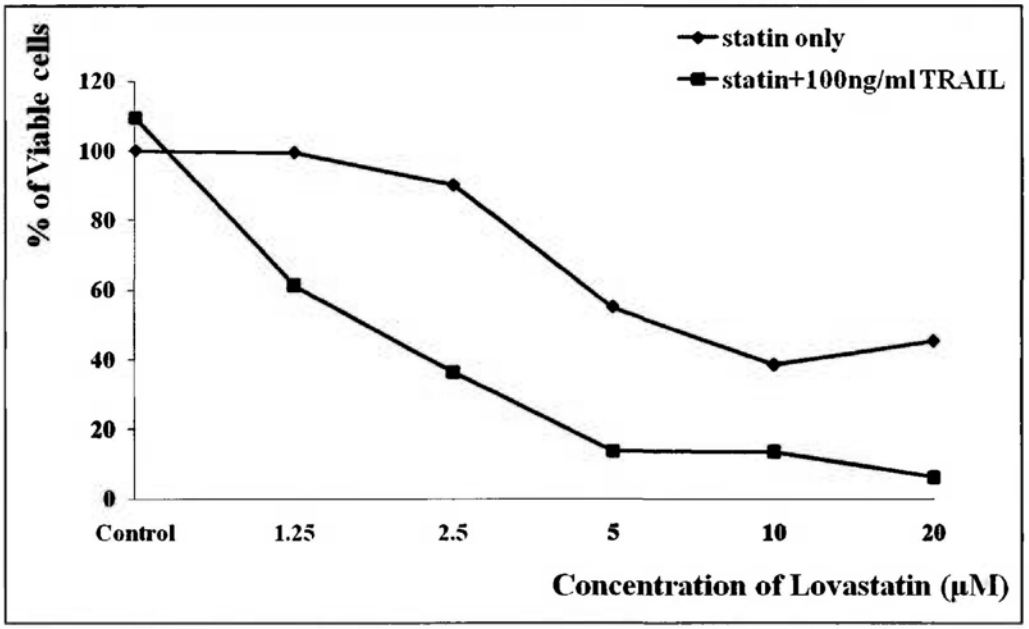
% of Viable cells
120
100
80
60
40
20
0
Control
1.25
2.5
5
10
20
Concentration of Lovastatin (µM)
statin only
statin+100ng/ml TRAIL

C.

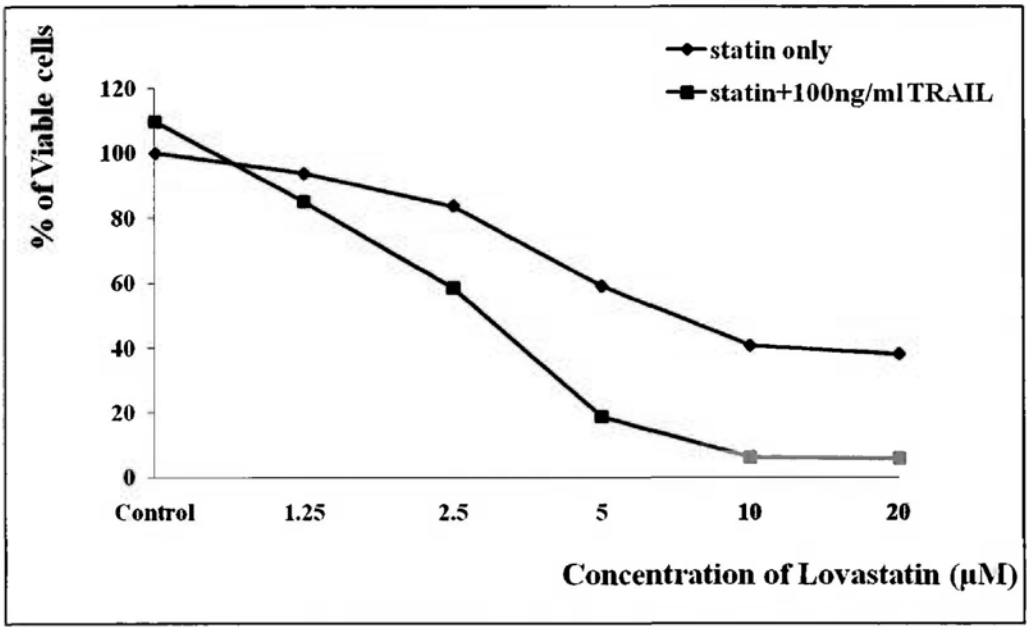
% of Viable cells
statin only
statin+100ng/ml TRAIL
120
100
80
60
40
20
0
Control
1.25
2.5
5
10
20
Concentration of Lovastatin (µM)

D.

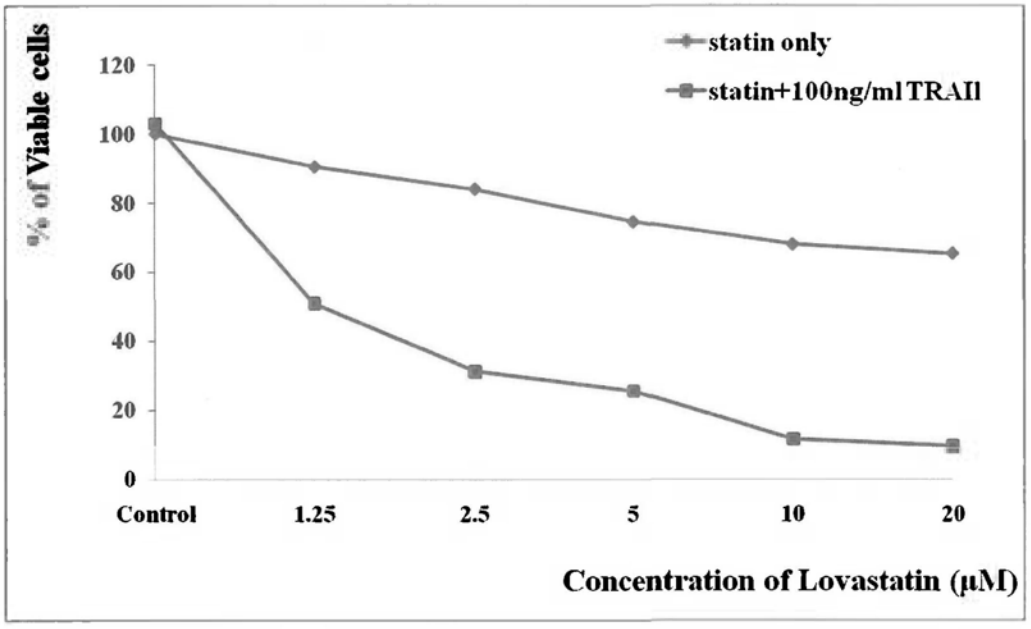
% of Viable cells
statin only
statin+100ng/ml TRAIl
120
100
80
60
40
20
0
Control
1.25
2.5
5
10
20
Concentration of Lovastatin (µM)

**Figure 2-7 Anti-proliferation effect of lovastatin alone versus lovastatin plus TRAIL for 48 hours.**

Cell death in the combined lovastatin and TRAIL groups was significantly greater than in the lovastatin only group for the A172 (A), M059J (B), M059K (C), and U87 MG (D) cells. Data are the mean ± S.D. of two separate experiments with similar trends.

### 2.3.4 Cell cycle analysis by PI staining

Screening PI stained cells by flow cytometry is a reliable method of classifying the different stages of cells. The U87 MG cells were treated with different concentrations of lovastatin (Vehicle-DMSO, 1.25 μM, 5 μM, and 20 μM) for 48 hours. The U87 MG cells in the G0/G1 phase were significantly increased by 16.0%, 32.0%, and 35.0% separately after incubation with 1.25 μM, 5 μM, and 20 μM of lovastatin.

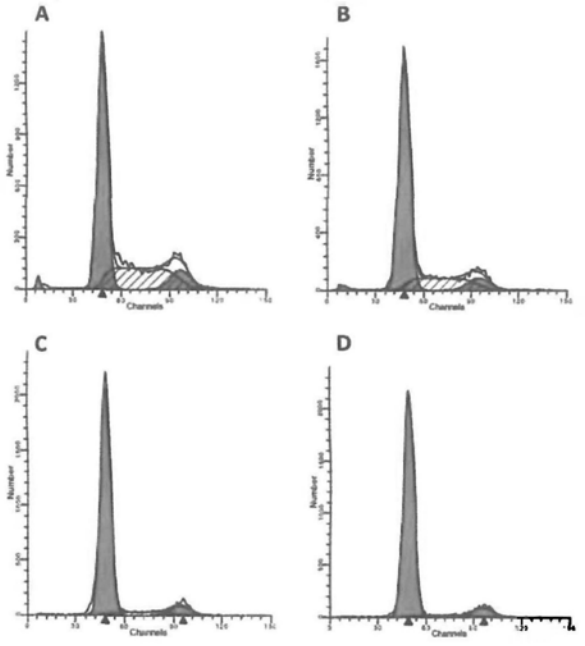
A
B
C
D
Number
Channels

E.

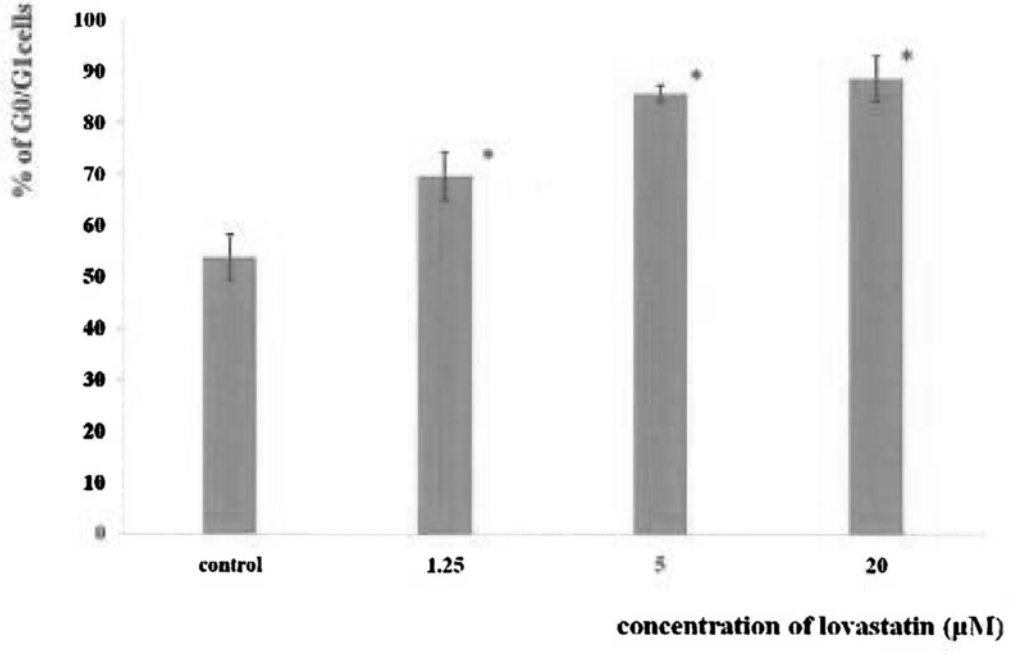
% of G0/G1cells
100
90
80
70
60
50
40
30
20
10
0
control
1.25
5
20
concentration of lovastatin (μM)

**Figure 2-8 Cell cycle determination on U87 MG cells**

When U87 MG cells were treated with lovastatin, the cells were arrested in the G0/G1 phase. The number of arrested cells in the control group (A) was significantly lower than the number of arrested cells in the 1.25 μM (B), 5 μM (C), and 20 μM (D) lovastatin groups. (E) Percentage of cells arrested after treatment with 1.25 μM, 5 μM, and 20 μM of lovastatin. Data are the mean ± S.D. of three separate experiments. * $p < 0.05$ when compared with the control group.

### 2.3.5 Apoptosis detected by Annexin V/PI staining

Our previous data showed that cell viability was decreased in cells treated with lovastatin and/or TRAIL. However, cell death occurs in two different modes: apoptosis and necrosis. Flow cytometry is the traditional measurement used to identify live cells, apoptotic cells, and necrotic cells by labeling with annexin V or PI. The newly enrolled cell lines, U87 MG and T98G, were analyzed after undergoing one of four treatments for 48 hours, including vehicle-DMSO, 100 ng/ml of TRAIL, 20 μM of lovastatin, and 20 μM of lovastatin plus 100 ng/ml of TRAIL. According to the flow cytometry results, the percentages of apoptotic cells in the U87 MG cells undergoing the four treatments were 1.69%, 5.44%, 12.59%, and 53.23%, respectively (Figure 2-9). Compared with the control

group, only the lovastatin group and lovastatin plus TRAIL group were statistically different. The T98G glioblastoma cells had 29.62%, 71.81%, 65.03%, and 87.97% apoptotic cells in the control, TRAIL, lovastatin, and lovastatin plus TRAIL groups (Figure 2-10).

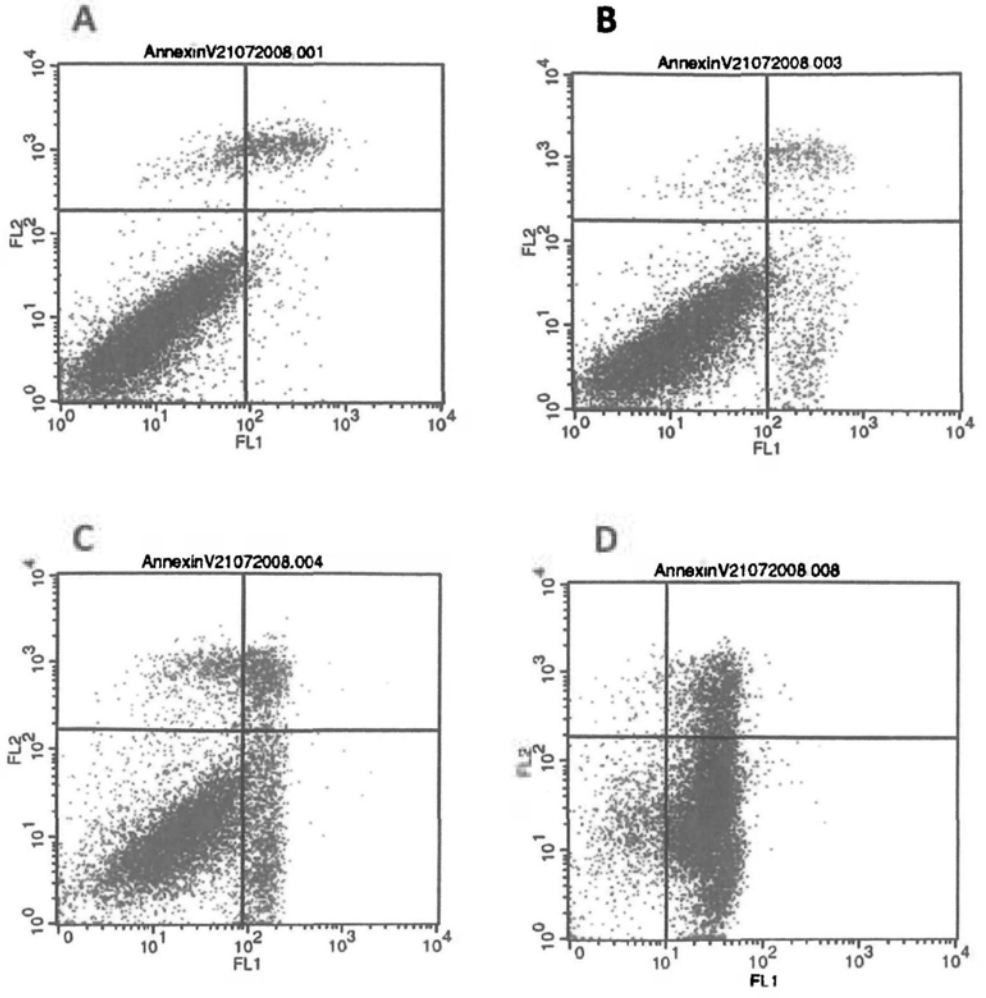

**E.**

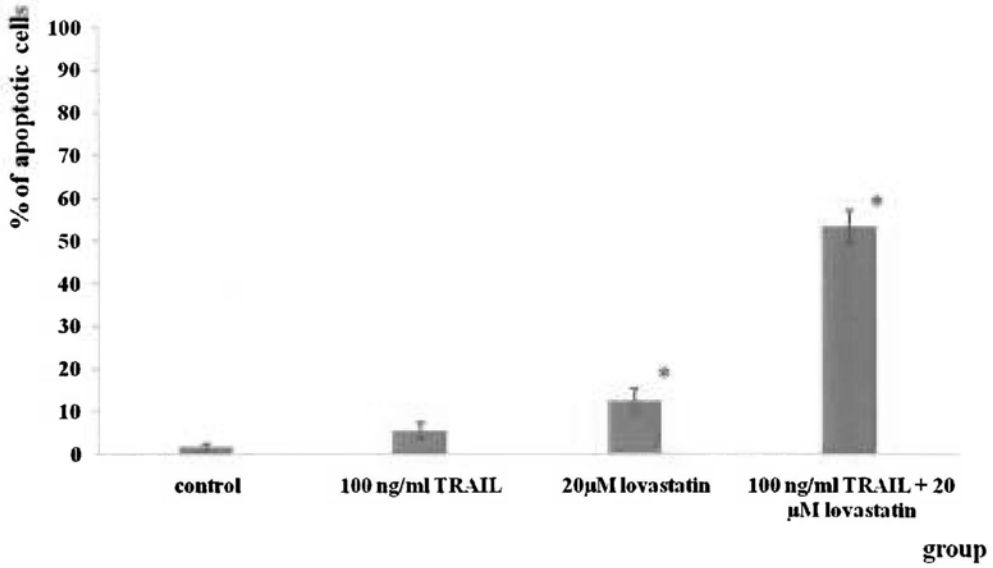


**Figure 2-9 Apoptosis detected by Annexin V/PI staining of U87 MG cells**

No statistical difference was identified between the control group (A) and TRAIL group (B). However, the other two treatments induced significant apoptosis in the U87 MG cells, especially in the TRAIL plus lovastatin group (C and D). (E) Percentage increase in apoptotic cells after treatment with lovastatin or lovastatin plus TRAIL. Data are the mean ± S.D. of three separate experiments. * $p < 0.05$ when compared with the control group.

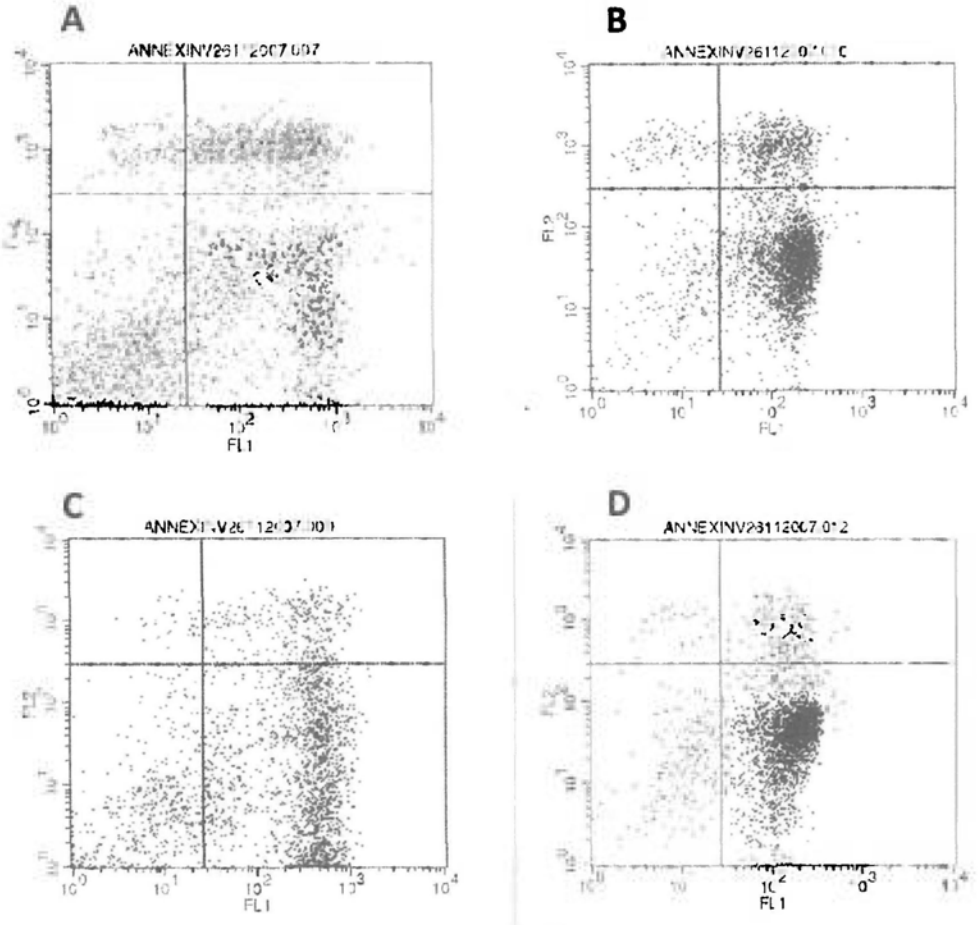
A
B
C
D
FL1
FL1

E.

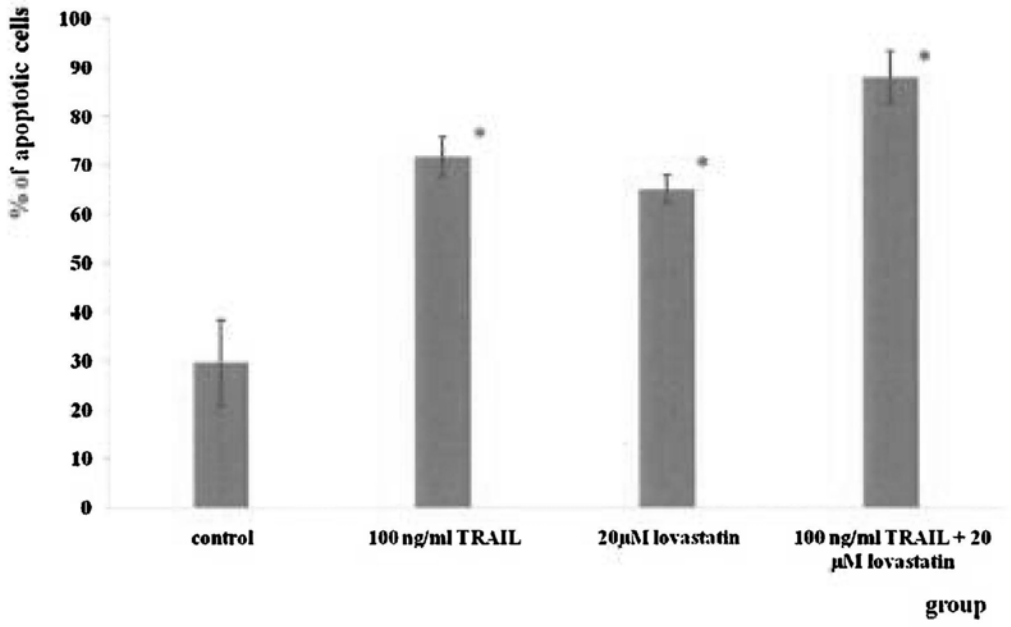


**Figure 2-10 Apoptosis detected by Annexin V/PI staining of T98G cells**

Unlike U87 MG, the apoptotic cells were significantly increased in all treatment groups, including TRAIL group (B) lovastatin group (C), and TRAIL plus lovastatin group (D). (E) Percentage of apoptotic cells in each treatment group in the T98G cells. Data are the mean ± S.D. of three separate experiments. * $p < 0.05$ when compared with the control group.

## 2.4 Discussion

It has been known that glioblastoma multiforme is the most common type of primary brain tumour and regards as one of the malignant tumour that the most difficult to cure. A suitable treatment that can significantly prolong the survival of glioblastoma patients remains elusive. Thus, translational researchers are constantly searching for new regimes and hope that the results will be useful for patients. The discovery of the tumour necrosis factor-related apoptosis-inducing ligand (TRAIL) was good news for cancer research. This ligand induces apoptosis in a wide range of cancer cells without harming normal cells. Unfortunately, several cancer cells, such as glioblastoma cells, pancreatic cancer, and melanoma, are resistant to TRAIL attack at different levels. It is thus important to find a reagent that can sensitise cells to TRAIL attack. The current strategies to enhance TRAIL sensitivity are chemotherapy and radiotherapy (Kim, Oh et al. 2010; El Fajoui, Toscano et al. 2011), but the severe side effects to normal cells are observed. Our previous work has demonstrated that lovastatin is a potential drug that can stimulate sensitivity to TRAIL (Chan, Chen et al. 2008). To our knowledge, this study represents the first time that TRAIL has been combined with a non-traditional anti-tumour drug for cancer therapy. In this project, two grade IV human glioblastoma multiforme cells lines, U87 and T98G, were newly recruited and used to demonstrate the effects of lovastatin and TRAIL on high grade glioma and determine the possible reason why lovastatin sensitises human glioblastoma cells to TRAIL attack.

According to the result of the MTT assay and flow cytometry, the T98G cells were sensitive to TRAIL-induced apoptosis, even at extra low doses. In contrast, the U87 MG cells were resistant to TRAIL attack, except for those in the high-dose group at 72 hours. As in other human glioblastoma cells that we have tested in the past, a lovastatin-induced anti-proliferation effect was observed in the U87 MG cells. The cell viability decreased to around 30% at high doses of lovastatin at 48 hours. However, the effect was limited, and was not statistically significant. The MTT assay and BrdU cell proliferation assay also showed the synergistic effect of TRAIL and lovastatin on U87 MG cells in a dose-dependent and time-dependent manner. However, the anti-proliferation effect of the combined treatment did not increase significantly between 48 and 72 hours of incubation. This may be related to the short half-life of TRAIL, which reduces the persistence of the anti-proliferation effect (Rozanov, Savinov et al. 2009). This indicates that the continuous administration of TRAIL may better than intermittent administration to provide a stable concentration of TRAIL in the blood.

Several previous studies have confirmed that lovastatin may arrest cells in the G0/G1 phase and then induce apoptosis in certain cancer cells, including colorectal cancer, prostate cancer, breast cancer, lung cancer, and pancreatic cancer (Gauthaman, Fong et al. 2009). These are important findings for cancer therapy, because not only statins are safe drugs that have been used in clinic for a long period, but also induce apoptosis without inflammatory response. Our

previous studies and this study reveal similar results in human glioblastoma cells using flow cytometry. In this study, we found U87 MG cells were arrested in G0/G1 phase by lovastatin in a dose dependent manner. Especially in high dose (20 μM) group, up to 90% of the U87 MG cells were arrested in the G0/G1 phase. Annexin V and PI double-staining is an easy and feasible method to detect the mode of cell death. In our project, we found lovastatin only produced 1.2 folds toxicity to TRAIL-induced apoptosis in TRAIL-sensitive T98G cells while 10 folds increase could be observed in TRAIL-resistant U87 MG cells. These results present that no obvious improvement could be found in TRAIL-sensitive GBM by TRAIL and lovastatin combination therapy. But lovastatin would be effective to treat TRAIL-resistant GBM, indicating that synergy of TRAIL and lovastatin might be a feasible regime to glioblastoma patients. However, the mechanism of TRAIL-induced attack by lovastatin is not clear and needs further investigation.

# Chapter Three How does lovastatin sensitise TRAIL-induced apoptosis in TRAIL-resistant GBM cells

## 3.1 Introduction

The tumour necrosis factor related apoptosis-inducing ligand (TRAIL) has been widely studied in the past 15 years. Due to its special property of targeting attacks on cancer cells without apparent damage to normal cells, TRAIL is regarded as a potential therapy for cancer patients (Wu 2009). However, its efficacy as a single agent is not satisfactory in many cancer cells. This may be due to TRAIL resistance, especially in certain highly malignant tumours such as pancreatic cancer (Hinz, Trauzold et al. 2000), melanoma (Fulda, Kufer et al. 2001), and neuroblastoma (Eggert, Grotzer et al. 2001). Thus, TRAIL is usually used as an adjuvant agent with radiotherapy, chemotherapy, or other treatment (Wu 2009). In the previous part, we have demonstrated that TRAIL and lovastatin in combination have a synergistic effect on human glioblastoma cells, indicating lovastatin can sensitise human glioblastoma cells to TRAIL-induced apoptosis. However, the mechanism of this phenomenon is not yet clear.

It has been known that the expression of death receptor is a major factor of TRAIL resistance (Srivastava 2001). We suppose that lovastatin sensitises TRAIL-induced apoptosis on human glioblastoma cells by dysregulating the expression of TRAIL receptor. Moreover, it has been reported that the NF-κB pathway possibly contributes to the mechanism of TRAIL resistance (Kavurma, Schoppet et al. 2008). Several studies have also reported that the expression of death receptors are regulated by the NF-κB pathway (Ravi, Bedi et al. 2001; Kwon, Choi et al. 2008; Lin, Ding et al. 2011). In addition, it has been

confirmed that lovastatin reduces NF-κB activity (Guijarro, Kim et al. 1996; Lin, Liu et al. 2005). We thus further hypothesize that lovastatin sensitises death receptor expression via the regulation of the NF-κB pathway. Furthermore, TRAIL induces apoptosis mainly through extrinsic pathway while lovastatin induces apoptosis via intrinsic pathway. Therefore, lovastatin sensitises TRIL-induced apoptosis might also due to the simultaneous triggering of the intrinsic and extrinsic apoptotic pathways, which amplify the apoptotic signal. In this part of the study, we mainly discuss the role of death receptor and NF-κB pathway in lovastatin-induced TRAIL attack.

## 3.2 Materials and Methods

### 3.2.1 Cell lines and cell cultures

A172, M059J, M059K, and U87 MG were purchased from the American Tissue Culture Collection (ATCC). They were all malignant glioblastoma cells that belong to different pathological stages. A172 was isolated from the tumour of a 53-year-old male and cultured in Dulbecco's modified Eagle's Medium (DMEM) (Gilbo, Grand Island, NY). Both the M059J and M059K cell lines were derived from the same male patient, who was 33 years old and had not received treatment. M059J cells lack DNA-dependent protein kinase activity, whereas M059K express normal levels of this enzyme. These two cell lines were cultured in Dulbecco's modified Eagle's Medium (DMEM)/F12 medium

(Gibco, Grand Island, NY). U87 MG is GBM cells which is classified as grade IV glioblastoma cells. It was isolated from a 44-year-old female patient and maintained in Eagle's Minimum Essential Medium (MEM) (Gibco, Grand Island, NY). All of the media were supplemented with 10% fetal bovine serum (FBS) (HyClone, Logan, UT), 100U/mL of penicillin, and 100g/mL of streptomycin (Gibco, Grand Island, NY) and the cells were cultured at 37°C with 5% $CO_2$/95% air. The media were changed every two to three days. When the confluence reached around 90%, cells was passaged using 0.05% Trypsin-EDTA (Gibco, Grand Island, NY).

Stromal cells, named 5059, derived from human umbilical cord were also used. The cells were cultured in Dulbecco's modified Eagle's Medium (DMEM) (Gilbo, Grand Island, NY).

### 3.2.2 Western blotting

Based on the results of the MTT assay, three concentrations (1.25 μM, 5 μM, and 20 μM) of lovastatin and 100 ng/ml of TRAIL were chosen to treat the cells for 48 hours. The 5059 cells were also treated with 5 μM of lovastatin for 48 hours to investigate the effect of lovastatin on normal cells. The total protein was extracted from the cultured cells using a cell scraper and RIPA buffer (1X PBS, 1% Nonidet P-40 (NP-40), 0.5% sodium deoxycholate, and 0.1% sodium dodecyl sulfate (SDS), pH 7.6 with 1X protease inhibitors (Roche, Basel,

Switzerland) and 100 μg/ml of phenylmethy-sulphonyl-fluoride (PMSF)). The cells were homogenized by gauge needles and incubated on ice for 30 minutes. The samples were then centrifuged at 13,000 rpm for 30 minutes at 4°C and the supernatants were collected as total protein. The concentration of total protein was tested by Bio-Rad DC Protein Assay (Bio-Rad Laboratories, Inc. Hercules, CA) in accordance with the manufacturer's instruction. Each sample containing 40 μg of protein was separated by SDS-PAGE using 10% polyacrylamide gels and then transferred to nitrocellulose blotting membranes (Amersham Biosciences, Piscataway, NJ). The membranes were blocked in 5% non-fat milk for one hour at room temperature, probed with DR4 (CHEMICON, Temecula, CA, 1:1000), DR5 (Cell Signaling Technology, Beverly, MA, 1:1000), DcR1 (Cell Signaling Technology, Beverly, MA, 1:1000), NF-κB p65 (Cell Signaling Technology, Beverly, MA, 1:1000), phospho-NF-κB p65 (Cell Signaling Technology, Beverly, MA, 1:1000), IκBα (Cell Signaling Technology, Beverly, MA, 1:1000), phospho- IκBα (Cell Signaling Technology, Beverly, MA, 1:1000), phospho- IKK α/β (Cell Signaling Technology, Beverly, MA, 1:1000), phospho-JNK (Cell Signaling Technology, Beverly, MA, 1:1000), Erk (Cell Signaling Technology, Beverly, MA, 1:1000), phospho- Erk (Cell Signaling Technology, Beverly, MA, 1:1000), p38 (Santa Cruz Biotechnology, Santa Cruz, CA, 1:1000), caspase-8 (Santa Cruz Biotechnology, Santa Cruz, CA, 1:1000), Bax (Cell Signaling Technology, Beverly, MA, 1:1000), or Smac (Santa Cruz Biotechnology, Santa Cruz, CA, 1:1000) antibody overnight at 4°C, and then incubated with specific secondary antibody (Santa Cruz Biotechnology, Santa Cruz, CA) for one hour at room temperature. The membranes were then

infiltrated with chemiluminescence (Amersham Biosciences, Piscataway, NJ) to detect the target protein signal. Each membrane was stripped and the expression of GAPDH (Santa Cruz Biotechnology, Santa Cruz, CA, 1:5000) detected as an internal reference to ensure equal loading.

### 3.2.3 mRNA level of DR5 as detected by real-time PCR

Real-time PCR, also known as quantitative real-time PCR (Q-PCR), is widely used to amplify and quantify a targeted DNA molecule at the same time. In this project, real-time PCR was used to quantify the mRNA expression of DR5 in human glioblastoma cells treated with 20 μM lovastatin.

In brief, 1? $0^5$ cells were seeded into six-well plates 24 hours in advance of the experiments. The cells were treated with vehicle-DMSO or 20 μM lovastatin. At the end of the incubation, the cells were harvested for RNA extraction. RNA was extracted using an RNA extraction kit (Geneisland, Taiwan) according to the manufacturer's protocol. 1 μg of RNA was used for the reverse transcription using the Reverse Transcription System (Promega, Madison, WI). The 20μl reaction mix was set up as follows.

| Component | Volume (µl) |
|---|---|
| $MgCl_2$ (25 mM) | 4 |
| Reverse Transcription 10X Buffer | 2 |
| dNTP (10 mM) | 2 |
| Recombinant RNasin® Ribonulease Inhibitor | 0.5 |
| AMV Reverse Transcriptase | 1 |
| Oligo T Primer | 0.5 |
| RNA sample | 1 |
| Nuclease-free water | 9 |
| **Total** | **20** |

The reaction mix was placed in a thermal cycler running a program of 25℃ for 5 minutes, 42℃ for 1 hour, 70℃ for 15 minutes, and 4℃ for 30 minutes. The cDNA of each sample was generated as the product of the reverse transcription, and was used as the template for further real-time PCR. The reaction mix was set up as follows.

| Component | Volume (μl) |
|---|---|
| 2X SYBR Green | 5 |
| Forward Primer | 0.5 |
| Reverse Primer | 0.5 |
| cDNA sample | 1 |
| Nuclease-free water | 3 |
| **Total** | **10** |

The reaction mix was placed in a thermal cycler (ABI 7900HT) running the following program.

| Temperature and duration | Number of cycles |
|---|---|
| 95℃, 2 minutes | 1 |
| 95℃, 0.5 minutes | 1 |
| 60℃, 0.5 minutes | 45 |
| 72℃, 1 minutes | |
| 72℃, 5 minutes | 1 |

The mRNA expression of actin was also detected as an internal reference to ensure equal loading.

The following primer profiles were used.

DR5 forward: 5 -GTCCTGCTGCAGGTCGTACC-3

reverse: 5 -GATGTCACTCCAGGGCGTAC-3

Actin forward: 5 -GATGAGATTGGCATGGCTTT-3

reverse: 5 -AGAGAAGTGGGGTGGCTTTT-3

### 3.2.4 NF-κB activity as measured by dual-luciferase reporter assay

The change of NF-κB signaling induced by lovastatin was detected by dual-luciferase reporter assay. In our experiment, the luciferase activities of firefly (*Photinus pyralis*) encoded by the NF-κB plasmid and Renilla (*Renilla reniformis*) encoded by internal control pRL-CMV vector were investigated sequentially through enzymatic activity (Figure 3-1).

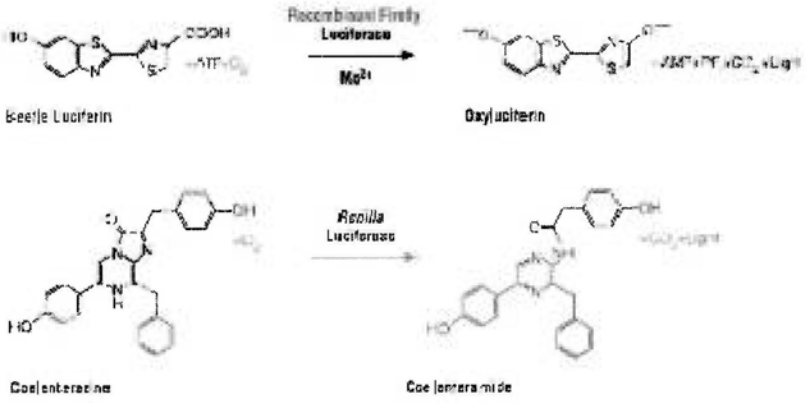


**Figure 3-1 Bioluminescent reactions catalyzed by firefly and *Renilla* luciferases**

$5\times10^4$ cells were seeded into 24-well plates with appropriate complete medium. After cell attachment, the NF-κB-luciferase reporter plasmid (600 ng / well) (Figure 3-2) and pRL-CMV vector (5 ng / well) (Figure 3-3) were co-transfected into human glioblastoma cells using lipofectamine 2000 Transfection Reagent (Invitrogen, Carlsbad, CA). After six hours incubation, the medium contain lipofectamine 2000 was discarded and fresh completed medium was added. 24 hours after transfection, the cells were treated with 20 μM lovastatin (TRC Inc., Ontario, Canada) for 1, 3, and 6 hours.

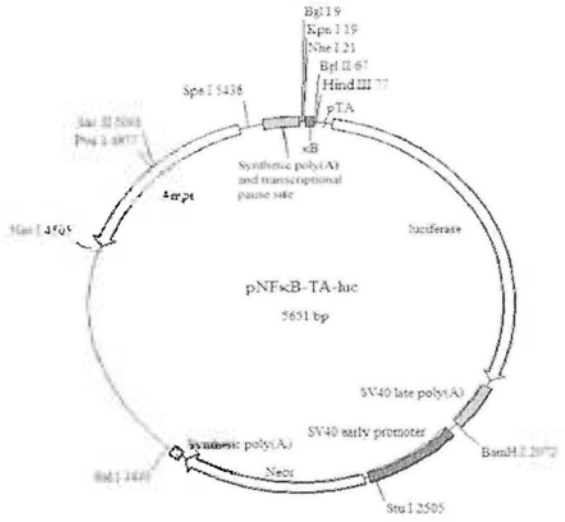


**Figure 3-2 Map of NF-κB-luciferase plasmid**

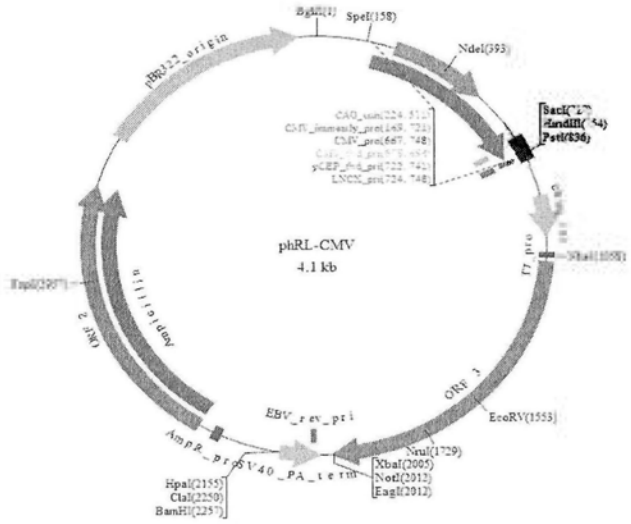


**Figure 3-3 Map of *Renilla*-luciferase vector**

After the incubation period, cell lysates were harvested and the luciferase signals were detected by Dual-Luciferase Reporter Assay System (Promega, USA). Briefly, the culture medium containing different concentration of lovastatin was discarded and PBS was used to wash cells. Then, 100 μl 1X Passive Lysis Buffer was added to each well and the plate was shook at room temperature for 15 minutes. Consequently, the lysates were transferred into 1.5 ml Eppendorf tubes and centrifuged at 10,000 g at 4℃ for 5 minutes. After centrifugation, the supernatant was moved to a new tube.

20 μl cell lysate extracted by the above method was added into the 96-well plate and then mixed with 100μl Luciferase Assay Buffer II. Then, the firefly luminescence encoded by the NF-κB was tested by luminometer (Spectra Rainbow, TECAN). After quantification, the firefly luminescence was quenched and the *Renilla* luciferase encoded by the internal control pRL-CMV vector was simultaneously initiated by adding Stop & Glo Reagent. Finally, the signal from *Renilla* luciferase was also measured by luminometer (Spectra Rainbow, TECAN). The NF-κB activity was normalized by the internal control, *Renilla*.

### 3.2.5 Statistical analysis

The data were presented as the mean ? one standard deviation (SD) for at least three separate determinations for each group. Differences between the groups were examined for statistical significance using a Student's *t*-test or one-way

ANOVA followed by a Student's *t*-test. $P<0.05$ was used to indicate a statistically significant difference.

## 3.3 Results

### 3.3.1 Expression of TRAIL receptors in human glioblastoma cells

It is known that TRAIL induces apoptosis mainly through the extrinsic pathway (receptor pathway) and the expression of death receptors and decoy receptors are the major factors for TRAIL resistance. Four human glioblastoma cell lines that resist TRAIL attack were used to determine the expression of TRAIL receptors. Cells were treated with vehicle-DMSO; 1.25 μM, 5 μM, and 20 μM of lovastatin; and 100 ng/ml of TRAIL. The number of decoy receptors of TRAIL was not significantly greater after incubation with the various concentrations of lovastatin (Figure 3-4; data for DcR 2 not shown). In the four human glioblastoma cell lines, the DR4 expression was similar across treatments (Figure 3-5). However, the protein level of DR5 was significantly up-regulated after stimulation with lovastatin. A higher expression of DR5 was found in the high-dose group, especially in the A172 and U87 MG cells (Figure 3-6). However, the DR5 expression was not significantly changed when cells treated with TRAIL only.

A.

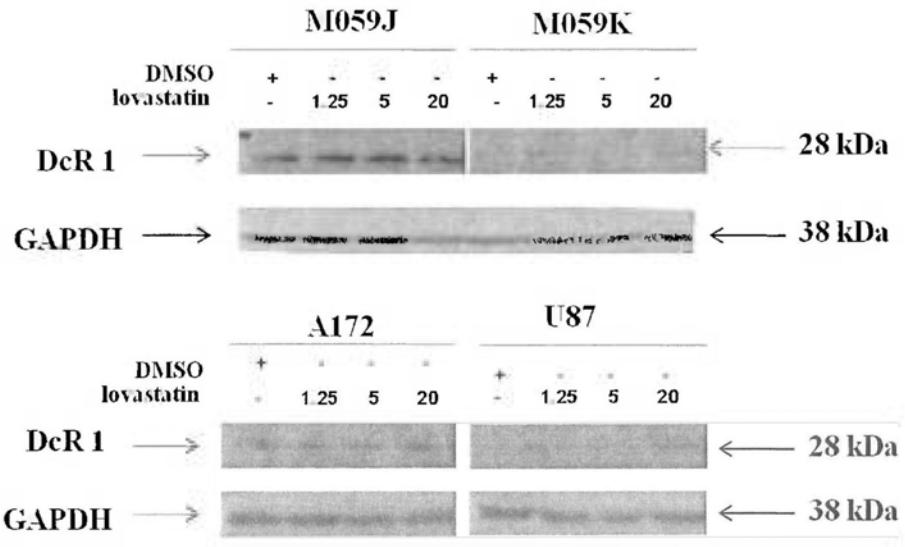


B.

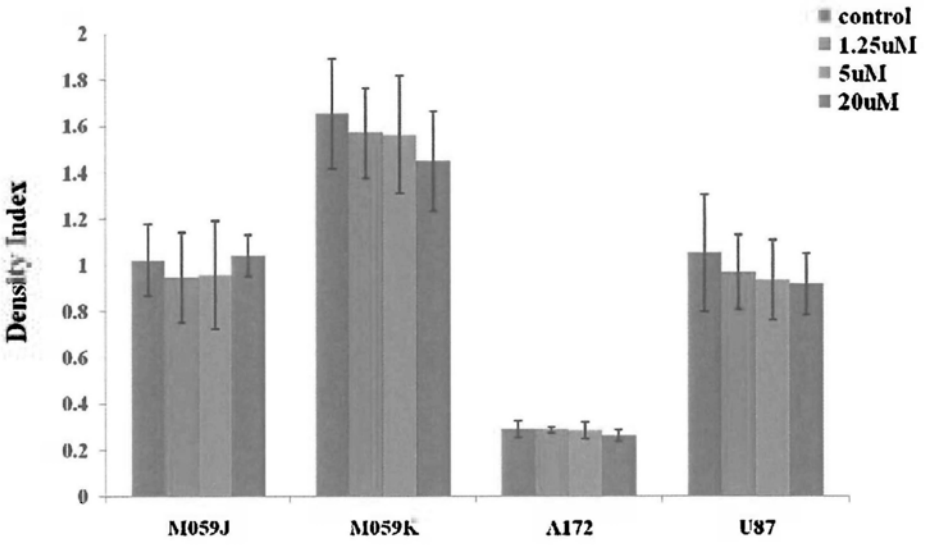


**Figure 3-4 Decoy receptor 1 expression in human glioblastoma cells**

Representative Western blots were shown (A). The target bands were normalized to GAPDH and the index of densities was calculated (B).

A.

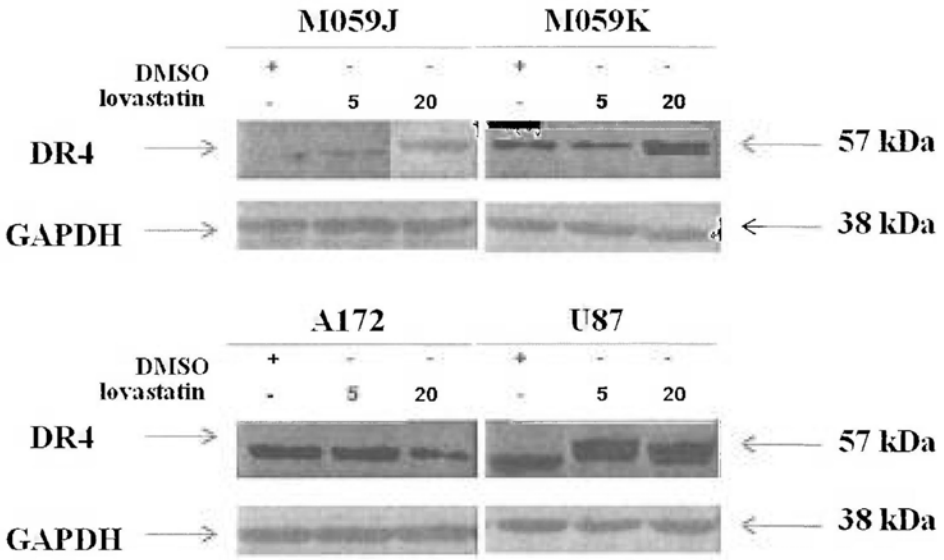


B.

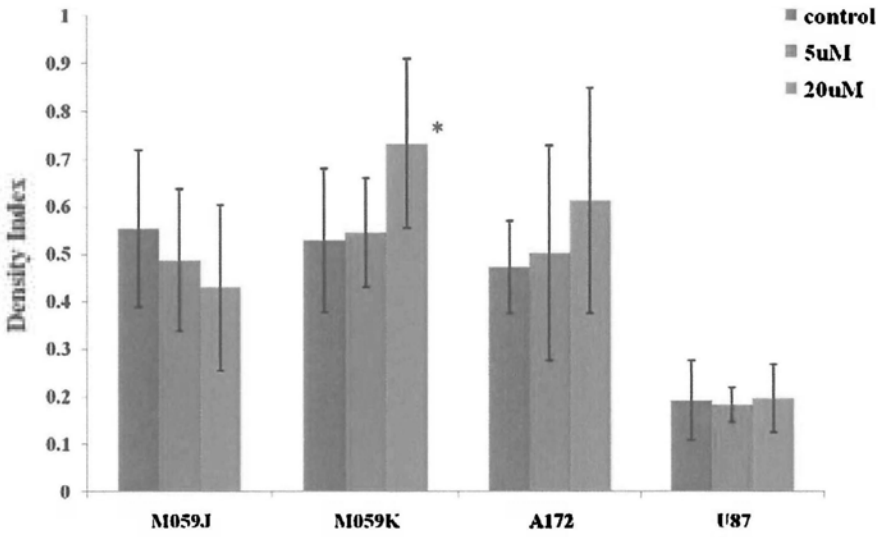


**Figure 3-5 DR4 expression in human glioblastoma cells**

Representative Western blots were shown (A). The target bands were normalized to GAPDH and the index of densities was calculated (B).

**A.**

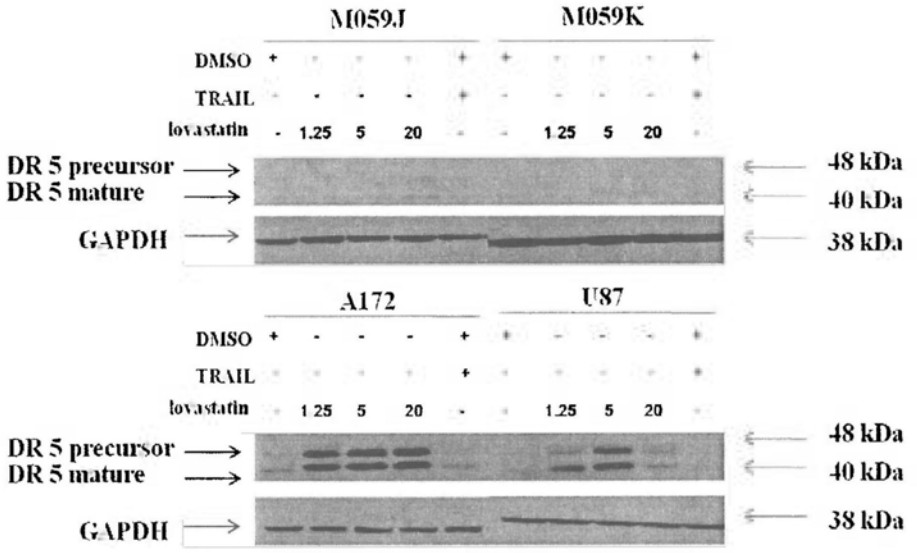


**B.**

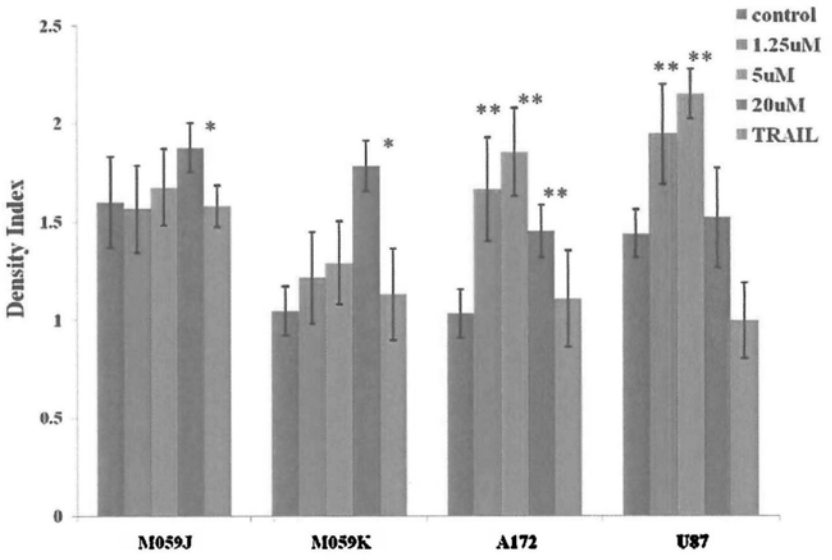


**Figure 3-6 DR5 expression in human glioblastoma cells**

Representative Western blots were shown (A). The target bands were normalized to GAPDH and the index of densities was calculated (B).

### 3.3.2 mRNA level of DR 5 in human glioblastoma cells

Real-time PCR is a precise method that allows both the detection and quantificaiton of specific sequences in a DNA sample. In this project, four huamn glioblastoma cell lines treated with 20 μM lovastatin was examined to detect the change in DR5 mRNA expression. The trend of DR5 mRNA expression was similar to the results obtained using western blot analysis. In the M059K cells, the DR5 mRNA level was not significantly increased by sensitization with lovastatin, whereas DR5 mRNA expression was obviously up-regulated in the other three cell lines after treatment with lovastatin. (Figure 3-7).

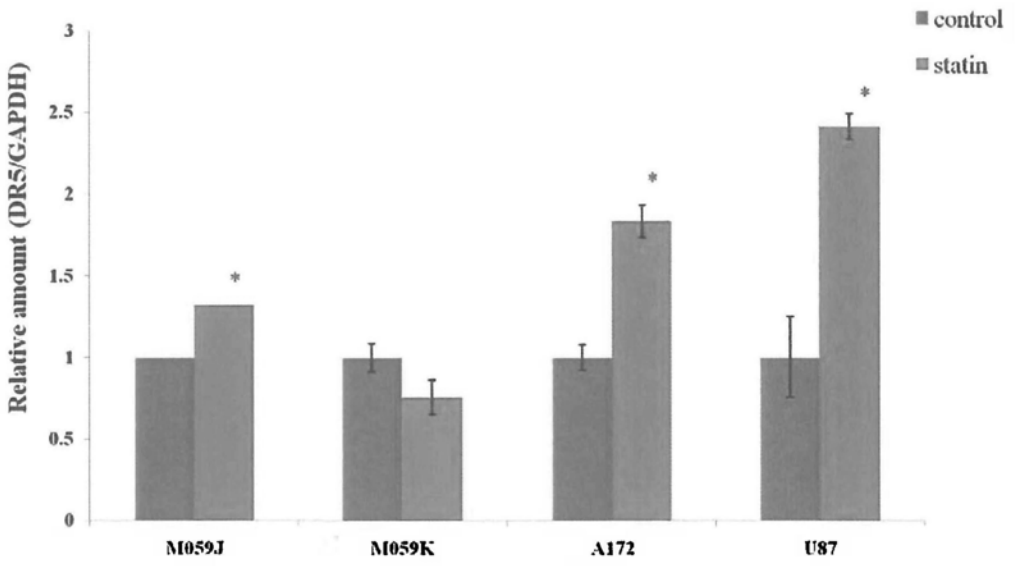


**Figure 3-7 mRNA level of DR5 in human glioblastoma cells**

M509J, M059K, A172, and U87 MG were treated with 20 μM lovastatin. Data are the mean ± S.D. of three separate experiments with similar trends.

### 3.3.3 DR5 expression in human stromal cells after treated with lovastatin

Based on the results that we obtained before, the protein expression of DR5 was significantly up-regulated in human glioblastoma cell lines. At the same time, 5059 stromal cells derived from human umbilical cord were tested after treatment with 5 μM of lovastatin. Distinct from the glioblastoma cells, lovastatin-induced DR5 up-regulation was not found in 5059 cells (Figure 3-8).

A.

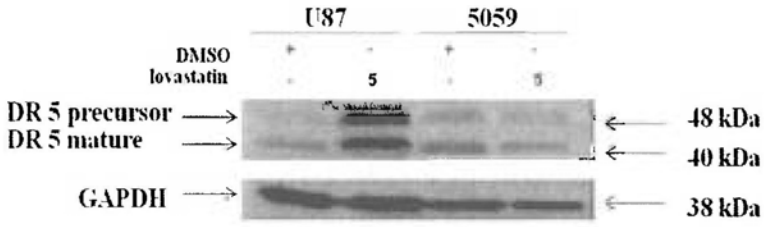


B.

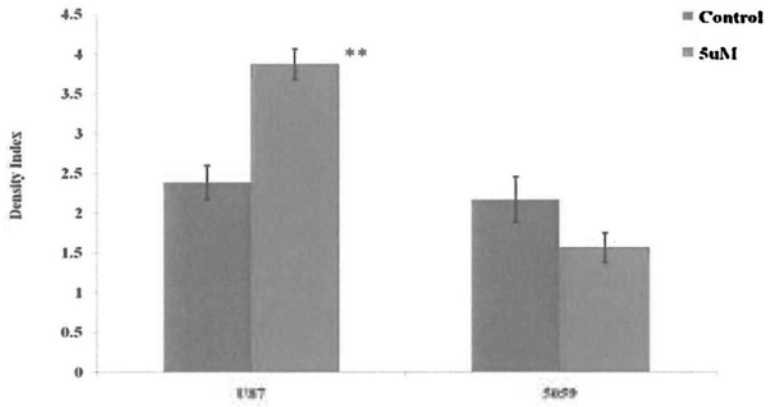


**Figure 3-8 DR5 expression in human stromal cells**

Representative Western blots were shown (A). The index of densities was calculated (B).

### 3.3.4 Change of NF-κB activity in human glioblastoma cells as detected by dual-luciferase reporter assay

In Dual-Luciferase Reporter Assay System, Firefly and *Renilla* luciferases were applied. Because of their distinct evolutionary origins, their respective bioluminescent can be easily discriminated. Therefore, it can efficiently detect the change of signaling pathways by co-transfection of pathway luciferase reporter plasmid and internal control pRL-CMV vector. In our project, the cells transfected with NF-κB-luciferase plasmid and *Renilla*-luciferase plasmid were treated with 20 μM lovastatin for 1, 3, and 6 hours. Within six hours after lovastatin treatment, the NF-κB activity of M059J, M059K and U87 were markedly decreased. However, there was no different in A172 (Figure 3-9).

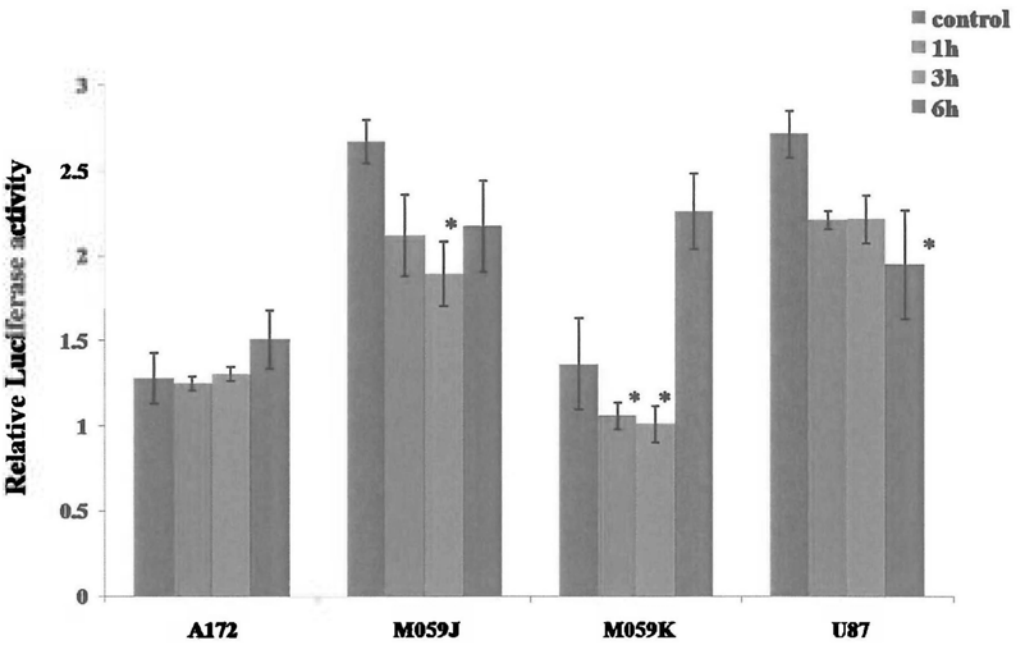


**Figure 3-9 NF-κB activity in human glioblastoma cells**

### 3.3.5 Change in the NF-κB pathway in human glioblastoma cells induced by lovastatin

M059J, M059K, A172, and U87 MG were treated with different concentrations of lovastatin (Vehicle-DMSO, 1.25 μM, 5 μM, and 20 μM) for 30 minutes, 3, 6, 12, and 24 hours. In the M059K cells, the total NF-κB p65 expression was not significantly changed by lovastatin. However, expression of the phosphorylated type of NF-κB p65, which is the active type of NF-κB, was significantly decreased in a dose-dependent manner, especially at 24 hours after incubation. In addition, phospho-IKK α/β and phospho-IκBα, which control the activation of NF-κB, were also down-regulated (Figure 3-10).

**A.**

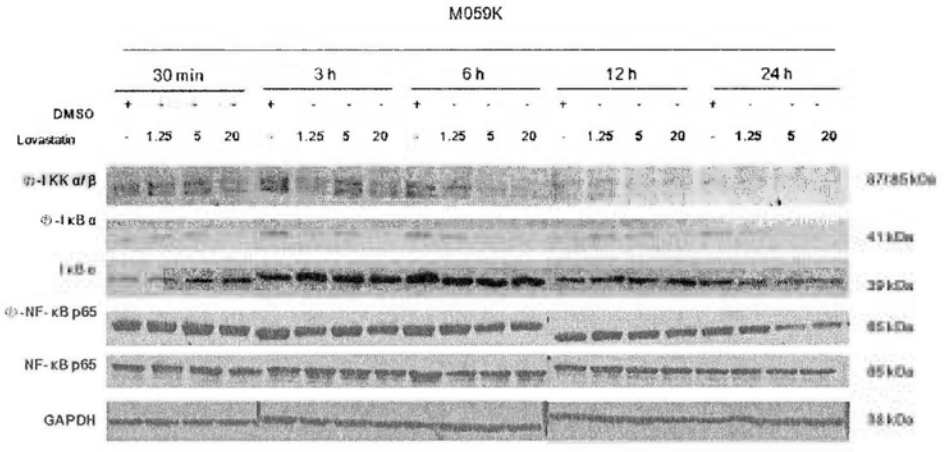

**B.**

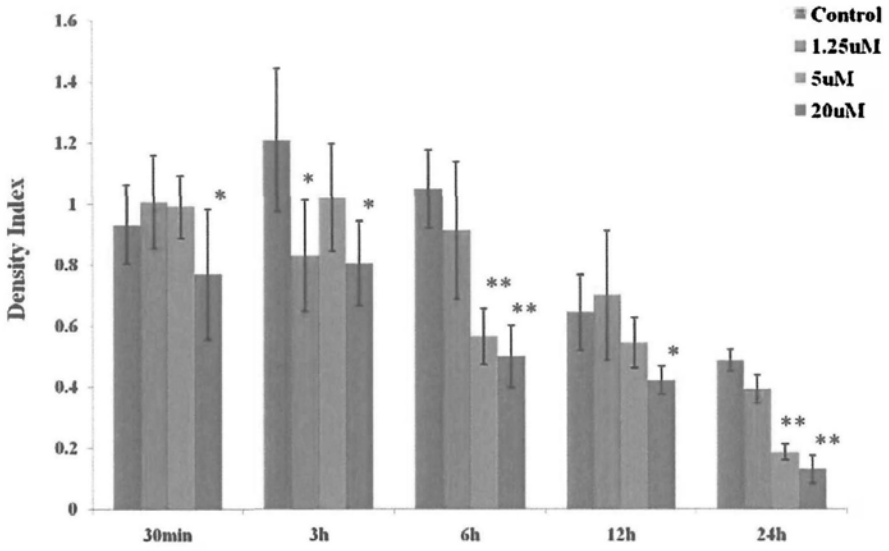
Control
1.25uM
5uM
20uM
Density Index
1.6
1.4
1.2
1
0.8
0.6
0.4
0.2
0
30min
3h
6h
12h
24h

C.

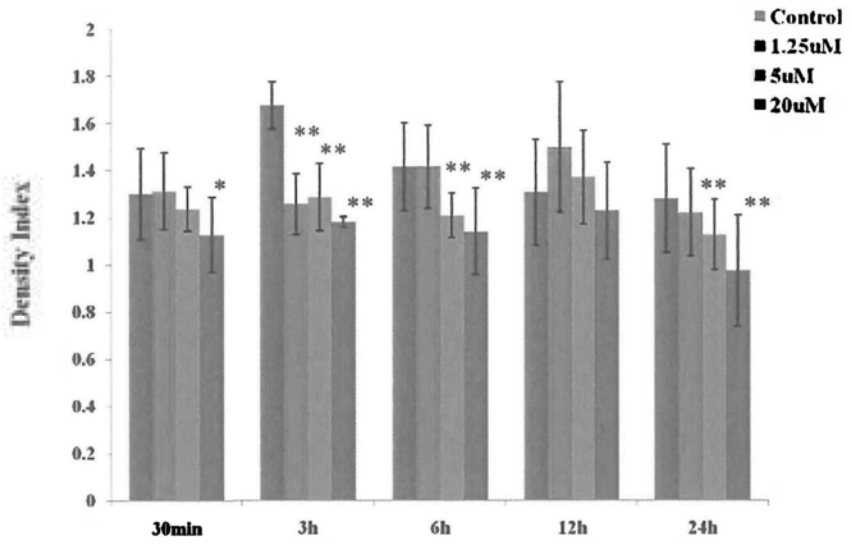
Control
1.25uM
5uM
20uM
Density Index
2
1.8
1.6
1.4
1.2
1
0.8
0.6
0.4
0.2
0
30min
3h
6h
12h
24h

**D.**

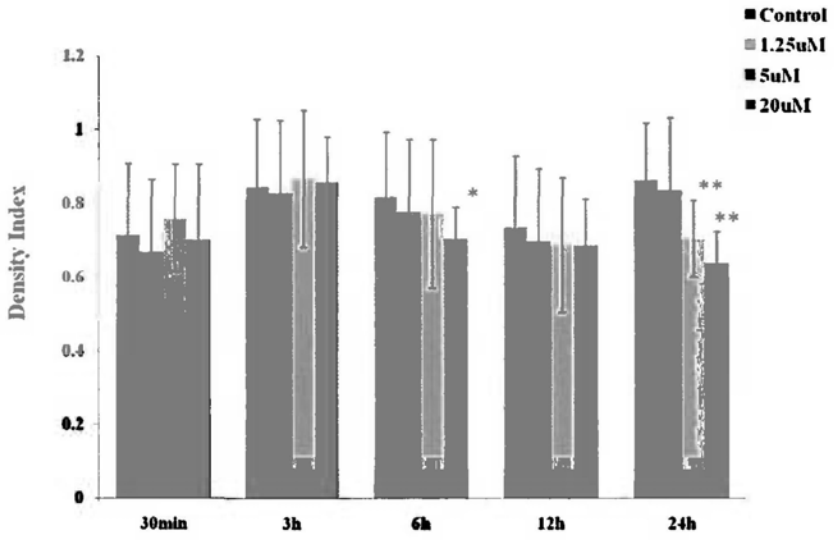


**Figure 3-10 Effect of lovastatin on NF-κB pathway in M059K at different time points**

Lovastatin caused the down-regulation of active NF-κB in a time-dependent and dose-dependent manner in M059K cells. Representative Western blots were shown (A). The target bands of phosphorylated IKK α/β (B), phosphorylated IκBα (C), and phosphorylated NF-κB p65 (D) were normalized to GAPDH and the index of densities was calculated.

The NF-κB expression in the other cell lines was also tested at 24 hours. Figure 3-11(A) shows that the phospho-NF-κB level was decreased in the cells treated with lovastatin. The phospho-IκBα expression was also down-regulated in a dose-dependent manner after treatment with lovastatin, whereas total IκBα expression was up-regulated. The most obvious difference could be found in the high dose (20 μM) lovastatin group (Figure 3-11).

**A.**

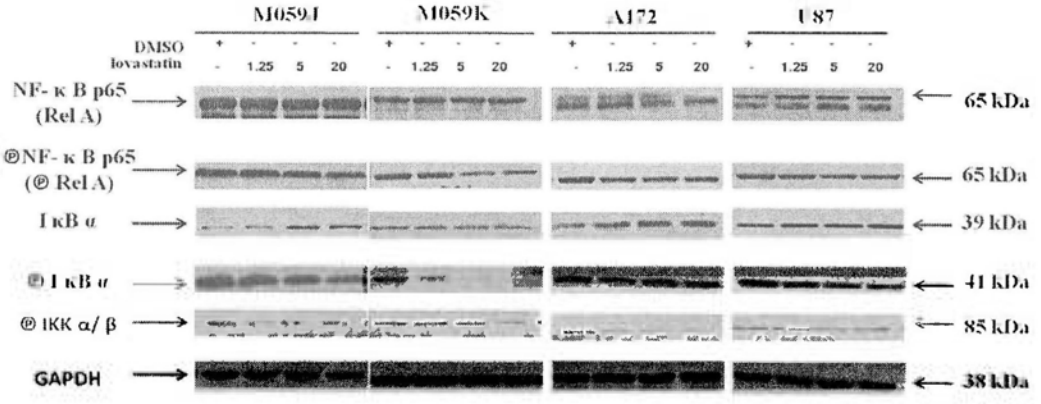

**B.**

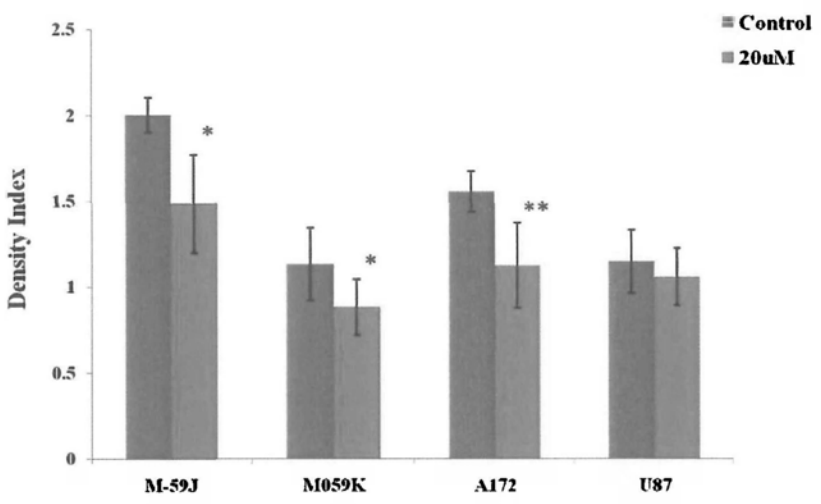
Control
20uM
Density Index
2.5
2
1.5
1
0.5
0
*
*
**
M-59J
M059K
A172
U87

**C.**

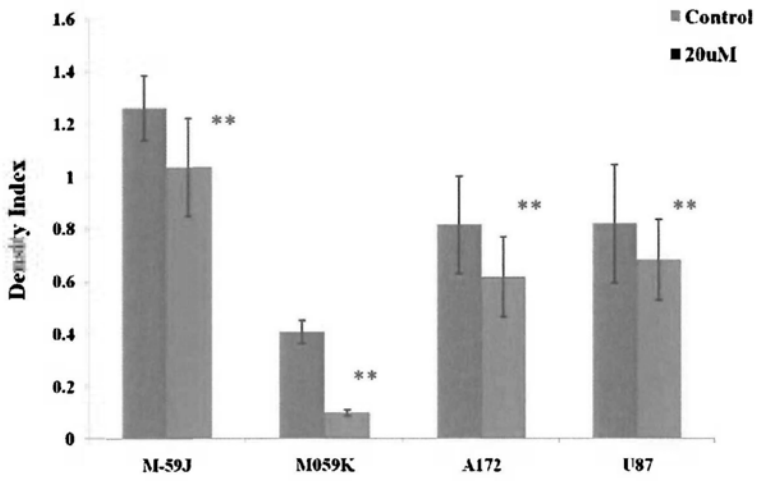
Control
20uM
Density Index
1.6
1.4
1.2
1
0.8
0.6
0.4
0.2
0
**
**
**
**
M-59J
M059K
A172
U87

D.

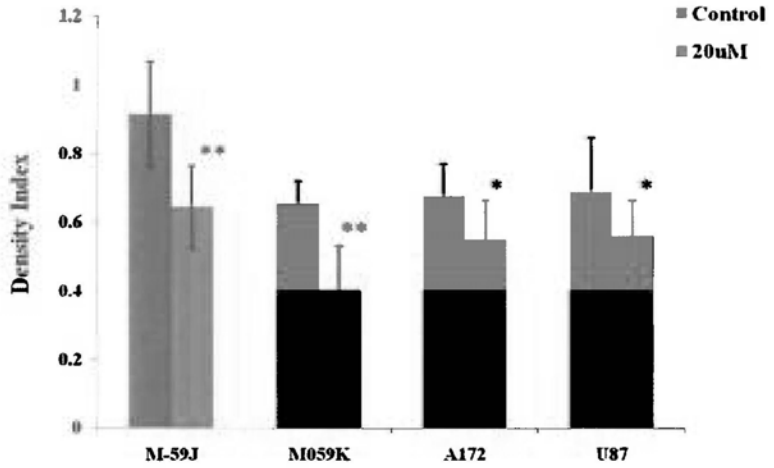


**Figure 3-11 Decrease in expression of active NF-κB in human glioblastoma cells due to lovastatin**

Representative Western blots were shown (A). The obvious difference cloud be found at high dose group. The target bands of phosphorylated IKK α/β (B), phosphorylated IκBα (C), and phosphorylated NF-κB p65 (D) were normalized to GAPDH and the index of densities was calculated. The marked difference was found at high dose of lovastatin treatment.

### 3.3.6 Expression of death receptors in human glioblastoma cells following the inhibition of NF-κB

To confirm the role of NF-κB in the regulation of death receptors, Bay, which is an inhibitor of IκBα phosphorylation, was applied to block the activation of the NF-κB pathway. After treatment with Bay for 48 hours, the DR5 expression showed a similar trend to the DR5 expression in glioblastoma cells treated with lovastatin (Figure 3-12).

**A.**

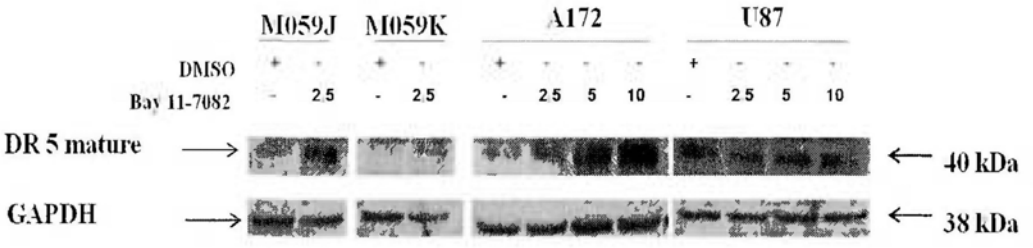

**B.**

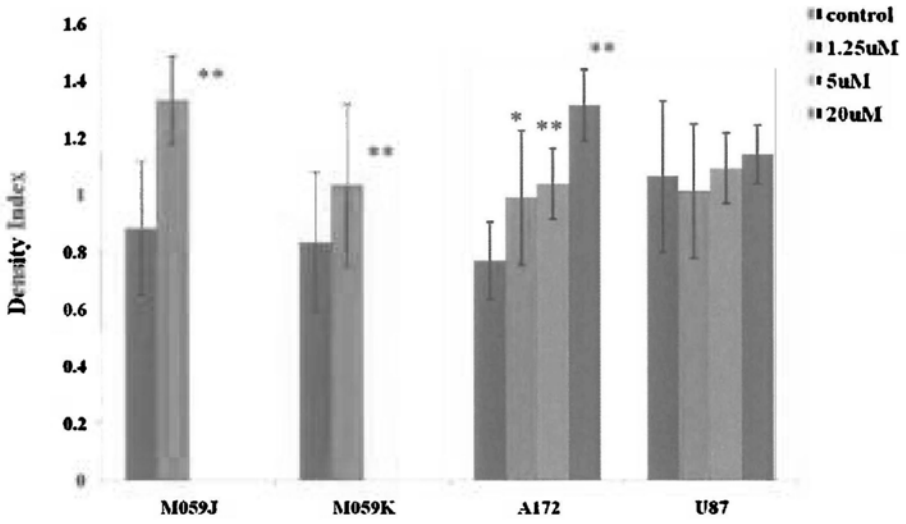


**Figure 3-12 DR5 expression sensitised by an NF-κB inhibitor**

The expression of DR5 was increased in a dose-dependent fashion after inhibition of the NF-κB pathway by an IκBα inhibitor. Representative Western blots were shown (A). The target bands were normalized to GAPDH and the index of densities was calculated (B).

### 3.3.7 Lovastatin affects the regulation of downstream molecules in the apoptotic pathway

Downstream molecules in the apoptotic pathway were observed in M059J, M059K, and A172 cells treated with different concentrations of lovastatin for 48 hours. The level of Bax, which improves the intrinsic apoptotic pathway, was significant increased after the cells had been treated with lovastatin. However, there was no obvious change in the expression of Smac between the treated and untreated groups. Caspase-8, which is regarded as the main apoptotic molecule in the extrinsic pathway, was also tested. In the high-dose group, the caspase-8 level was significantly down-regulated, with an associated up-regulation of cleaved caspase-8 (Figure 3-13). This implies an interaction between the intrinsic and extrinsic pathways after lovastatin treatment.

**A.**

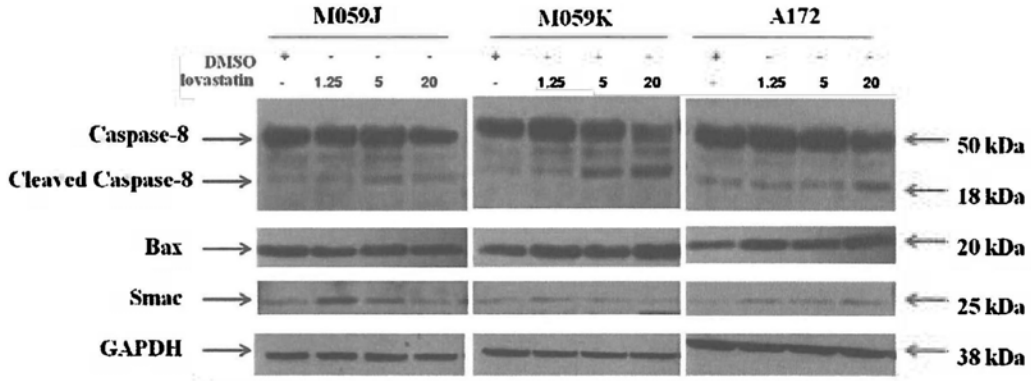
M059J
M059K
A172
DMSO
lovastatin
1.25
5
20
Caspase-8
Cleaved Caspase-8
Bax
Smac
GAPDH
50 kDa
18 kDa
20 kDa
25 kDa
38 kDa

**B.**

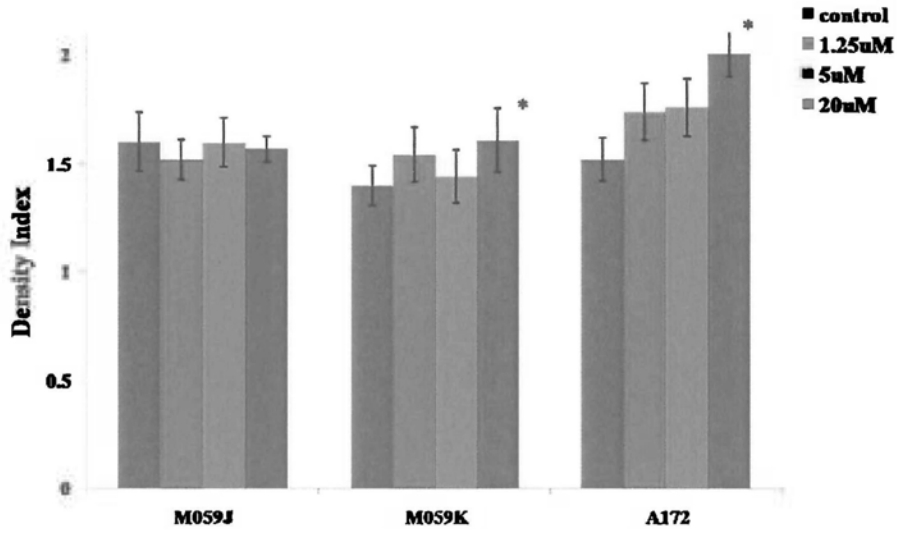
control
1.25uM
5uM
20uM
Density Index
1.5
1
0.5
0
M059J
M059K
A172
*
*

C.

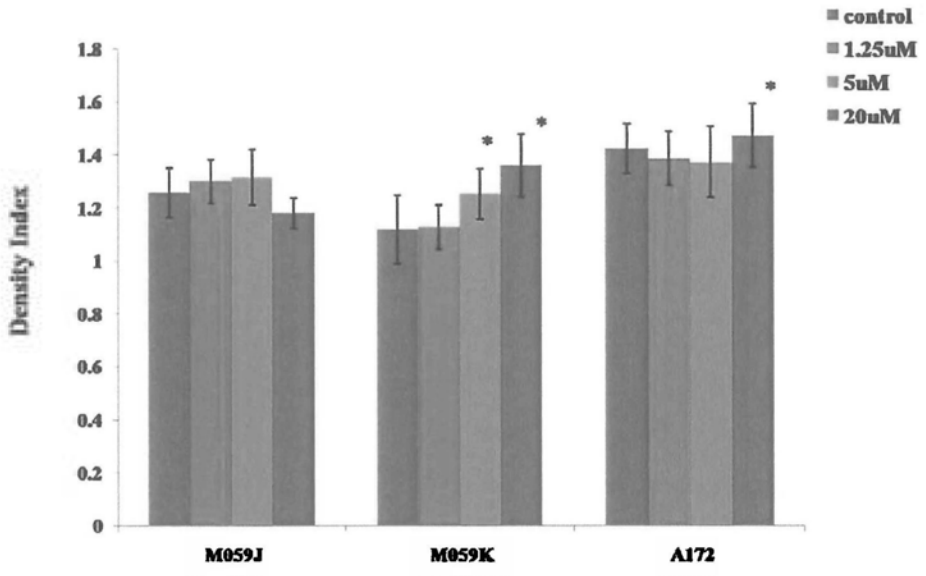


**Figure 3-13 Lovastatin affected both the intrinsic and extrinsic apoptotic pathways**

Representative Western blots were shown (A). The target bands of Bax (B), and cleaved caspase-8 (C) were normalized to GAPDH and the index of densities was calculated.

### 3.3.8 Regulation of the MAPK pathway induced by lovastatin treatment in human glioblastoma cells

The MAPK pathway was also chosen for further examination after glioblastoma cells were treated with lovastatin for 24 hours. The extracted protein from the cell samples was then used to detect the protein expression of JNK, Erk, and p38. The data revealed that the expression of phosphorylated Erk was significantly decreased, whereas JNK and p38 were up-regulated after lovastatin treatment (Figure 3-14).

A.

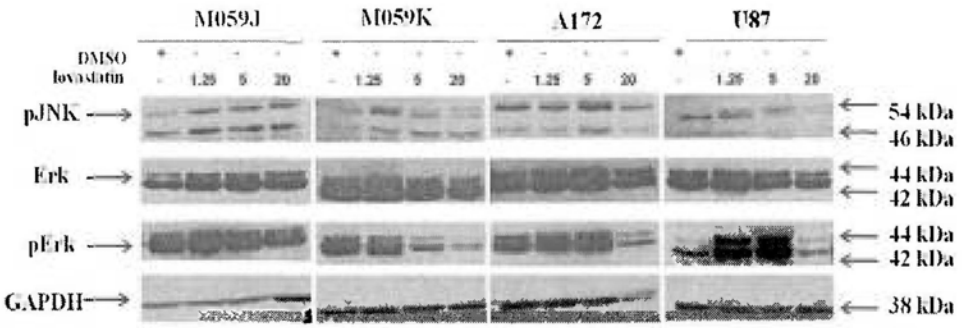


B.

C.

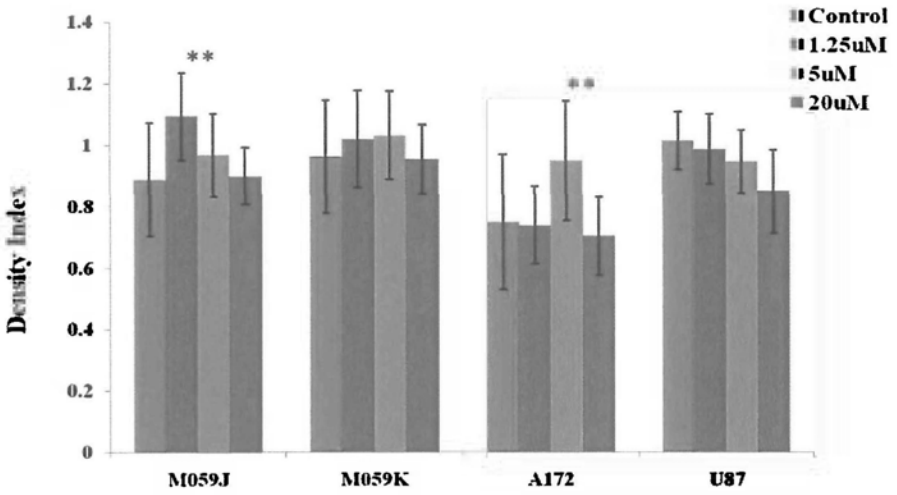
Control
1.25uM
5uM
20uM
Density Index
1.4
1.2
1
0.8
0.6
0.4
0.2
0
**
**
M059J
M059K
A172
U87

D.

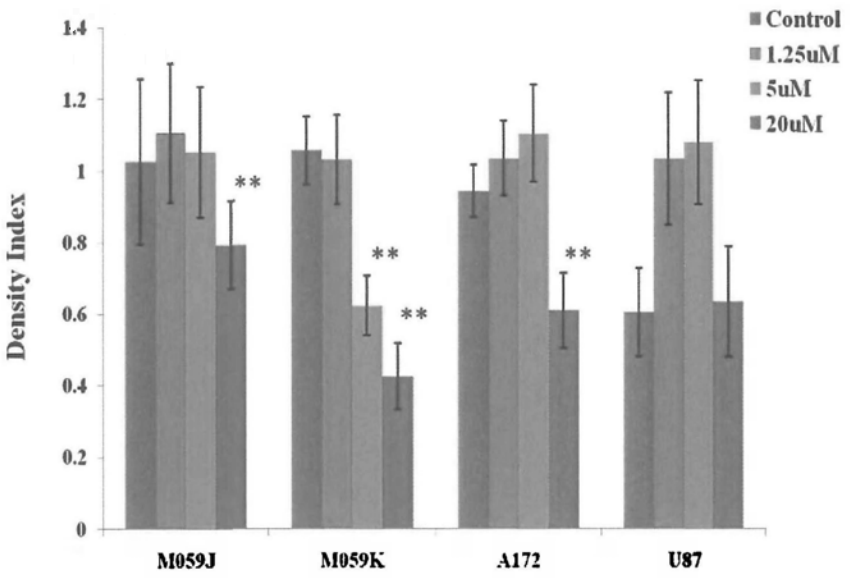
Control
1.25uM
5uM
20uM
Density Index
1.4
1.2
1
0.8
0.6
0.4
0.2
0
**
**
**
**
M059J
M059K
A172
U87

E.

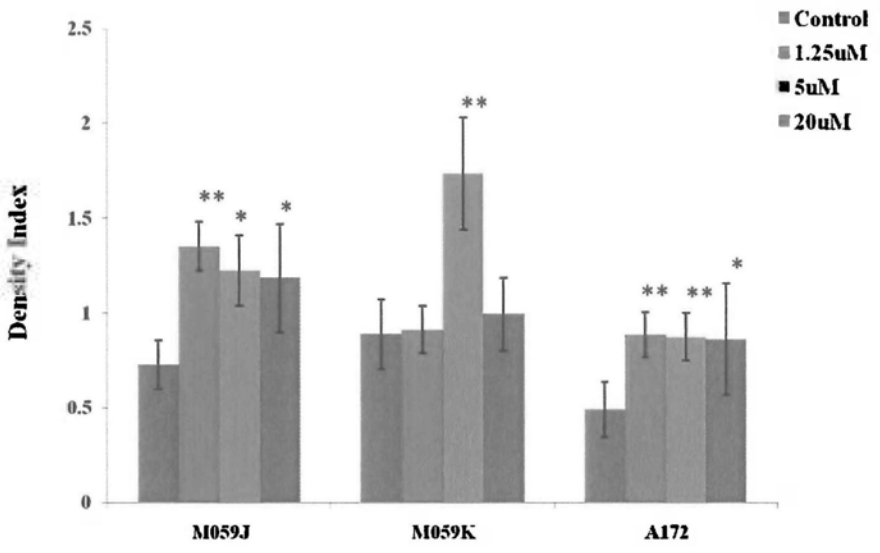


**Figure 3-14 Regulation of the MAPK signal by lovastatin in human glioblastoma cells**

When human glioblastoma cells were cultured with lovastatin, the Erk signal was significantly decreased and the JNK and p38 expression were up-regulated. Representative Western blots were shown (A and B). The target bands of phosphorylated JNK (C), phosphorylated Erk (D) and p38 (E) were normalized to GAPDH and the index of densities was calculated.

## 3.4 Discussion

In this study, we demonstrate that lovastatin and TRAIL have a synergistic apoptotic effect on human glioblastoma cells. This may be related to the triggering of both the intrinsic and extrinsic apoptotic pathways at the same time. However, the reason for TRAIL-induced apoptosis in human glioblastoma cells sensitised by lovastatin is still not clear. It has been known that TRAIL resistance is affected by multi-factor and the expression of death receptor is one of the major factors (Srivastava 2001). Western blot and real-time PCR were utilized in this study to detect the expression of TRAIL receptors, both death receptors and decoy receptors, in cells treated with lovastatin. The protein and mRNA expression results showed distinct lovastatin-induced DR5 up-regulation in the A172, M059J, and U87 cells. In the M059K cells, the protein expression of DR5 was also significantly elevated after treatment with lovastatin in a dose-dependent manner. However, a similar result was not found in the real-time PCR data, suggesting that post-translational modification may affect the expression of DR5 in M059K cells. According to these results, DR5 could be a potential biomarker for clinic to screen glioblastoma patients who are sensitive to TRAIL treatment. If the DR5 expressions of patients are negative, it indicates that they are resistant to TRAIL treatment and need to be administrated with lovastatin to sensitise TRAIL-induced apoptosis. In addition, comparison of the control groups of the M059J, M059K, and A172 lines showed that DR5 expression in the A172 group was higher than that in the Ma09J and M059K

groups. This may explain why A172 is more sensitive to TRAIL attack than the other two types of glioblastoma cells.

Lovastatin is a systemic drug that affects the entire body. Thus, 5059 cells, which are stromal cells derived from human umbilical cord, were used to evaluate the effect of lovastatin on DR5 expression in normal cells. Compared with U87 MG cells, the DR5 expression was not up-regulated by lovastatin in the 5059 cells, indicating that lovastatin does not increase the DR5 expression in normal cells. This is important for TRAIL to maintain its property of targeted attack to cancer cells after receiving lovastatin treatment. However, the effect of lovastatin on DR5 regulation in other normal cells still needs to be investigated.

However, which signal pathway is involved in the lovastatin-induced DR5 up-regulation? Several studies have suggested that NF-κB may be responsible for the resistance to TRAIL-induced apoptosis, and accumulating evidence suggests that different NF-κB subunits have different effects on death receptor regulation (Chen, Kandasamy et al. 2003). Moreover, TRAIL and its receptors can sensitise the activation of NF-κB in many cells, such as HeLa and 293T cells, thereby inducing TRAIL resistance to cells more aggressively (Sheridan, Marsters et al. 1997).

Lovastatin, a 3-hydroxy-3-methylglutaryl-CoA (HMG-CoA) reductase inhibitor, is widely used in clinical practice for hypercholesterol patients. One of the mechanisms by which lovastatin decreases blood cholesterol is by modulating the inflammatory response. It is known that NF-κB not only has a dual effect on apoptosis, but also plays a critical role in other cellular functions, including inflammation and immune response. We thus hypothesize that lovastatin-induced TRAIL apoptosis may be related to the NF-κB pathway.

First, we investigated the NF-κB activity in human glioblastoma cells after treated with lovastatin. We found the NF-κB activity was rapidly reduced within six hours after incubation. Furthermore, we investigated protein expression changes in certain molecules in the NF-κB pathway before and after lovastatin treatment. It is known that active NF-κB may translocate into the nucleus and then display its functions. Our results also showed that the total NF-κB expression did not differ between the control group and the lovastatin treatment group. However, expression of the phosphorylated type of NF-κB, which is regarded as the active type, was significantly decreased after lovastatin treatment. We also investigated expression of the phosphorylated type of IκBα and IKK α/β, which play critical roles in NF-κB activation. We found that the expression of phospho-IκBα and phospho-IKK α/β were down-regulated, indicating that the activation of NF-κB was inhibited. To confirm that DR5 up-regulation is induced by lovastatin via the inactivation of the NF-κB pathway, we used Bay, which is an inhibitor of cytokine-induced IκBα phosphorylation,

as a treatment to examine the DR5 expression in human glioblastoma cells. The results were similar to those for cells treated with lovastatin, indicating that DR5 expression was increased due to NF-κB inactivation. This may explain how lovastatin sensitizes cells to TRAIL-induced apoptosis.

The apoptotic factors in the intrinsic apoptotic pathway and extrinsic apoptotic pathway were also determined. Caspase-8 is an important molecule in the extrinsic pathway, and it is known that the down-regulation of caspase-8 is related to TRAIL resistance (Zhang and Fang 2005). We found that the cleaved caspase-8 level was very low in the control group of A172, M059J and M059K cell lines. However, the cleaved caspase-8 expression was significantly increased after lovastatin treatment. Similar discoveries have been made in mammary carcinoma cells and hepatocytes (Kubota, Fujisaki et al. 2004; Shibata, Ito et al. 2004). These results imply that lovastatin may influence not only the intrinsic apoptotic pathway, but also the extrinsic pathway through Bcl-2 and Bax. It has been suggested that Bcl-2 may bind and sequester caspase-8 and block its function (Poulaki, Mitsiades et al. 2001). Bax functions in reverse to Bcl-2, but they may interact in the mitochondria to balance cell death. Several studies have reported that the Bax/Bcl-2 ratio may influence the efficacy of cancer treatments (Shi, Chen et al. 2010). The results in this study showed that Bax expression was significantly increased after lovastatin treatment and induced the up-regulation of cleaved caspase-8.

MAPK pathway is another possible pathway that induces cells resistant to TRAIL attack. A previous study has also demonstrated that lovastatin may induce apoptosis in macrophages and ovarian cancer cells through the activation of JNK (Liang, Liu et al. 2006; Liu, Liang et al. 2009). We thus hypothesize that the JNK pathway is another possible mechanism of lovastatin-induced apoptosis in human glioblastoma cells. Our results confirmed that lovastatin-induced apoptosis was not only induced by JNK activation, but also associated with Erk and p38, two other members of the MAPK pathway. According to western blot data, the protein expression of active JNK and p38 was increased whereas that of active Erk significantly was decreased. Other studies have also proposed that DR5 up-regulation may be mediated by the MAPK pathway in human medulloblastoma cells (Li, Fan et al. 2008). Changes in the MAPK pathway may also influence TRAIL-induced apoptosis by lovastatin. In conclusion, it appears that multiple interacting pathways are involved in lovastatin-induced DR5 up-regulation.

# Chapter Four Preclinical animal studies in nude mice model of GBM

## 4.1 Introduction

Animal experiments are an important part of translational research. They provide a connection between bench and bed, and offer valuable data for further clinical application. To improve the detection methods in such experiments, *in vivo* imaging systems such as magnetic resonance imaging (MRI), positron emission tomography (PET), bioluminescent imaging (BLI), and fluorescence imaging have been developed. These are non-invasive methods of quantifying the tumour burden and dynamically detecting micrometastasis (Lim, Modi et al. 2009).

Fluorescent imaging is an important part of *in vivo* imaging systems, which are limited by tissue absorption occurring only at wavelengths below 600 nm and poor tissue penetration. Fluorescent signals are particularly advantageous for use in non-living organisms, such histological slides. Bioluminescence is more popular for use in *in vivo* experiments. It has been concluded that the emission spectrum of luciferase (Luc) at 37癈 is mostly above 600 nm, and that it penetrates tissue very efficiently. However, it also has some limitations, chiefly that the procedure of luciferin oxidation by luciferase requires the presence of adenosine-5'-triphosphate (ATP). This means that bioluminescence can only be detected in living organisms. Cell lines expressing firefly luciferase are regarded as the most sensitive method for the optical detection of bioluminescence.

To detect signals both *in vivo* and histologically, we established an U87-GFP-Luc brain tumour model using a lentivirus transduction platform. After the subcutaneous brain tumour model was established, the *in vivo* effect of lovastatin and TRAIL was investigated.

## 4.2 Materials and Methods

### 4.2.1 Cell lines and cell cultures

U87 MG and 293T were purchased from the American Type Culture Collection (ATCC). The U87 MG, which is a glioblastoma multiforme cell line, was maintained in Eagle's Minimum Essential Medium (MEM) (Gibco, Grand Island, NY), and the 293T, which is a kidney epithelial cell line, was cultured in Dulbecco's Modified Eagle's Medium (DMEM) (Gibco, Grand Island, NY). Both the MEM and DMEM media were supplemented with 10% fetal bovine serum (FBS) (HyClone, Logan, UT), 100U/mL of penicillin, and 100g/mL of streptomycin (Gibco, Grand Island, NY), and the cells were incubated at 37℃ with 5% $CO_2$ /95% air. The media were changed every two to three days. When the confluence reached around 90%, cells was passaged using 0.05% Trypsin-EDTA (Gibco, Grand Island, NY).

### 4.2.2 Lentivirus production and transduction

293T cells produce lentivirus particles through the transient transfection of plasmids that encode for the components of the virion. The lentiviral vector can then be used to transduce the GFP-Luc gene through integration into the U87 MG genome.

293T cells were seeded into 100mm dishes and grown to about 80% confluency. The desired volume of each plasmid and chemical was calculated according to the following table.

| | **Amount required (μg/per 100 mm dish)** | **Required volume (μl/per 100 mm dish)** |
|---|---|---|
| pCMV-VSGS (Envelope plasmid) | 4 | |
| pMDL-G/P-RRE (Packaging plasmid) | 8 | |
| pRSV-REV (Packaging vector) | 6 | |
| Lenti-GFP-Luc # (Transfer vector) | 15 | |
| 2.5 M $CaCl_2$ | -- | 125 |
| 0.1X TE buffer | -- | * |
| 2X HBS | -- | 1,000 |
| **Total** | **--** | **2,000** |

* volume of TE buffer (μl) = 1,000 – volume of envelope plasmid, packaging plasmid, packaging vector, transfer vector, and $CaCl_2$.

# Lenti-GFP-Luc was kindly provided by Professor Gang Li (Dept. of O&T)

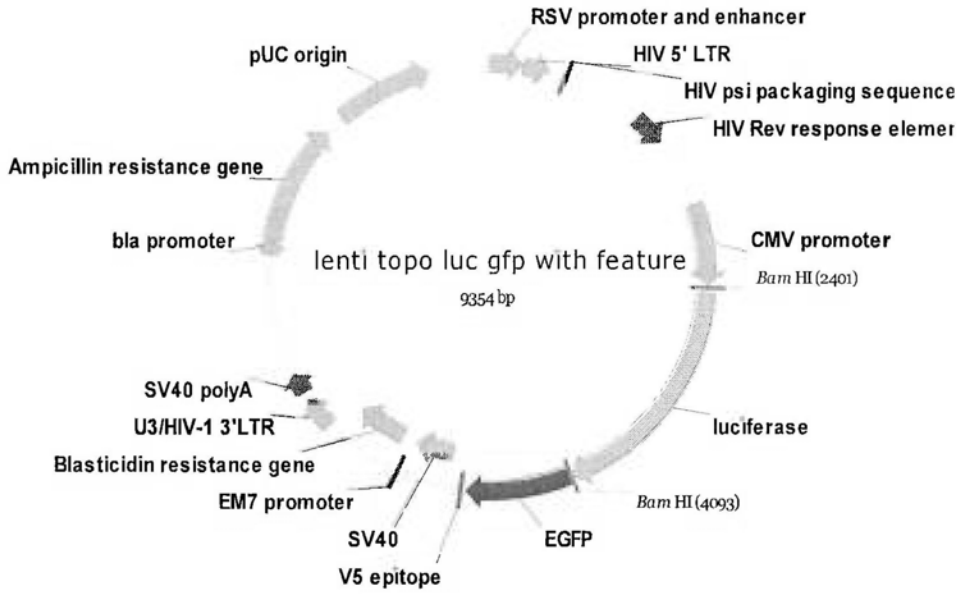


**Figure 4-1 Map of the transfer vector (lenti-GFP-Luc)**

DNA, $CaCl_2$ and TE buffer (10 mM of Tris pH 8.0, 1 mM of EDTA) were mixed in a 50ml conical vial. The mixture was slowly added into another 50 ml conical vial containing HEPES-buffered saline (HBS) (280 mM of NaCl, 50 mM of HEPES, 1.5 mM of $Na_2HPO_42 \cdot H_2O$, 10 mM of KCl, 12 mM of dextrose) while being vortexed at medium speed. The mixture was then pipetted immediately into each plate. Sixteen hours after transfection, the medium was aspirated and carefully replaced with 10 ml of fresh DMEM containing 10% FBS. After a further 48 hours growth, the viral supernatant was collected into 50 ml conical vials and centrifuged at 5,000 revolutions per minute (rpm) for 20 minutes at 4℃. The viral supernatant was filtered through a 0.22μm microfilter

and kept overnight at 4℃. On the second day, the viral supernatant was centrifuged again at 9,000 rpm overnight at 4℃. Finally, the supernatant was discarded and the virus pellet resuspended in TBS (800 mg of NaCl, 20 mg of KCl, 300 mg of Tris base in 100 ml of distilled water, pH 8.0).

Reverse transcription PCR and real-time PCR were used to determine the concentration of the virus. The viral supernatant was set as the template for reverse transcription using the Reverse Transcription System (Promega, Madison, WI). The 20μl reaction mix was set up as follows.

| **Component** | **Volume (μl)** |
|---|---|
| $MgCl_2$ (25 mM) | 2 |
| Reverse Transcription 5X Buffer | 4 |
| dNTP (10 mM) | 1 |
| Recombinant RNasin® Ribonulease Inhibitor | 0.5 |
| AMV Reverse Transcriptase | 0.5 |
| Random Primer | 1 |
| Viral supernatant | 1 |
| Diethyl pyrocarbonate (DEPC) water | 10 |
| **Total** | **20** |

The reaction mix was placed in a thermal cycler and run at a program of 25℃ for 5 minutes, 42℃ for 1 hour, 70℃ for 15 minutes, and 4℃ for 30 minutes. cDNA of the viral supernatant was generated as the product of the reverse transcription, and was used as the template for the real-time PCR. The reaction mix was set up as follows.

| **Component** | **Volume (µl)** |
|---|---|
| SYBR Green | 10 |
| Forward Primer | 0.5 |
| Reverse Primer | 0.5 |
| cDNA sample | 1 |
| Diethyl pyrocarbonate (DEPC) water | 8 |
| **Total** | **20** |

The reaction mix was placed in a thermal cycler, and the following program run.

| **Temperature and duration** | **Number of cycles** |
|---|---|
| 50℃, 2 minutes | 1 |
| 95℃, 10 minutes | 1 |
| 95℃, 15 seconds | 40 |
| 60℃, 1 minutes | |
| 60℃, 1 minutes | 1 |

5? $0^5$ U87 MG cells were seeded into each well of a six-well plate and cultured with MEM medium. After the cells had attached, the medium was exchanged for MEM medium containing the viral vector and polybrene. Sixteen hours after transduction, the medium was replaced again with fresh medium, and the cells were incubated for another 48 hours. The transduced cells were then subcultured onto a 100mm dish and selected with 10μg/ml of blasticidin (InvivoGen, San Diego, California).

### 4.2.3 Confirmation of the transduced cell lines

The transduced cells containing GFP gene were detected by fluorescence microscopy and digitally imaged (Nikon Inc, Tokyo, Japan). They were also tested by bioluminescence assay. In this process, exogenous luciferin is oxidized by luciferase to produce a bluish-green light. There is a positive correlation between the light density and the number of transduced cells.

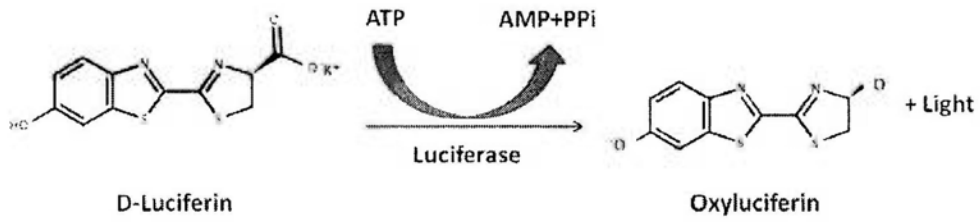


**Figure 4-2 Principle of bioluminescence assay**

1? $0^4$ U87-GFP-Luc cells were resuspended in PBS and seeded into a black 96-well plate. Then, 150 μg/ml of D-luciferin (Caliper LifeSciences, Hopkinton, MA) was added to the cell suspension and the cells were incubated at 37°C for 5 minutes. Immediately after incubation, the light intensity of each well was measured by a luminometer (VICTOR$^3$TM, Multilabel Counter, PerkinElmer).

### 4.2.4 Growth curve assay of the transduced cell line

The proliferation rate of the transduced U87 MG was investigated by comparison with untransduced U87 MG. 3.5? $0^4$ U87 MG and U87-GFP-Luc cells were separately seeded into a six-well plate with complete MEM medium. At 24, 48, 72, 96, and 120 hours after seeding, one well each of the U87 MG and U87-GFP-Luc was trypsinized and counted. The total number of cells and the culture time were used to draw a growth curve.

### 4.2.5 Establishment of the subcutaneous brain tumour model and treatment

All of the procedures were approved by the Animal Experiment Ethics Committee of the Chinese University of Hong Kong. Four-week-old nude male mice (n=30) were provided by the Laboratory Animal Services Center of the Chinese University of Hong Kong. Briefly, 5? $0^6$ U87-GFP-Luc cells were injected subcutaneously into the dorsal region of the mice. The animals were

allowed access to chow and water *ad libitum*. Their body weight, tumour size, and general condition were determined every two days.

The tumour volume was calculated by using the following formula.

Tumour Volume (V) = 0.5譏諡$^2$,

where a is the length and b the width of the tumour.

When the tumour volume reached 100 mm$^3$, the mice were randomly grouped and administrated with different concentration of lovastatin (control, 5 mg/Kg body weight · day and 10 mg/Kg body weight · day) with or without 200 ng TRAIL.

The lovastatin was converted to the active form by the following procedures: 480 mg of lovastatin was dissolved in 12.5 ml 96% ethanol. Then, 18 ml of 0.1 M NaOH was added and incubated at 50℃ for 2 hours. After incubation, the dissolved lovastatin was neutralized to pH 7 using 0.1 M HCl. Finally, the solution was diluted to the appropriate concentration by distilled water.

All of the nude mice received the lovastatin daily by intraperitoneal injection or peri-tumoral injection for 12 days. The nude mice of lovastatin plus TRAIL

group were peri-tumoral administrated with TRAIL during day 4 to day6 and day 10 and day12 after treatment start. During the experiment, the body weight, tumour size, and general condition were investigated every two days. IVIS images were also taken twice a week to confirm the tumour size. Thirteen days after the start of the treatment, the nude mice were sacrificed by an overdose of anesthetic. Tumour specimens and other organs were harvested for further experiments.

### 4.2.6 *In vivo* imaging system

During the observation, the tumour-bearing nude mice were imaged by an *in vivo* imaging system (Caliper, Hopkinton, MA). Before taking the images, luciferin (150 mg/kg body weight) was delivered by intraperitoneal (i.p.) injection. About seven minutes after the luciferin injection, the nude mice were anesthetized with isoflurane (Alfamedic Ltd. Hong Kong), which is an inhalational anesthetic. The appropriate exposure time was selected to prevent image saturation.

### 4.2.7 Immunohistochemical staining

The tumour specimens were fixed in 10% paraformaldehyde and processed for tissue sectioning. Paraffin-embedded sections (5 μm) were prepared for immunohistochemical staining.

In brief, the slides were put into an oven at 56°C for 30 minutes. They were then put into xylene to de-wax for 5 minutes. The xylene was changed three times. After the de-waxing procedure, the slides were hydrated in a graded series of concentrations of ethanol (100% → 95% → 80% → 70% → PBS). After washing with 0.003% Triton X-100, the slides were heated in 10 mM of sodium citrate buffer (pH 6.0) for 10 minutes and then cooled for another 10 minutes. The slides were washed in PBST and then immerged into 3% $H_2O_2$ for 10 minutes to block the endogenous peroxidase. The slides were then washed with 0.03% Triton X-100 again. Ten-percent normal blocking serum containing 0.3% Triton X-100 was used to block non-specific binding for 1 hour. The slides were then incubated with Ki-67 (Santa Cruz Biotechnology, Santa Cruz, CA, 1:50) and DR5 antibody (Cell Signaling Technology, Beverly, MA, 1:50) containing 0.3% Triton X-100 overnight at 4°C.

On the second day, the slides were washed again and incubated with specific biotinylated secondary antibody (Vector, Burlingame, CA, 1:100) for 1.5 hours at room temperature. After incubation and another three washes, the slides were incubated with horseradish peroxidase streptavidin (HRP Streptavidin) (Vector, Burlingame, CA, 1:200) for another 1.5 hours at room temperature. Finally, the slides were washed and incubated with a 0.05% DAB-plus reagent kit (Zymed, San Francisco, CA) for 1 to 5 minutes to allow the color to develop. The color reaction was stopped by immersing the slides in tap water. The slides were then

immersed in a graded series of concentrations of ethanol (70% → 80% → 95% → 100% → Xylene) before dehydration and mounting.

### 4.2.8 Expression of DR5 in tumour tissues as determined by western blotting

300 μl tissue lysis buffer (50 mM Tris-HCl (pH 7.4), 150 mM NaCl, 1% Triton X-100, 5 mM EDTA (pH 8.0) and 0.1% sodium dodecyl sulfate (SDS), with 1X protease inhibitors (Roche, Basel, Switzerland) and 100 μg/ml of phenylmethy-sulphonyl-fluoride (PMSF)) was added into per 100 mg tissue and then the samples were homogenized by pellet pestles cordless motor. After homogenization, the tissue samples were incubated on ice for 30 minutes. The samples were then centrifuged at 13,000 rpm for 30 minutes at 4°C and the supernatants were collected as total protein. The concentration of total protein was tested by Bio-Rad DC Protein Assay (Bio-Rad Laboratories, Inc. Hercules, CA) in accordance with the manufacturer's instruction. Each sample containing 40 μg of protein was separated by SDS-PAGE using 10% polyacrylamide gels and then transferred to nitrocellulose blotting membranes (Amersham Biosciences, Piscataway, NJ). The membranes were blocked in 5% non-fat milk for one hour at room temperature, probed with DR5 (Cell Signaling Technology, Beverly, MA, 1:1000) antibody overnight at 4°C, and then incubated with specific secondary antibody (Santa Cruz Biotechnology, Santa Cruz, CA) for one hour at room temperature. The membranes were then infiltrated with chemiluminescence (Amersham Biosciences, Piscataway, NJ) to detect the

target protein signal. Each membrane was stripped and the expression of GAPDH (Santa Cruz Biotechnology, Santa Cruz, CA, 1:5000) detected as an internal reference to ensure equal loading.

### 4.2.9 Statistical analysis

The data were presented as the mean ? one standard deviation (SD) for at least three separate determinations for each group. Differences between the groups were examined for statistical significance using a Student's *t*-test or one-way ANOVA followed by a Student's *t*-test. $P<0.05$ was used to indicate a statistically significant difference.

## 4.3 Results

### 4.3.1 Transduction rate observed by fluorescence microscopy

Green fluorescence protein (GFP) is widely used to label cells for observation by integrating the GFP gene into the cellular DNA. This allows researchers to detect specific types of cells both *in vitro* and *in vivo*. In this study, GFP was transduced into the U87 MG cells using a lentiviral system. After transduction, the cells were selected by blasticidin over a two-week period. During the selection, the transduction rate of the cells was determined daily by fluorescence microscopy (Figure 4-3).

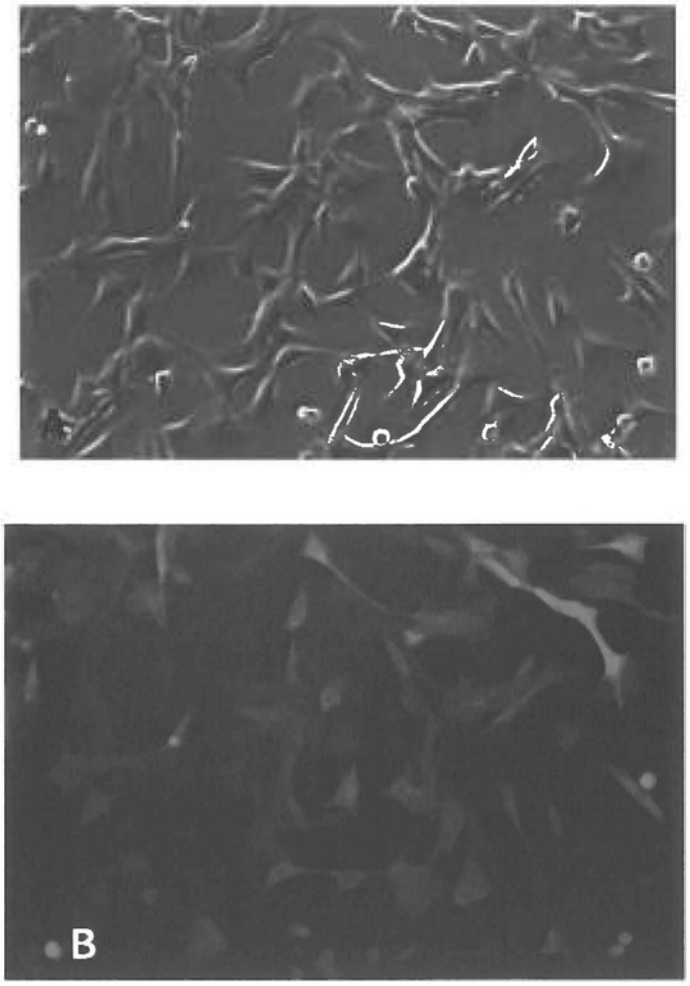


**Figure 4-3 Morphology of the transduced U87 MG**

After two weeks of selection by blasticidin, the transduced U87 MG cells were observed under an optical microscope (A) and a fluorescence microscope (B). Over 90% of the cells were transduced with GFP.

### 4.3.2 Bioluminescence assay of U87-GFP-Luc

The transduced U87 MG cells were used for the bioluminescence assay, which is a common method of confirming the transduction rate of luciferase. The assay was repeated at least three times using different passages of cell. Compared with the untransduced U87 MG, the transduced U87-GFP-Luc showed a significantly higher luminescence density (Figure 4-4).

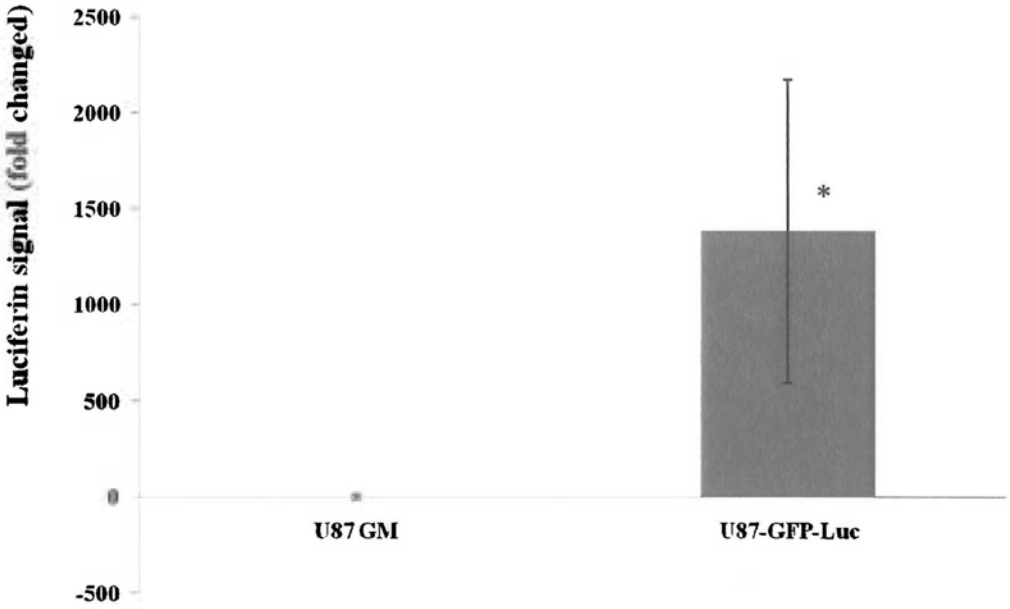


**Figure 4-4 Intensity of the luciferin signal in U87 MG and U87-GFP-Luc**

Exogenous luciferin was oxidized by luciferase in U87-GFP-Luc. Compared with U87 MG, the luciferin signal was 1,300-fold higher in the transduced U87 MG cells. Data are the mean ± S.D. of three separate experiments.

### 4.3.3 Cell proliferation of transduced and untransduced cells

The same amount of U87 MG and U87-GFP-Luc were seeded separately into a six-well plate. The growth curve showed that the growth rate became slow at about 96 hours after seeding. The observed growth patterns of the U87 MG and U87-GFP-Luc were similar (Figure 4-5).

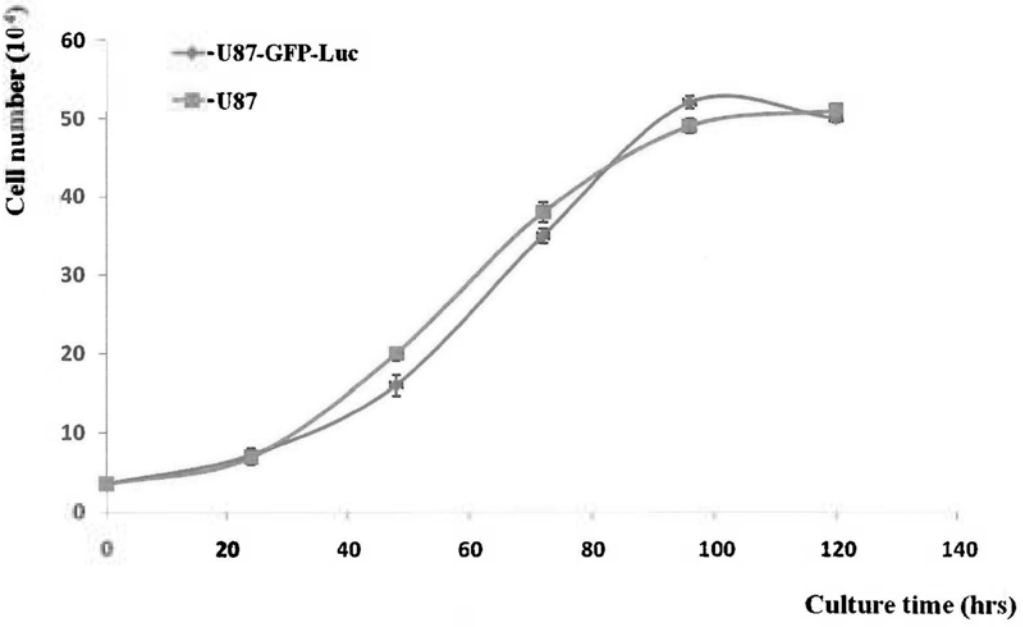


**Figure 4-5 Growth curves of transduced and untransduced U87 MG**

The growth rates of the two cell lines were the same regardless of whether the luciferase gene was present or absent. Data are the mean ± S.D. of three separate experiments.

### 4.3.4 Subcutaneous brain tumour model and IVIS image

The subcutaneous brain tumour model was established successfully by inoculation with 5? $0^6$ of U87-GFP-Luc. The body weight, tumour size, and general condition of nude mice were investigated. All of the mice recovered uneventfully from the tumour cell inoculation and received a normal diet. No anorexia, mania, or neurological symptoms were observed.

In most of the nude mice, a soft tumour mass was found at the inoculation site, which then disappeared slowly within three weeks of inoculation. After the three weeks had elapsed, solid masses were found that grew quickly (Figure 4.6). It took around one month to achieve a tumour volume of 100 $mm^3$, which is the threshold for treatment. Bioluminescence images of the nude mice were taken using IVIS to determine the tumour size and detect metastasis. The IVIS images showed that the luciferin intensity was consistent with the tumour size as measured with electronic calipers (Figure 4.7). However, no metastasis was found.

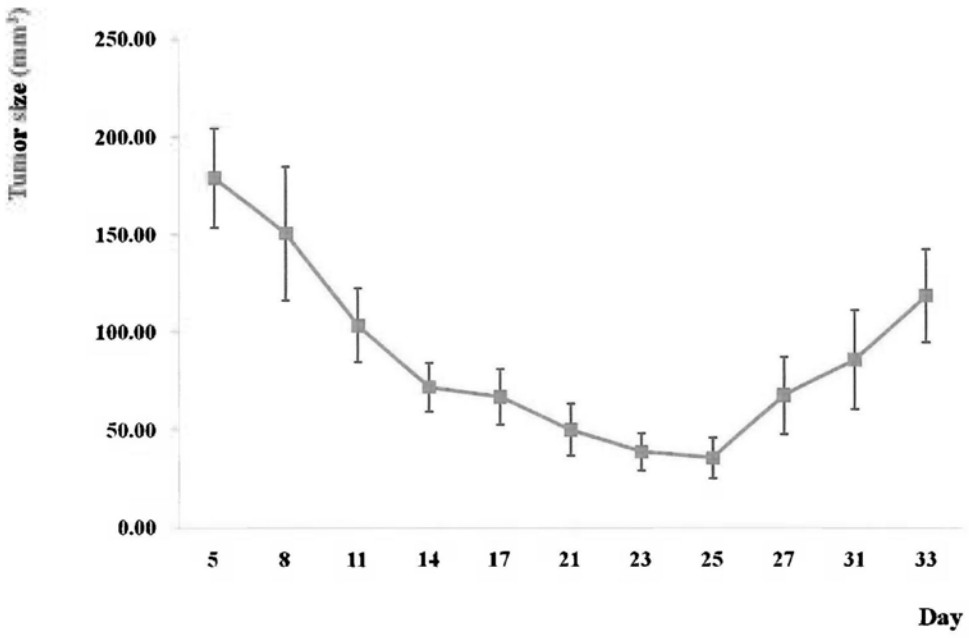


**Figure 4-6 Growth curve of transduced U87 MG in nude mice**

Initially, soft masses were found that were gradually absorbed until the tumour size was reduced to a minimum at around three weeks after inoculation. Subsequently, the tumours became harder and grew rapidly. Data are the mean ± S.D. of three separate experiments.

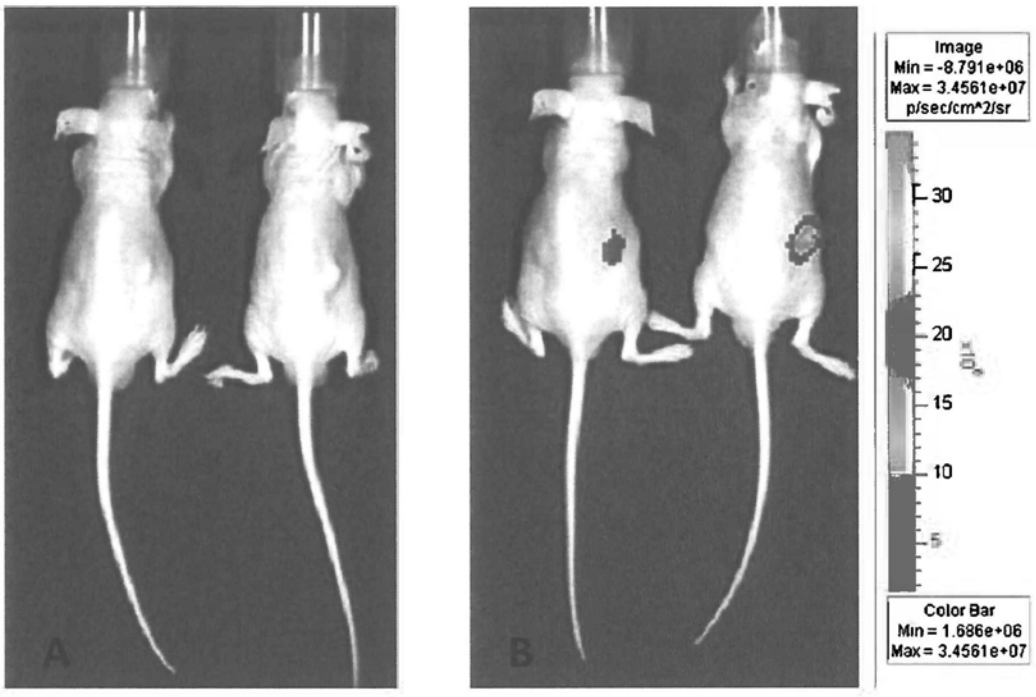


**Figure 4-7 IVIS imaging of the U87-GFP-Luc subcutaneous tumour model**

Subcutaneous tumours were found in the dorsal area. The larger tumours showed higher luciferin intensity, indicating a positive correlation between tumour size and bioluminescent signal.

### 4.3.5 Anti-tumour effect of lovastatin on glioblastoma animal model by intraperitoneal injection

U87 MG cells transduced with GFP and luciferase genes were used in our *in vivo* experiment. As mentioned, 5? $0^6$ U87-GFP-Luc cells were subcutaneously injected into the dorsal region of the model mice. It took around one month to achieve a tumour volume of 100 $mm^3$, which is regarded as the threshold for treatment. The mice were randomly divided into a control group (n=10), low-dose group (5 mg/Kg body weight · day lovastatin) (n=10), and high-dose group (10 mg/Kg body weight · day lovastatin) (n=10). During the observation, all of the animals received a normal diet and tolerated the treatment well. No neurological symptoms were found in any of the animals. Figure 4-8 shows the change in body weight of the mice after treatment. There was no difference between the control group and treatment group. However, thin limbs were found in the control group at the end of the investigation. The volume of subcutaneous tumour growth was also observed with electronic calipers. In the first week after treatment, the tumour size was not significantly different among the three groups. However, in the second week, the tumour growth rate was quite different. The tumour size in the control group increased markedly, whereas the tumours in the treatment group enlarged slowly. Statistical differences were found between the low- and high-dose lovastatin groups on day 12 after initiation of the treatment compared with the control group (811.59? 56.95; 478.52? 25.92 *v.s.* 1600.43? 73.82) (Figure 4-9). The IVIS imaging system was again used. The bioluminescent density was higher in the control group

than in the treatment group ($8.70\times10^{10}$ *v.s.* $3.33\times10^{10}$, $1.87\times10^{10}$) at the end of the observation. However, the luciferin density did not accord with the tumour size in all cases (Figure 4-10, Figure 4-11 and Figure 4-12).

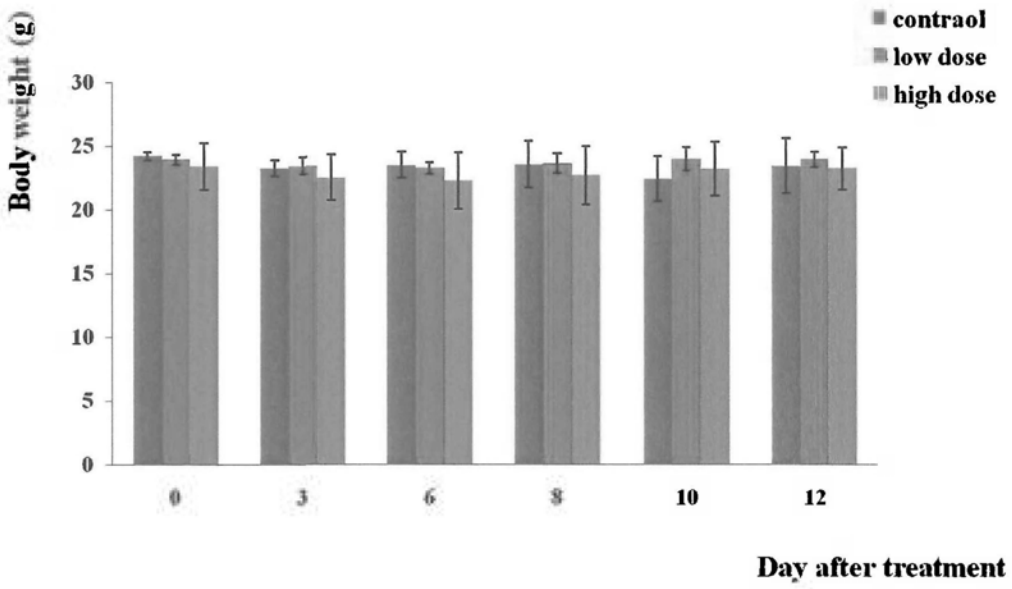


**Figure 4-8 Body weight change in the subcutaneous mouse model after treatment**

The animals received treatment daily via intraperitoneal injection. All of the nude mice were tolerant of the treatment and the body weight of each group was similar during the observation.

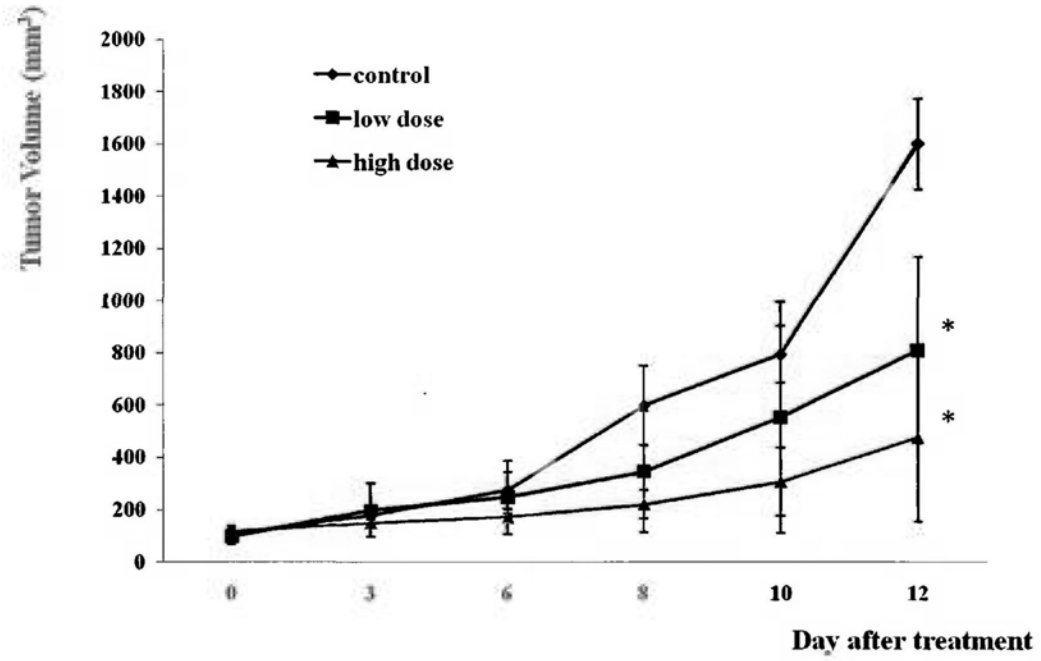


**Figure 4-9 Tumour volume in the subcutaneous mouse model after intraperitoneal administration of lovastatin**

Nude mice with subcutaneous brain tumours were randomly divided into three groups. The tumour volume of the mice receiving lovastatin was significantly smaller than that of the control group. The high-dose group showed the greatest anti-tumour effect. Data are the mean ± S.D. * $p < 0.05$ when compared with the control group.

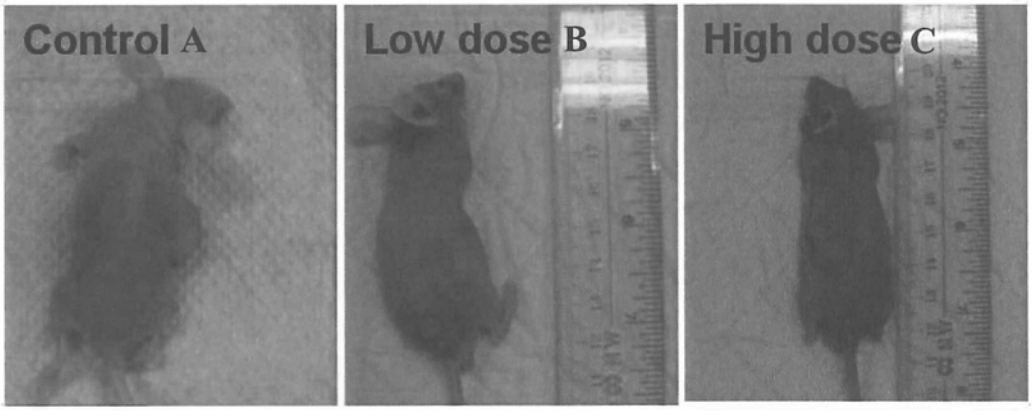


**Figure 4-10 Nude mice bearing subcutaneous brain tumours receiving lovastatin treatment by intraperitoneal injection**

Subcutaneous tumour model mice receiving different treatments, including control (A), 5 mg/Kg body weight • day lovastatin (B), and 10 mg/Kg body weight • day lovastatin (C) on day 13 after treatment.

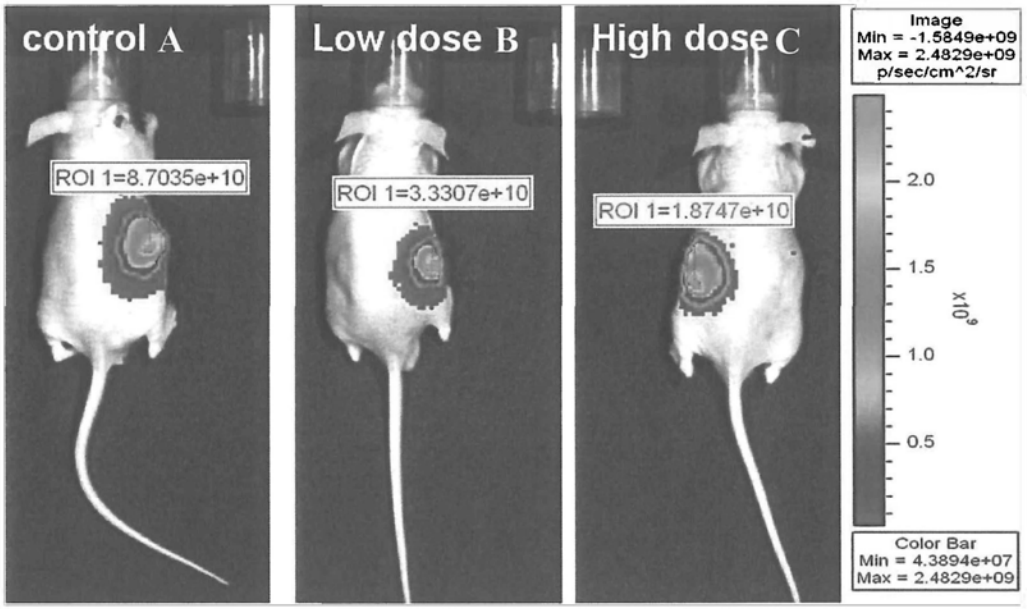


**Figure 4-11 IVIS imaging of the subcutaneous brain tumour mouse model**

Subcutaneous tumour model mice receiving different treatments, including control (A), 5 mg/Kg body weight • day lovastatin (B), and 10 mg/Kg body weight • day lovastatin (C) on day 13 after treatment.

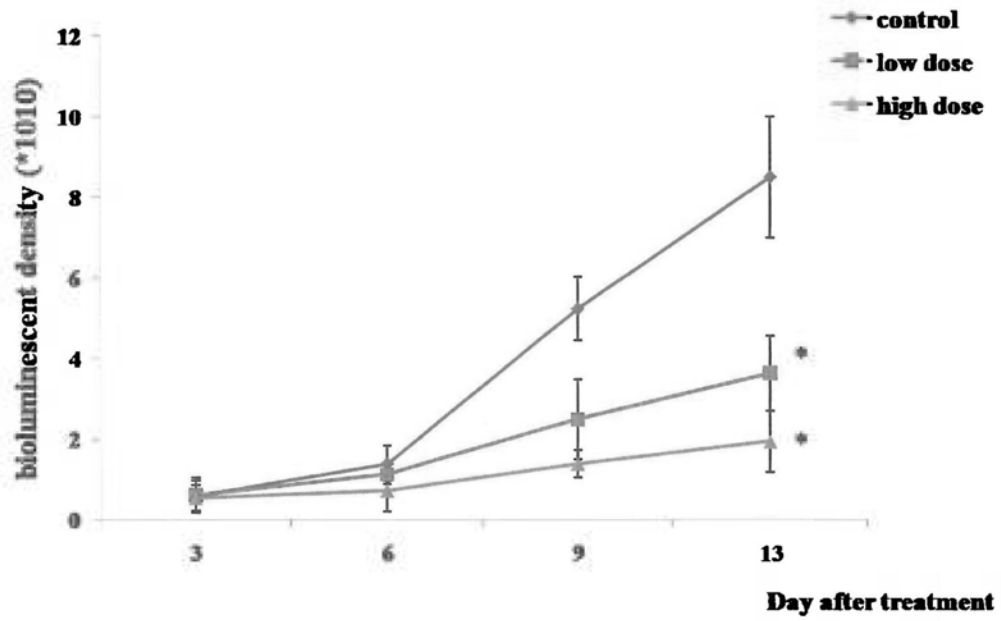


**Figure 4-12 The bioluminescent density of the tumour in the subcutaneous mouse model after intraperitoneal administration of lovastatin**

The bioluminescent density of nude mice with subcutaneous brain tumours were detected using IVIS system. Data are the mean ± S.D. * $p < 0.05$ when compared with the control group.

### 4.3.6 The Ki-67 expression of tumour tissue collected from nude mice receiving intraperitoneal administration of lovastatin as detected by immunohistochemical staining

After continuous intraperitoneal treatment of lovastatin for 12 days, the nude mice were sacrificed and tumour specimens were collected. The macroscopic appearances of all of the samples were smooth, solid, and with new blood vessel formation. Moreover, microvascular proliferation, cellular variety, and nuclear atypia were observed by haematoxylin and eosin staining both in control and lovastatin treatment groups (Data not shown). Ki-67 (Antigen KI-67) which is a specific proliferation marker for brain tumours was also determined using immunohistochemical staining. Compared with control group, the Ki-67 expression of high dose lovastatin group was markedly decreased (Figure 4-13). It indicated that lovastatin reduced the proliferation of tumour cells.

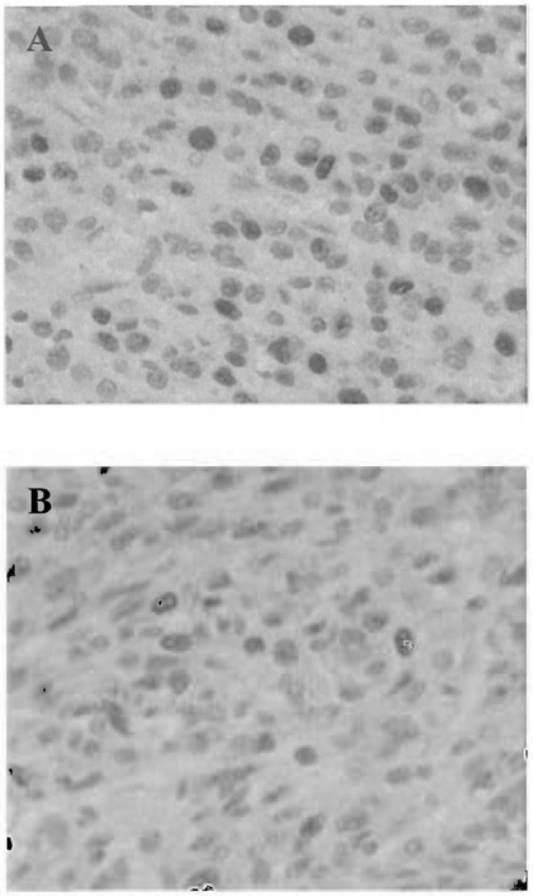


**Figure 4-13 The expression of Ki-67 in tumour tissue was detected by immunohistochemical staining**

The brown crystals that could be seen in the cell nuclei were the positive signal of Ki-67. The Ki-67 expression of lovastatin treatment group (B) was markedly lower than the control group (A).

### 4.3.7 The DR5 protein expression of tumour tissue collected from nude mice receiving intraperitoneal administration of lovastatin as determined by western blotting

It had been confirmed from our *in vitro* work that lovastatin sensitised TRAIL-induced apoptosis through up-regulation of DR5. Although intraperitoneal administration of lovastatin could inhibit tumour proliferation, the protein expression of DR5 in tumour tissue is uncertain. Therefore, the DR5 protein expression of tumour tissue samples collected from nude mice receiving intraperitoneal administration of lovastatin was detected by western blotting. We found that the DR5 expression in lovastatin group was similar to the control group (Figure 4-14).

A.

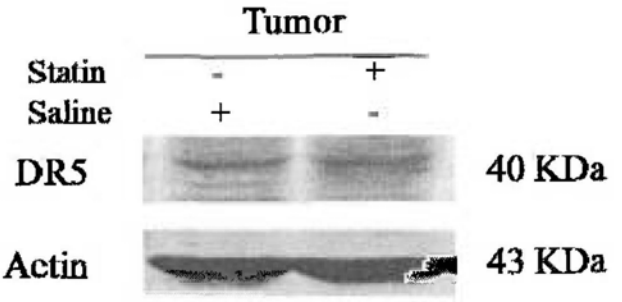


B.

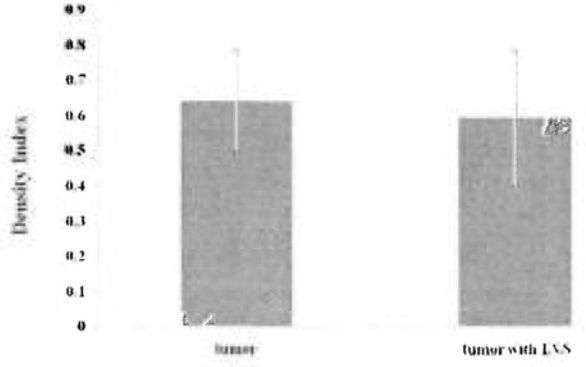


**Figure 4-14 The DR5 protein expression in tumour tissues harvested from nude mice receiving intraperitoneal administration of lovastatin**

Nude mice bearing subcutaneous glioblastoma received intraperitoneal administration of lovastatin. After 12 days treatment, the DR5 protein expression was not increased. Representative Western blots was shown (A). The target bands were normalized to GAPDH and the index of densities was calculated (B).

### 4.3.8 The DR5 protein expression of tumour tissue collected from nude mice receiving local peri-tumoral administration of lovastatin as investigated by western blotting and immunohistochemical staining

The subcutaneously brain tumour nude mice were randomly divided into two groups, including control group and lovastatin group (10 mg/Kg body weight • day). All animals received placebo or lovastatin daily by local peri-tumoral injection for 12 days. After treatment, the tumour tissue and liver tissue were harvested and the DR5 expression was tested using western blotting and immunohistochemical staining. Figure 4-15 showed the DR5 protein expression in tumour tissue and normal liver tissue. The DR5 protein expression was up-regulated after nude mice receiving local peri-tumoral administration of lovastatin, whereas the DR5 level in normal liver tissue was not changed. In addition, the increased DR5 expression was also observed in lovastatin-treated tissue (Figure 4-16).

**A.**

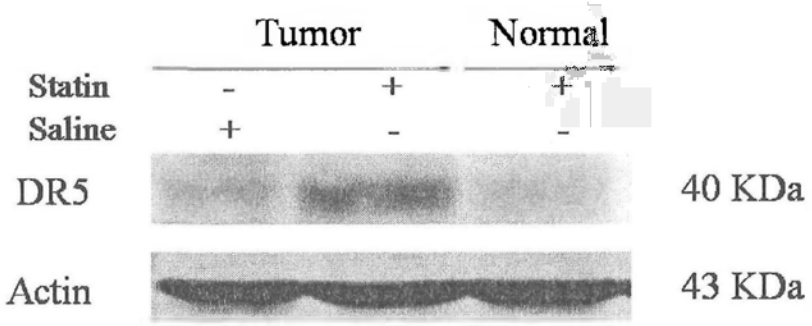

B.

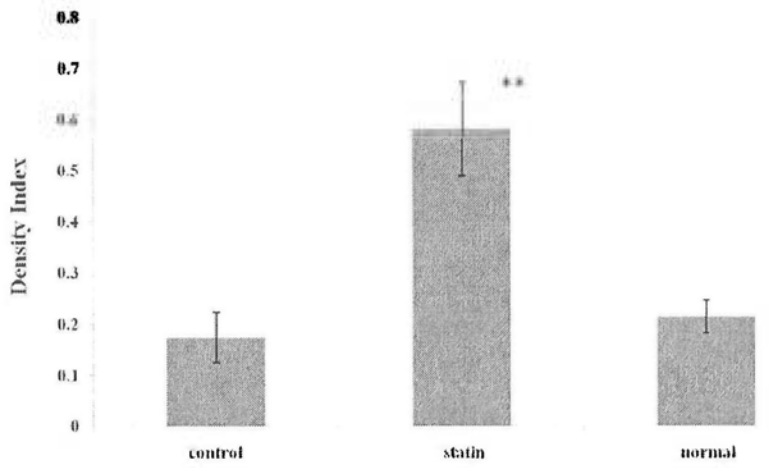


**Figure 4-15 The DR5 protein expression in tumour tissues harvested from nude mice receiving peri-tumoral administration of lovastatin**

Nude mice bearing subcutaneous glioblastoma received local peri-tumoral administration of lovastatin. After 12 days treatment, the DR5 protein expression in tumour tissue was markedly increased while the expression in normal liver tissue was not changed. Representative Western blots was shown (A). The target bands were normalized to GAPDH and the index of densities was calculated (B).

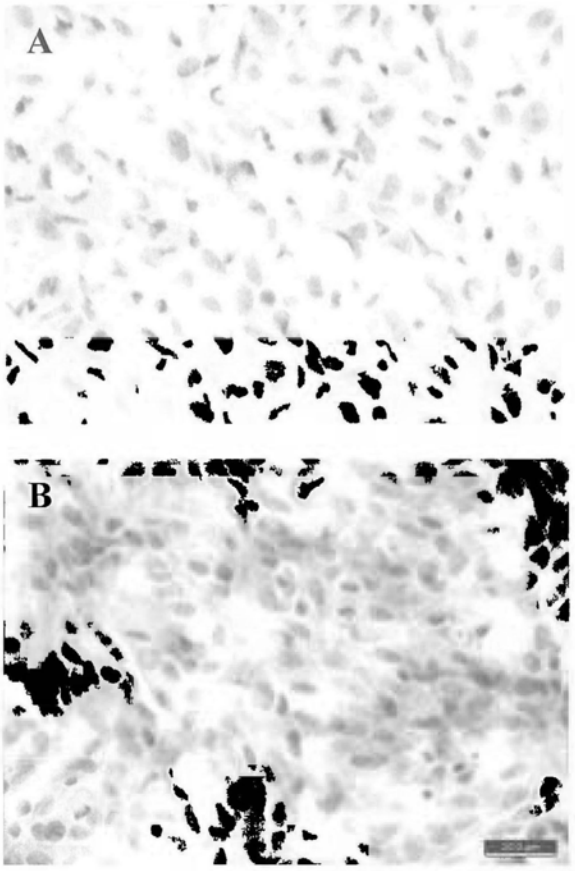


**Figure 4-16 The expression of DR5 in tumour tissue was detected by immunohistochemical staining**

Compared with control group (A), the DR5 expression of lovastatin treatment group (B) was significantly increased.

### 4.3.9 Synergistic effect of lovastatin and TRAIL on subcutaneous brain tumour model *in vivo*

The nude mice bearing subcutaneous brain tumour which achieved 100 $mm^3$ were randomly divided into a control group, lovastatin group (5 mg/Kg body weight · day lovastatin), and lovastatin plus TRAIL group (5 mg/Kg body weight · day lovastatin plus 200 ng TRAIL). The volume of subcutaneous tumour growth was observed by electronic calipers and IVIS system. The tumour size of lovastatin group and combination therapy group was significantly smaller than control group (Figure 4-17 and Figure 4-18). Especially in lovastatin plus TRAIL group, the tumour size was markedly suppressed during the treatment. The similar result was also observed by IVIS system. The luciferase signal of lovastatin plus TRAIL group was significantly week than control group or lovastatin group (Figure 4-19 and Figure 4-20).

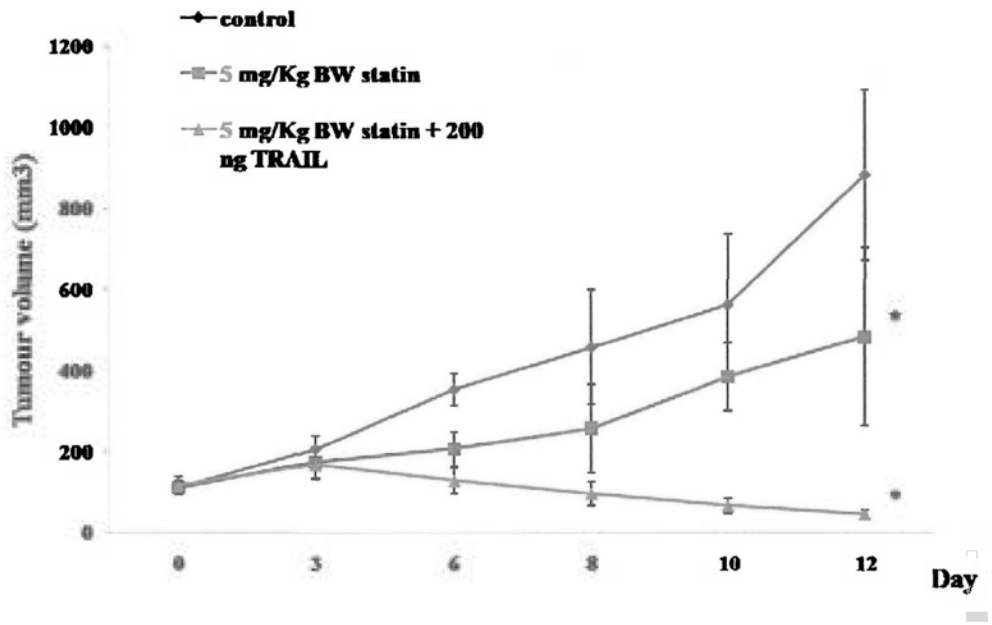


**Figure 4-17 Tumour volume in the subcutaneous mouse model after local peri-tumoral administration of lovastatin**

Nude mice with subcutaneous brain tumours were randomly divided into three groups. The tumour volume of the mice receiving lovastatin plus TRAIL was markedly diminished. Data are the mean ± S.D. * $p < 0.05$ when compared with the control group.

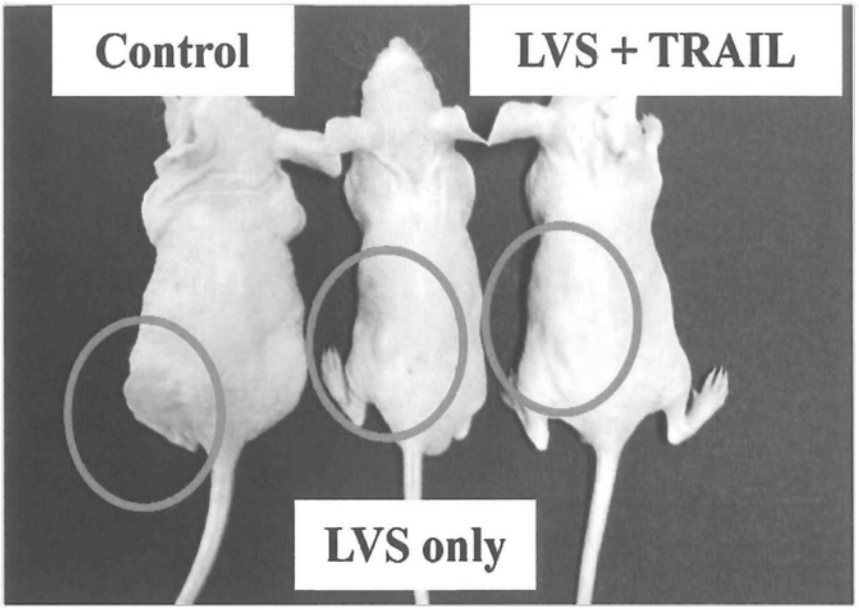


**Figure 4-18 Nude mice bearing subcutaneous brain tumours receiving peri-tumoral administration of lovastatin with/ without TRAIL**

Subcutaneous tumour model mice receiving different treatments, including control, 5 mg/Kg body weight • day lovastatin, and 5 mg/Kg body weight • day lovastatin plus 200 ng TRAIL on day 13 after treatment.

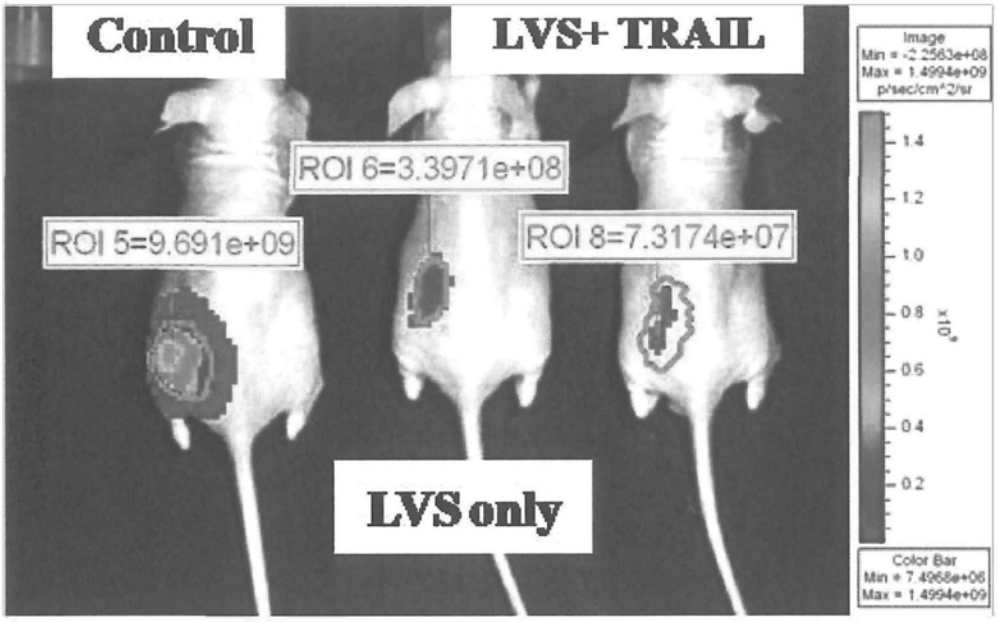


**Figure 4-19 IVIS imaging of the subcutaneous brain tumour mice receiving local peritumoral administration of lovastatin plus TRAIL**

Subcutaneous tumour model mice receiving different treatments, including control, 5 mg/Kg body weight • day lovastatin, and 5 mg/Kg body weight • day lovastatin plus 200 ng TRAIL on day 13 after treatment.

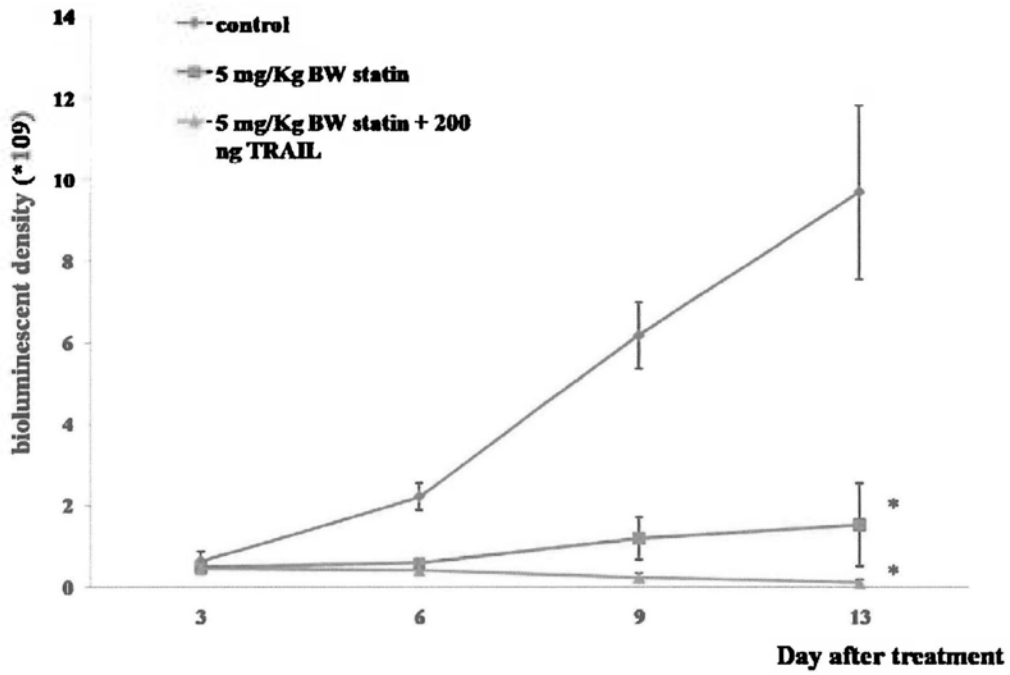


**Figure 4-20 The bioluminescent density of the tumour in the subcutaneous mouse model after local peri-tumoral administration of lovastatin with/ without TRAIL**

The bioluminescent density of nude mice with subcutaneous brain tumours were detected using IVIS system. Data are the mean ± S.D. * $p < 0.05$ when compared with the control group.

## 4.4 Discussion

*In vivo* imaging systems, such as MRI, PET, bioluminescence imaging (BLI), and fluorescence imaging, are widely accepted in animal experiments as providing meaningful data for pre-clinical trials. They are non-invasive, and allow researchers to obtain dynamic images. Among the various *in vivo* image modalities, bioluminescence and fluorescence imaging are more acceptable in animal experiments because they are quick and easy to perform and allow a high throughput. Compared with fluorescence imaging, bioluminescence imaging is more sensitive and shows minimal background signals from animal tissue (Troy, Jekic-McMullen et al. 2004). Thus, bioluminescence imaging is more attractive for *in vivo* experiments.

Bioluminescence imaging can reveal tumour development earlier, even if the tumour is unpalpable, undergoes necrosis, or micrometastasizes. Recently, it has been reported that the modified bioluminescence gene significantly improves the sensitivity of bioluminescence imaging, and makes the detection of single cells *in vivo* possible (Kim, Urban et al. 2010). Bioluminescence image also has an advantage for orthotopic models, which usually require a great quantity of animals to be sacrificed at each time point. To date, firefly luciferase remains the most common gene used in bioluminescence imaging. To set up the platform for luciferase-based bioluminescence imaging in this study, U87 MG cells expressing luciferase were used. The GFP gene was also transduced for histological testing and the identification of luciferase-positive cells.

In this study, we used the lentiviral transduction system which can integrate into the genome of non-proliferating cells (Bukrinsky, Haggerty et al. 1993). Unlike traditional transfection, the selection period for transduction is relatively shorter, and the transduced cells selected by the specific antibiotics are more stable. These advantages were displayed in our data. U87 MG cells transduced with GFP and luciferase gene were selected for two weeks by specific antibiotics, and the transduction rate was above 90%. In contrast, it takes at least one month for a stable cell line to be created with a traditional transfection system.

Several previous studies have confirmed the tumourigenesis property of the U87 MG cell line in nude mice. To confirm the carcinogenesis of transduced U87 MG cells, we observed the growth pattern of transduced and untransduced U87 MG cells. The results showed the growth curves of U87 MG and U87-GFP-Luc were similar; indicating that cell proliferation was not interrupted by lentiviral transduction or GFP and luciferase expression. Both fluorescent and bioluminescent signals were detected in the different cell passages, indicating that the lentivirus transduction was successful and persistent, and that the bioluminescent signal was transferred to the cell progeny. This is important for *in vivo* imaging, as it allows tumour development to be tracked over a long period.

The growth curve of U87-GFP-Luc cells in the nude mice was also investigated. Fake tumours were found in most of the mice at the early stage. These masses

were soft in quality and were absorbed slowly. This phenomenon may be related to an immune reaction to human cancer cells in nude mice, which still have a normal B cell function. Once the immune reaction period had expired, solid tumours emerged and grew quickly. It has been demonstrated that at least 800 cells are needed to detect bioluminescent signals, and that there is a positive correlation between cell number and signal density (Bai, Yan et al. 2011). According to our results, the luciferin density was detectable earlier, even when the tumour was not obvious and could not be measured accurately with electronic calipers. It is important for researchers to exactly determine the tumour development as early as possible.

*In vivo* imaging system is a non-invasive, reliable, and real-time method for used in animal experiments. This part of work established a stable luciferase-based *in vivo* imaging platform that is suitable for long-term observations. The GFP gene was also transduced into the cells of interest as a marker of positive transduction and use for the fluorescence imaging of non-living cells or tissue.

After the subcutaneous brain tumour model bearing luciferase gene was well established, the *in vivo* antitumour effect of lovastatin and TRAIL were evaluated using the above model. Nude mice bearing subcutaneous brain tumours were given different doses of lovastatin with / without TRAIL by different administrated method. All of the animals were tolerant of the dose of

lovastatin (5 mg/Kg body weight • day and 10 mg/Kg body weight • day lovastatin) and 200 ng TRAIL given by intraperitoneal or peri-tumoral injection. During the observation, all of the animals received a normal diet and the body weight of each group was similar, although the animals in control were obviously thin, indicating that the energy consumption in this group was greater than that in the treatment group.

The results also show that intraperitoneal injection of lovastatin treatment dose-dependently decreased tumour volume in nude mice subcutaneously. However, it must be noted that lovastatin only slowed down the tumour growth rate in our experiment. This indicates that lovastatin is insufficiently efficacious as a single reagent for cancer therapy, and needs to be combined with other drugs to amplify its antitumour effect. The Ki-67 expression detected by immunohistochemical staining also confirmed the inhibitory effect of tumour proliferation by lovastatin. However, intraperitoneal administration of lovastatin can not increase the DR5 protein expression in tumour tissues. It might due to the poor infiltration of lovastatin to tumour tissue after intraperitoneal administration.

In order to elevate the DR5 expression in tumour tissue, the method of administration was changed. After receiving local peri-tumoral administration of lovastatin, the DR5 protein expression was significantly upregulated. In

addition, the result of immunohistochemical staining also confirmed the lovastatin-induced DR5 upregulation in tumour tissue of nude mice. Furthermore, the normal liver tissues from the subcutaneous brain tumor mice receiving lovastatin treatment were also harvested. We found the DR5 expression of normal liver tissue was not increased even after receiving lovastatin treatment. It presents that local peri-tumoral administration of lovastatin only induced DR5 expression in tumour tissue but not in normal tissue. It further implies that normal tissues will not be attacked by TRAIL after local injection of lovastatin.

Moreover, the synergistic effect of lovastatin and TRAIL on glioblastoma animal model was also investigated. First, the nude mice bearing subcutaneous brain tumor were received lovastatin treatment for up-regulating DR5 expression in tumour tissue. Consequently, TRAIL was given in the interval of the treatment. After 12 days treatment, lovastatin produced synergistic effect with TRAIL to inhibit tumour growth in nude mice. This regime not only inhibits the growth rate of the tumour but also diminishs the tumour volume.

Another discovery that is worthy of note is the relationship between tumour size and luciferin intensity. In some cases, the tumour size in the low-dose lovastatin group was smaller than that in the high-dose group. However, the luciferin intensity in the low-dose group was higher. This indicates that measuring tumour volume with electron calipers is not the most accurate method of

evaluating the growth rate of tumours. Necrotic centers may occur and contribute to an increase in physical tumour size (Vaupel, Kallinowski et al. 1989) but a decrease in luciferin density. Thus, it is confirmed again *in vivo* imaging systems are a better method of detecting tumour growth and location.

# Chapter Five

# Conclusion and Future Prospects

## 5.1 Summary of results

1. Efficacy of lovastatin and TRAIL in combination

Lovastatin and TRAIL in combination were found to have a synergistic antitumour effect in four human glioblastoma cell lines, including A172, M059J, M059K, and U87 MG. The major mode of cell death is apoptosis.

2. Mechanism by which lovastatin sensitises TRAIL-induced apoptosis.

(a) TRAIL-induced apoptosis is sensitised by lovastatin through an increase in DR5 expression, indicating DR5 is a potential biomarker for screening glioblastoma patients who need to receive lovastatin therapy for upregulating DR5 expression in tumour tissue.

(b) The up-regulation of DR5 is related to the NF-κB pathway. The down-regulation of activated NF-κB p65 raised the DR5 expression via inactivation of phosphorylated IκBα and phosphorylated IKK α/β.

(c) MAPK pathway is also related to the up-regulation of DR5 through a decrease in ERK/MAPK expression and an increase in JNK/p38 expression.

3. Preclinical animal studies in nude mice model of GBM

(a) Lovastatin significantly inhibits the tumour growth rate by intraperitoneal injection, but not increased the DR5 expression in tumour tissue.

(b) DR5 expression in tumour tissue is markedly increased with peri-tumoral injection of lovastatin.

(c) A synergistic effect of lovastatin and TRAIL was found *in vivo*, suggesting combination of lovastatin and TRAIL is a feasible treatment strategy for TRAIL-resistant GBM.

## 5.2 Conclusion

Our study shows that lovastatin and TRAIL have a synergistic anti-tumour effect on glioblastoma both *in vitro* and *in vivo*. Lovastatin sensitises TRAIL-induced apoptosis through the up-regulation of DR5. This may be due to the interaction of multiple pathways, including the down-regulation of NF-kB p65 and ERK/MAPK expression and the up-regulation of JNK/p38 expression. The proposed mechanism is graphically represented in Figure 5.

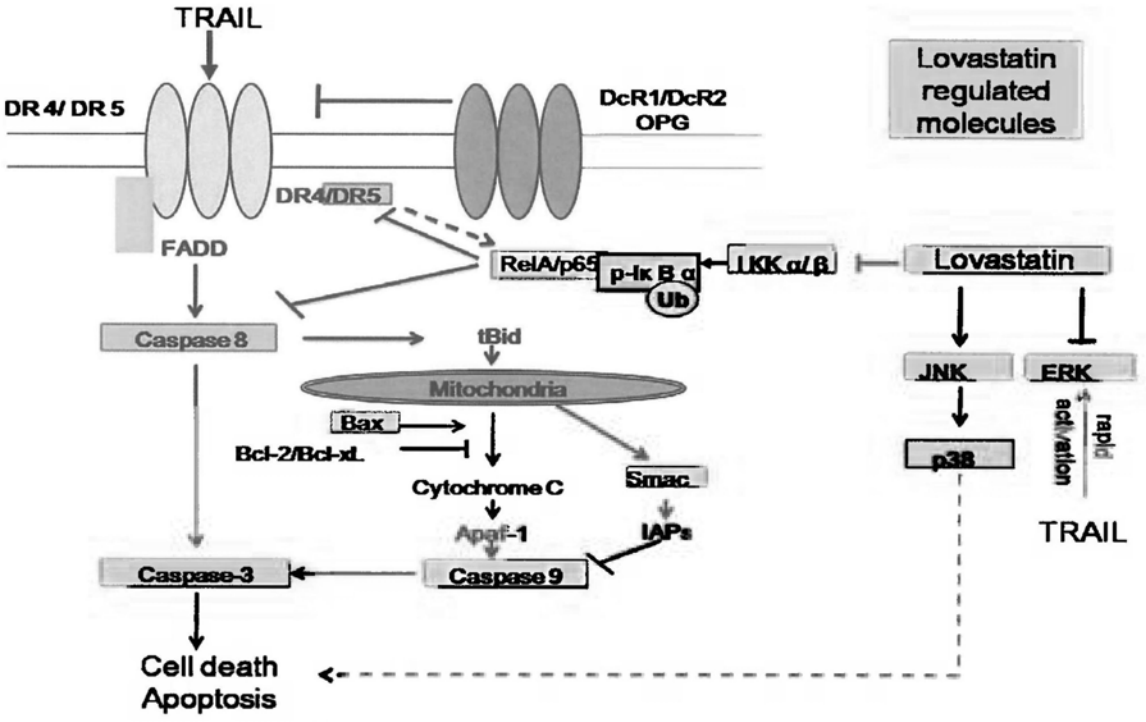


**Figure 5 Schematic representation of the mechanism of TRAIL-induced apoptosis sensitised by lovastatin in human glioblastoma cells**

## 5.3 Future prospects

Our study confirms the synergistic antitumour effect of TRAIL and lovastatin on human glioblastoma both *in vitro* and *in vivo*, and indicates that the mechanism of TRAIL-induced apoptosis by lovastatin involves the interaction of multiple pathways. These findings provide new insights into glioblastoma therapy. However, the orthotopic model was not performed in this project. It is necessary to confirm the effect of the blood-brain barrier on treatment efficacy.

In addition, we have confirmed that the lovastatin-sensitised TRAIL-induced apoptosis is affected by multiple pathways. In order to understand its mechanism clearly, it is important to select more signal pathway that might be related using RNA array. Moreover, the drugs which regulate NF-κB pathway might have potential to elevate the expression of death receptor and could be selected as another sensitiser of TRAIL-induced apoptosis.

# References


(1994). "Randomised trial of cholesterol lowering in 4444 patients with coronary heart disease: the Scandinavian Simvastatin Survival Study (4S)." Lancet **344**(8934): 1383-1389.

(2001). "Randomized trial of procarbazine, lomustine, and vincristine in the adjuvant treatment of high-grade astrocytoma: a Medical Research Council trial." J Clin Oncol **19**(2): 509-518.

Abayasiriwardana, K. S., D. Barbone, et al. (2007). "Malignant mesothelioma cells are rapidly sensitized to TRAIL-induced apoptosis by low-dose anisomycin via Bim." Mol Cancer Ther **6**(10): 2766-2776.

Aggarwal, B. B. (2004). "Nuclear factor-kappaB: the enemy within." Cancer Cell **6**(3): 203-208.

Aktas, O., U. Schulze-Topphoff, et al. (2007). "The role of TRAIL/TRAIL receptors in central nervous system pathology." Front Biosci **12**: 2912-2921.

Albayrak, B., A. F. Samdani, et al. (2004). "Intra-operative magnetic resonance imaging in neurosurgery." Acta Neurochir (Wien) **146**(6): 543-556; discussion 557.

Almasan, A. and A. Ashkenazi (2003). "Apo2L/TRAIL: apoptosis signaling, biology, and potential for cancer therapy." Cytokine Growth Factor Rev **14**(3-4): 337-348.

Anita C. Bellail, P. M., Chunhai Hao (2009). Targeting of TRAIL apoptotic pathways for glioblastoma therapies, in CNS Caner - Models, markers, prognostic factors, targets and therapeutic approaches. E. G. Meir, Humana Press: 977-1099.

Aranha, M. M., P. M. Borralho, et al. (2007). "NF-kappaB and apoptosis in colorectal tumourigenesis." Eur J Clin Invest **37**(5): 416-424.

Arts, H. J., S. de Jong, et al. (2004). "Chemotherapy induces death receptor 5 in epithelial ovarian carcinoma." Gynecol Oncol **92**(3): 794-800.

Ashkenazi, A. (2002). "Targeting death and decoy receptors of the tumour-necrosis factor superfamily." Nat Rev Cancer **2**(6): 420-430.

Ashkenazi, A. and V. M. Dixit (1998). "Death receptors: signaling and modulation." Science **281**(5381): 1305-1308.

Ashkenazi, A., R. C. Pai, et al. (1999). "Safety and antitumor activity of recombinant soluble Apo2 ligand." J Clin Invest **104**(2): 155-162.

Bai, X., Y. Yan, et al. (2011). "Tracking long-term survival of intramyocardially delivered human adipose tissue-derived stem cells using bioluminescence imaging." Mol Imaging Biol **13**(4): 633-645.

Barrios-Gonzalez, J. and R. U. Miranda (2010). "Biotechnological production and applications of statins." Appl Microbiol Biotechnol **85**(4): 869-883.

Berger, M. S. (1994). "Malignant astrocytomas: surgical aspects." Semin Oncol **21**(2): 172-185.

Blais, L., A. Desgagne, et al. (2000). "3-Hydroxy-3-methylglutaryl coenzyme A reductase inhibitors and the risk of cancer: a nested case-control study." Arch Intern Med **160**(15): 2363-2368.

Bock, H. C., M. J. Puchner, et al. (2010). "First-line treatment of malignant glioma with carmustine implants followed by concomitant radiochemotherapy: a multicenter experience." Neurosurg Rev **33**(4): 441-449.

Bodmer, J. L., P. Meier, et al. (2000). "Cysteine 230 is essential for the structure and activity of the cytotoxic ligand TRAIL." J Biol Chem **275**(27): 20632-20637.

Bukrinsky, M. I., S. Haggerty, et al. (1993). "A nuclear localization signal within HIV-1 matrix protein that governs infection of non-dividing cells." Nature **365**(6447): 666-669.

Cafforio, P., F. Dammacco, et al. (2005). "Statins activate the mitochondrial pathway of apoptosis in human lymphoblasts and myeloma cells." Carcinogenesis **26**(5): 883-891.

Capala, J., B. H. Stenstam, et al. (2003). "Boron neutron capture therapy for glioblastoma multiforme: clinical studies in Sweden." J Neurooncol **62**(1-2): 135-144.

CBTRUS (2002-2006). "2010 CBTRUS Statistical Report Tables."

Chakravarti, A., J. S. Loeffler, et al. (2002). "Insulin-like growth factor receptor I mediates resistance to anti-epidermal growth factor receptor therapy in primary human glioblastoma cells through continued activation of phosphoinositide 3-kinase signaling." Cancer Res **62**(1): 200-207.

Chan, D. Y., G. G. Chen, et al. (2008). "Lovastatin sensitized human glioblastoma cells to TRAIL-induced apoptosis." J Neurooncol **86**(3): 273-283.

Chan, K. K., A. M. Oza, et al. (2003). "The statins as anticancer agents." Clin Cancer Res **9**(1): 10-19.

Chandy, T., G. S. Das, et al. (2000). "5-Fluorouracil-loaded chitosan coated polylactic acid microspheres as biodegradable drug carriers for cerebral tumours." J Microencapsul **17**(5): 625-638.

Chawla-Sarkar, M., S. I. Bae, et al. (2004). "Downregulation of Bcl-2, FLIP or IAPs (XIAP and survivin) by siRNAs sensitizes resistant melanoma cells to Apo2L/TRAIL-induced apoptosis." Cell Death Differ **11**(8): 915-923.

Chen, J., X. Sun, et al. (2010). "Cisplatin-enhanced sensitivity of glioblastoma multiforme U251 cells to adenovirus-delivered TRAIL in vitro." Tumour Biol **31**(6): 613-622.

Chen, X., K. Kandasamy, et al. (2003). "Differential roles of RelA (p65) and c-Rel subunits of nuclear factor kappa B in tumor necrosis factor-related apoptosis-inducing ligand signaling." Cancer Res **63**(5): 1059-1066.

Chen, X., H. Thakkar, et al. (2001). "Constitutively active Akt is an important regulator of TRAIL sensitivity in prostate cancer." Oncogene **20**(42): 6073-6083.

Chinnaiyan, A. M., K. O'Rourke, et al. (1995). "FADD, a novel death domain-containing protein, interacts with the death domain of Fas and initiates apoptosis." Cell **81**(4): 505-512.

Chinnaiyan, A. M., U. Prasad, et al. (2000). "Combined effect of tumor necrosis factor-related apoptosis-inducing ligand and ionizing radiation in breast cancer therapy." Proc Natl Acad Sci U S A **97**(4): 1754-1759.

Cummins, J. M., M. Kohli, et al. (2004). "X-linked inhibitor of apoptosis protein (XIAP) is a nonredundant modulator of tumor necrosis factor-related apoptosis-inducing ligand (TRAIL)-mediated apoptosis in human cancer cells." Cancer Res **64**(9): 3006-3008.

Cusack, J. C., Jr., R. Liu, et al. (2000). "Inducible chemoresistance to 7-ethyl-10-[4-(1-piperidino)-1-piperidino]-carbonyloxycamptothe cin (CPT-11) in colorectal cancer cells and a xenograft model is overcome by inhibition of nuclear factor-kappaB activation." Cancer Res **60**(9): 2323-2330.

Daniels, R. A., H. Turley, et al. (2005). "Expression of TRAIL and TRAIL receptors in normal and malignant tissues." Cell Res **15**(6): 430-438.

Davis, F. G., N. Malinski, et al. (1996). "Primary brain tumor incidence rates in four United States regions, 1985-1989: a pilot study." Neuroepidemiology **15**(2): 103-112.

Degli-Esposti, M. A., P. J. Smolak, et al. (1997). "Cloning and characterization of TRAIL-R3, a novel member of the emerging TRAIL receptor family." J Exp Med **186**(7): 1165-1170.

Dolcet, X., D. Llobet, et al. (2005). "NF-kB in development and progression of human cancer." Virchows Arch **446**(5): 475-482.

Dorr, J., I. Bechmann, et al. (2002). "Lack of tumor necrosis factor-related apoptosis-inducing ligand but presence of its receptors in the human brain." J Neurosci **22**(4): RC209.

Dorsey, J. F., A. Mintz, et al. (2009). "Tumor necrosis factor-related apoptosis-inducing ligand (TRAIL) and paclitaxel have cooperative in vivo effects against glioblastoma multiforme cells." Mol Cancer Ther **8**(12): 3285-3295.

Downs, J. R., M. Clearfield, et al. (1998). "Primary prevention of acute coronary events with lovastatin in men and women with average cholesterol levels: results of AFCAPS/TexCAPS. Air Force/Texas Coronary Atherosclerosis Prevention Study." JAMA **279**(20): 1615-1622.

Duffau, H., L. Capelle, et al. (2003). "Usefulness of intraoperative electrical subcortical mapping during surgery for low-grade gliomas located within eloquent brain regions: functional results in a consecutive series of 103 patients." J Neurosurg **98**(4): 764-778.

Edwards, C. J. and T. D. Spector (2002). "Statins as modulators of bone formation." Arthritis Res **4**(3): 151-153.

Edwards, P. A. and J. Ericsson (1999). "Sterols and isoprenoids: signaling molecules derived from the cholesterol biosynthetic pathway." Annu Rev Biochem **68**: 157-185.

Egan, L. J. and M. Toruner (2006). "NF-kappaB signaling: pros and cons of altering NF-kappaB as a therapeutic approach." Ann N Y Acad Sci **1072**: 114-122.

Eggert, A., M. A. Grotzer, et al. (2001). "Resistance to tumor necrosis factor-related apoptosis-inducing ligand (TRAIL)-induced apoptosis in neuroblastoma cells correlates with a loss of caspase-8 expression." Cancer Res **61**(4): 1314-1319.

Ehtesham, M., P. Kabos, et al. (2002). "Induction of glioblastoma apoptosis using neural stem cell-mediated delivery of tumor necrosis factor-related apoptosis-inducing ligand." Cancer Res **62**(24): 7170-7174.

El Fajoui, Z., F. Toscano, et al. (2011). "Oxaliplatin Sensitizes Human Colon Cancer Cells to TRAIL Through JNK-Dependent Phosphorylation of Bcl-xL." Gastroenterology **141**(2): 663-673.

Emery, J. G., P. McDonnell, et al. (1998). "Osteoprotegerin is a receptor for the cytotoxic ligand TRAIL." J Biol Chem **273**(23): 14363-14367.

Endo, A., M. Kuroda, et al. (1976). "Competitive inhibition of 3-hydroxy-3-methylglutaryl coenzyme A reductase by ML-236A and ML-236B fungal metabolites, having hypocholesterolemic activity." FEBS Lett **72**(2): 323-326.

Figueiredo, E. G., J. W. Faria, et al. (2010). "Treatment of recurrent glioblastoma with intra-arterial BCNU [1, 3-bis (2-chloroethyl)-1-nitrosourea]." Arq Neuropsiquiatr **68**(5): 778-782.

Fiveash, J. B., G. Y. Gillespie, et al. (2008). "Enhancement of glioma radiotherapy and chemotherapy response with targeted antibody therapy against death receptor 5." Int J Radiat Oncol Biol Phys **71**(2): 507-516.

Fox, N. L., R. Humphreys, et al. (2010). "Tumor Necrosis Factor-related apoptosis-inducing ligand (TRAIL) Receptor-1 and Receptor-2 agonists for cancer therapy." Expert Opin Biol Ther **10**(1): 1-18.

Frank, S., U. Kohler, et al. (1999). "Expression of TRAIL and its receptors in human brain tumors." Biochem Biophys Res Commun **257**(2): 454-459.

French, L. E. and J. Tschopp (2002). "Defective death receptor signaling as a cause of tumor immune escape." Semin Cancer Biol **12**(1): 51-55.

Frese, S., F. Pirnia, et al. (2003). "PG490-mediated sensitization of lung cancer cells to Apo2L/TRAIL-induced apoptosis requires activation of ERK2." Oncogene **22**(35): 5427-5435.

Frick, M., J. Dulak, et al. (2003). "Statins differentially regulate vascular endothelial growth factor synthesis in endothelial and vascular smooth muscle cells." Atherosclerosis **170**(2): 229-236.

Fulda, S., M. U. Kufer, et al. (2001). "Sensitization for death receptor- or drug-induced apoptosis by re-expression of caspase-8 through demethylation or gene transfer." Oncogene **20**(41): 5865-5877.

Gaiser, T., M. R. Becker, et al. (2008). "TRAIL-mediated apoptosis in malignant glioma cells is augmented by celecoxib through proteasomal degradation of survivin." Neurosci Lett **442**(2): 109-113.

Gajewski, T. F. (2007). "On the TRAIL toward death receptor-based cancer therapeutics." J Clin Oncol **25**(11): 1305-1307.

Gauthaman, K., C. Y. Fong, et al. (2009). "Statins, stem cells, and cancer." J Cell Biochem **106**(6): 975-983.

Geletneky, K., A. D. Hartkopf, et al. (2010). "Therapeutic implications of the enhanced short and long-term cytotoxicity of radiation treatment followed by oncolytic parvovirus H-1 infection in high-grade glioma cells." Bioeng Bugs **1**(6): 429-433.

Genc, S., M. Y. Egrilmez, et al. (2009). "TNF-related apoptosis-inducing ligand level in Alzheimer's disease." Neurol Sci **30**(3): 263-267.

Germershausen, J. I., V. M. Hunt, et al. (1989). "Tissue selectivity of the cholesterol-lowering agents lovastatin, simvastatin and pravastatin in rats in vivo." Biochem Biophys Res Commun **158**(3): 667-675.

Ghosh, S. and M. Karin (2002). "Missing pieces in the NF-kappaB puzzle." Cell **109 Suppl**: S81-96.

Goffman, T. E., L. J. Dachowski, et al. (1992). "Long-term follow-up on National Cancer Institute Phase I/II study of glioblastoma multiforme treated with iododeoxyuridine and hyperfractionated irradiation." J Clin Oncol **10**(2): 264-268.

Goldstein, J. L. and M. S. Brown (1990). "Regulation of the mevalonate pathway." Nature **343**(6257): 425-430.

Goncharenko-Khaider, N., D. Lane, et al. (2010). "The inhibition of Bid expression by Akt leads to resistance to TRAIL-induced apoptosis in ovarian cancer cells." Oncogene **29**(40): 5523-5536.

Grandi, P., J. Fernandez, et al. (2010). "Targeting HSV-1 virions for specific binding to epidermal growth factor receptor-vIII-bearing tumor cells." Cancer Gene Ther **17**(9): 655-663.

Griffith, T. S., W. A. Chin, et al. (1998). "Intracellular regulation of TRAIL-induced apoptosis in human melanoma cells." J Immunol **161**(6): 2833-2840.

Griffith, T. S. and D. H. Lynch (1998). "TRAIL: a molecule with multiple receptors and control mechanisms." Curr Opin Immunol **10**(5): 559-563.

Griffith, T. S., S. R. Wiley, et al. (1999). "Monocyte-mediated tumoricidal activity via the tumor necrosis factor-related cytokine, TRAIL." J Exp Med **189**(8): 1343-1354.

Gross, A., J. Jockel, et al. (1998). "Enforced dimerization of BAX results in its translocation, mitochondrial dysfunction and apoptosis." EMBO J **17**(14): 3878-3885.

Grund, K., R. Ahmadi, et al. (2008). "Troglitazone-mediated sensitization to TRAIL-induced apoptosis is regulated by proteasome-dependent degradation of FLIP and ERK1/2-dependent phosphorylation of BAD." Cancer Biol Ther **7**(12): 1982-1990.

Guijarro, C., Y. Kim, et al. (1996). "Lovastatin inhibits lipopolysaccharide-induced NF-kappaB activation in human mesangial cells." Nephrol Dial Transplant **11**(6): 990-996.

Hall, M. A. and J. L. Cleveland (2007). "Clearing the TRAIL for Cancer Therapy." Cancer Cell **12**(1): 4-6.

Halpin, R. A., E. H. Ulm, et al. (1993). "Biotransformation of lovastatin. V. Species differences in in vivo metabolite profiles of mouse, rat, dog, and human." Drug Metab Dispos **21**(6): 1003-1011.

Hao, C., F. Beguinot, et al. (2001). "Induction and intracellular regulation of tumor necrosis factor-related apoptosis-inducing ligand (TRAIL) mediated apotosis in human malignant glioma cells." Cancer Res **61**(3): 1162-1170.

Harikumar, K. B., B. Sung, et al. (2010). "Escin, a pentacyclic triterpene, chemosensitizes human tumor cells through inhibition of nuclear factor-kappaB signaling pathway." Mol Pharmacol **77**(5): 818-827.

Hatanpaa, K. J., S. Burma, et al. (2010). "Epidermal growth factor receptor in glioma: signal transduction, neuropathology, imaging, and radioresistance." Neoplasia **12**(9): 675-684.

He, Q., J. Shi, et al. (2010). "Dihydroartemisinin upregulates death receptor 5 expression and cooperates with TRAIL to induce apoptosis in human prostate cancer cells." Cancer Biol Ther **9**(10): 819-824.

Hebert, P. R., J. M. Gaziano, et al. (1997). "Cholesterol lowering with statin drugs, risk of stroke, and total mortality. An overview of randomized trials." JAMA **278**(4): 313-321.

Hefti, M., G. von Campe, et al. (2008). "5-aminolevulinic acid induced protoporphyrin IX fluorescence in high-grade glioma surgery: a one-year experience at a single institutuion." Swiss Med Wkly **138**(11-12): 180-185.

Hegi, M. E., A. C. Diserens, et al. (2005). "MGMT gene silencing and benefit from temozolomide in glioblastoma." N Engl J Med **352**(10): 997-1003.

Hetschko, H., V. Voss, et al. (2008). "Pharmacological inhibition of Bcl-2 family members reactivates TRAIL-induced apoptosis in malignant glioma." J Neurooncol **86**(3): 265-272.

Hindler, K., C. S. Cleeland, et al. (2006). "The role of statins in cancer therapy." Oncologist **11**(3): 306-315.

Hinz, S., A. Trauzold, et al. (2000). "Bcl-XL protects pancreatic adenocarcinoma cells against CD95- and TRAIL-receptor-mediated apoptosis." Oncogene **19**(48): 5477-5486.

Hoffmann, O., F. Zipp, et al. (2009). "Tumour necrosis factor-related apoptosis-inducing ligand (TRAIL) in central nervous system inflammation." J Mol Med (Berl) **87**(8): 753-763.

Hong Kong Cancer Registry, H. A. ( 2010).

Horiot, J. C., W. van den Bogaert, et al. (1988). "European Organization for Research on Treatment of Cancer trials using radiotherapy with multiple fractions per day. A 1978-1987 survey." Front Radiat Ther Oncol **22**: 149-161.

Hotta, T., H. Suzuki, et al. (2003). "Chemotherapeutic agents sensitize sarcoma cell lines to tumor necrosis factor-related apoptosis-inducing ligand-induced caspase-8 activation, apoptosis and loss of mitochondrial membrane potential." J Orthop Res **21**(5): 949-957.

Hu, W. H., H. Johnson, et al. (1999). "Tumor necrosis factor-related apoptosis-inducing ligand receptors signal NF-kappaB and JNK activation and apoptosis through distinct pathways." J Biol Chem **274**(43): 30603-30610.

Hua, M. Y., H. L. Liu, et al. (2011). "The effectiveness of a magnetic nanoparticle-based delivery system for BCNU in the treatment of gliomas." Biomaterials **32**(2): 516-527.

Hymowitz, S. G., H. W. Christinger, et al. (1999). "Triggering cell death: the crystal structure of Apo2L/TRAIL in a complex with death receptor 5." Mol Cell **4**(4): 563-571.

Irmler, M., M. Thome, et al. (1997). "Inhibition of death receptor signals by cellular FLIP." Nature **388**(6638): 190-195.

Jackson, S. M., J. Ericsson, et al. (1997). "Signaling molecules derived from the cholesterol biosynthetic pathway." Subcell Biochem **28**: 1-21.

Jacobs, M. D. and S. C. Harrison (1998). "Structure of an IkappaBalpha/NF-kappaB complex." Cell **95**(6): 749-758.

Jeremias, I. and K. M. Debatin (1998). "TRAIL induces apoptosis and activation of NFkappaB." Eur Cytokine Netw **9**(4): 687-688.

Jo, M., T. H. Kim, et al. (2000). "Apoptosis induced in normal human hepatocytes by tumor necrosis factor-related apoptosis-inducing ligand." Nat Med **6**(5): 564-567.

Jorg-Christian Tonn, M. W., James T. Rutka (2010). Oncology of CNS Tumors, Springer.

Kavurma, M. M., M. Schoppet, et al. (2008). "TRAIL stimulates proliferation of vascular smooth muscle cells via activation of NF-kappaB and induction of insulin-like growth factor-1 receptor." J Biol Chem **283**(12): 7754-7762.

Kim, C. H. and S. Gupta (2000). "Expression of TRAIL (Apo2L), DR4 (TRAIL receptor 1), DR5 (TRAIL receptor 2) and TRID (TRAIL receptor 3) genes in multidrug resistant human acute myeloid leukemia cell lines that overexpress MDR 1 (HL60/Tax) or MRP (HL60/AR)." Int J Oncol **16**(6): 1137-1139.

Kim, J. B., K. Urban, et al. (2010). "Non-invasive detection of a small number of bioluminescent cancer cells in vivo." PLoS One **5**(2): e9364.

Kim, S., M. W. Gaber, et al. (2009). "The inhibition of glioma growth in vitro and in vivo by a chitosan/ellagic acid composite biomaterial." Biomaterials **30**(27): 4743-4751.

Kim, S. M., J. H. Oh, et al. (2010). "Irradiation enhances the tumor tropism and therapeutic potential of tumor necrosis factor-related apoptosis-inducing ligand-secreting human umbilical cord blood-derived mesenchymal stem cells in glioma therapy." Stem Cells **28**(12): 2217-2228.

Kim, S. U. (2011). "Neural stem cell-based gene therapy for brain tumors." Stem Cell Rev **7**(1): 130-140.

Kita, M., T. Okawa, et al. (1989). "[Radiotherapy of malignant glioma--prospective randomized clinical study of whole brain vs local irradiation]." Gan No Rinsho **35**(11): 1289-1294.

KJ, Z. (1979). "Histological typing of tumors of the central nervous system." International histological classification of tumors, no. 21. World Health Organization, Geneva.

Knight, M. J., C. D. Riffkin, et al. (2001). "Analysis of FasL and TRAIL induced apoptosis pathways in glioma cells." Oncogene **20**(41): 5789-5798.

Kremer, P., M. Fardanesh, et al. (2009). "Intraoperative fluorescence staining of malignant brain tumors using 5-aminofluorescein-labeled albumin." Neurosurgery **64**(3 Suppl): 53-60; discussion 60-51.

Kubota, T., K. Fujisaki, et al. (2004). "Apoptotic injury in cultured human hepatocytes induced by HMG-CoA reductase inhibitors." Biochem Pharmacol **67**(12): 2175-2186.

Kuijlen, J. M., E. Bremer, et al. (2010). "Review: on TRAIL for malignant glioma therapy?" Neuropathol Appl Neurobiol **36**(3): 168-182.

Kumamoto, H. and K. Ooya (2005). "Expression of tumor necrosis factor alpha, TNF-related apoptosis-inducing ligand, and their associated molecules in ameloblastomas." J Oral Pathol Med **34**(5): 287-294.

Kusama, T., M. Mukai, et al. (2001). "Inhibition of epidermal growth factor-induced RhoA translocation and invasion of human pancreatic cancer cells by 3-hydroxy-3-methylglutaryl-coenzyme a reductase inhibitors." Cancer Res **61**(12): 4885-4891.

Kwon, D., K. Choi, et al. (2008). "Hydrogen peroxide enhances TRAIL-induced cell death through up-regulation of DR5 in human astrocytic cells." Biochem Biophys Res Commun **372**(4): 870-874.

Lane, D., N. Goncharenko-Khaider, et al. (2010). "Ovarian cancer ascites protects from TRAIL-induced cell death through alphavbeta5 integrin-mediated focal adhesion kinase and Akt activation." Oncogene **29**(24): 3519-3531.

Laperriere, N. J., P. M. Leung, et al. (1998). "Randomized study of brachytherapy in the initial management of patients with malignant astrocytoma." Int J Radiat Oncol Biol Phys **41**(5): 1005-1011.

Lawrence, D., Z. Shahrokh, et al. (2001). "Differential hepatocyte toxicity of recombinant Apo2L/TRAIL versions." Nat Med **7**(4): 383-385.

Laws, E. R., I. F. Parney, et al. (2003). "Survival following surgery and prognostic factors for recently diagnosed malignant glioma: data from the Glioma Outcomes Project." J Neurosurg **99**(3): 467-473.

LeBlanc, H., D. Lawrence, et al. (2002). "Tumor-cell resistance to death receptor--induced apoptosis through mutational inactivation of the proapoptotic Bcl-2 homolog Bax." Nat Med **8**(3): 274-281.

Lee, S., H. Yagita, et al. (2010). "Optimized combination therapy using bortezomib, TRAIL and TLR agonists in established breast tumors." Cancer Immunol Immunother **59**(7): 1073-1081.

Lee, S. H., H. S. Kim, et al. (2003). "Increased expression of FLIP, an inhibitor of Fas-mediated apoptosis, in stomach cancer." APMIS **111**(2): 309-314.

Lee, S. J., M. J. Ha, et al. (1998). "Inhibition of the 3-hydroxy-3-methylglutaryl-coenzyme A reductase pathway induces p53-independent transcriptional regulation of p21(WAF1/CIP1) in human prostate carcinoma cells." J Biol Chem **273**(17): 10618-10623.

Lee, T. J., J. T. Lee, et al. (2006). "Acquired TRAIL resistance in human breast cancer cells are caused by the sustained cFLIP(L) and XIAP protein levels and ERK activation." Biochem Biophys Res Commun **351**(4): 1024-1030.

Lefranc, F., J. Brotchi, et al. (2005). "Possible future issues in the treatment of glioblastomas: special emphasis on cell migration and the resistance of migrating glioblastoma cells to apoptosis." J Clin Oncol **23**(10): 2411-2422.

Leibel, S. A. and G. E. Sheline (1987). "Radiation therapy for neoplasms of the brain." J Neurosurg **66**(1): 1-22.

Lemke, D. M. (2004). "Epidemiology, diagnosis, and treatment of patients with metastatic cancer and high-grade gliomas of the central nervous system." J Infus Nurs **27**(4): 263-269.

Leong, S., R. B. Cohen, et al. (2009). "Mapatumumab, an antibody targeting TRAIL-R1, in combination with paclitaxel and carboplatin in patients with advanced solid malignancies: results of a phase I and pharmacokinetic study." J Clin Oncol **27**(26): 4413-4421.

Leverkus, M., M. Neumann, et al. (2000). "Regulation of tumor necrosis factor-related apoptosis-inducing ligand sensitivity in primary and transformed human keratinocytes." Cancer Res **60**(3): 553-559.

Li, H., H. Zhu, et al. (1998). "Cleavage of BID by caspase 8 mediates the mitochondrial damage in the Fas pathway of apoptosis." Cell **94**(4): 491-501.

Li, P., S. Jayarama, et al. (2010). "Akt-phosphorylated mitogen-activated kinase-activating death domain protein (MADD) inhibits TRAIL-induced apoptosis by blocking Fas-associated death domain (FADD) association with death receptor 4." J Biol Chem **285**(29): 22713-22722.

Li, Y., X. Fan, et al. (2008). "Hepatocyte growth factor enhances death receptor-induced apoptosis by up-regulating DR5." BMC Cancer **8**: 325.

Liang, S. L., H. Liu, et al. (2006). "Lovastatin-induced apoptosis in macrophages through the Rac1/Cdc42/JNK pathway." J Immunol **177**(1): 651-656.

Lim, E., K. D. Modi, et al. (2009). "In vivo bioluminescent imaging of mammary tumors using IVIS spectrum." J Vis Exp(26).

Lin, R., J. Liu, et al. (2005). "Lovastatin reduces nuclear factor kappaB activation induced by C-reactive protein in human vascular endothelial cells." Biol Pharm Bull **28**(9): 1630-1634.

Lin, T., Z. Ding, et al. (2011). "2-Tellurium-bridged beta-cyclodextrin, a thioredoxin reductase inhibitor, sensitizes human breast cancer cells to TRAIL-induced apoptosis through DR5 induction and NF-kappaB suppression." Carcinogenesis **32**(2): 154-167.

Liu, H., S. L. Liang, et al. (2009). "Statins induce apoptosis in ovarian cancer cells through activation of JNK and enhancement of Bim expression." Cancer Chemother Pharmacol **63**(6): 997-1005.

Louis, D. N., H. Ohgaki, et al. (2007). "The 2007 WHO classification of tumours of the central nervous system." Acta Neuropathol **114**(2): 97-109.

Lu, W., Q. Sun, et al. (2006). "Cationic albumin-conjugated pegylated nanoparticles allow gene delivery into brain tumors via intravenous administration." Cancer Res **66**(24): 11878-11887.

Maranzano, E., P. Anselmo, et al. (2011). "Treatment of recurrent glioblastoma with stereotactic radiotherapy: long-term results of a mono-institutional trial." Tumori **97**(1): 56-61.

Mariani, S. M. and P. H. Krammer (1998). "Differential regulation of TRAIL and CD95 ligand in transformed cells of the T and B lymphocyte lineage." Eur J Immunol **28**(3): 973-982.

Mark Bernstein, M. S. B., Ed. (2008). Neuro-oncology. The Essentials, Thieme.

Marsters, S. A., J. P. Sheridan, et al. (1997). "A novel receptor for Apo2L/TRAIL contains a truncated death domain." Curr Biol **7**(12): 1003-1006.

Martelli, A. M., P. L. Tazzari, et al. (2003). "A new selective AKT pharmacological inhibitor reduces resistance to chemotherapeutic drugs, TRAIL, all-trans-retinoic acid, and ionizing radiation of human leukemia cells." Leukemia **17**(9): 1794-1805.

Massa, P. E., X. Li, et al. (2005). "Gene expression profiling in conjunction with physiological rescues of IKKalpha-null cells with wild type or mutant IKKalpha reveals distinct classes of IKKalpha/NF-kappaB-dependent genes." J Biol Chem **280**(14): 14057-14069.

Massy, Z. A. and C. Guijarro (2001). "Statins: effects beyond cholesterol lowering." Nephrol Dial Transplant **16**(9): 1738-1741.

Melloni, E., P. Secchiero, et al. (2005). "Functional expression of TRAIL and TRAIL-R2 during human megakaryocytic development." J Cell Physiol **204**(3): 975-982.

Minniti, G., M. Salvati, et al. (2011). "Correlation between O6-methylguanine-DNA methyltransferase and survival in elderly patients with glioblastoma treated with radiotherapy plus concomitant and adjuvant temozolomide." J Neurooncol **102**(2): 311-316.

Mori, T., R. Doi, et al. (2005). "Regulation of the resistance to TRAIL-induced apoptosis as a new strategy for pancreatic cancer." Surgery **138**(1): 71-77.

Muenchen, H. J., D. L. Lin, et al. (2000). "Tumor necrosis factor-alpha-induced apoptosis in prostate cancer cells through inhibition of nuclear factor-kappaB by an IkappaBalpha "super-repressor"." Clin Cancer Res **6**(5): 1969-1977.

Muhlenbeck, F., E. Haas, et al. (1998). "TRAIL/Apo2L activates c-Jun NH2-terminal kinase (JNK) via caspase-dependent and caspase-independent pathways." J Biol Chem **273**(49): 33091-33098.

Muldoon, L. L., M. A. Pagel, et al. (1999). "A physiological barrier distal to the anatomic blood-brain barrier in a model of transvascular delivery." AJNR Am J Neuroradiol **20**(2): 217-222.

Munshi, A., G. Pappas, et al. (2001). "TRAIL (APO-2L) induces apoptosis in human prostate cancer cells that is inhibitable by Bcl-2." Oncogene **20**(29): 3757-3765.

Nagai, S., K. Washiyama, et al. (2002). "Aberrant nuclear factor-kappaB activity and its participation in the growth of human malignant astrocytoma." J Neurosurg **96**(5): 909-917.

Naka, T., K. Sugamura, et al. (2002). "Effects of tumor necrosis factor-related apoptosis-inducing ligand alone and in combination with chemotherapeutic agents on patients' colon tumors grown in SCID mice." Cancer Res **62**(20): 5800-5806.

Nam, S. Y., G. A. Jung, et al. (2003). "Upregulation of FLIP(S) by Akt, a possible inhibition mechanism of TRAIL-induced apoptosis in human gastric cancers." Cancer Sci **94**(12): 1066-1073.

Nash, D. T. (2005). "Relationship of C-reactive protein, metabolic syndrome and diabetes mellitus: potential role of statins." J Natl Med Assoc **97**(12): 1600-1607.

Nelson, D. F., M. Diener-West, et al. (1988). "Combined modality approach to treatment of malignant gliomas--re-evaluation of RTOG 7401/ECOG 1374 with long-term follow-up: a joint study of the Radiation Therapy Oncology Group and the Eastern Cooperative Oncology Group." NCI Monogr(6): 279-284.

Nieder, C., N. Andratschke, et al. (2004). "Radiotherapy for high-grade gliomas. Does altered fractionation improve the outcome?" Strahlenther Onkol **180**(7): 401-407.

Nitsch, R., I. Bechmann, et al. (2000). "Human brain-cell death induced by tumour-necrosis-factor-related apoptosis-inducing ligand (TRAIL)." Lancet **356**(9232): 827-828.

Nubel, T., W. Dippold, et al. (2004). "Lovastatin inhibits Rho-regulated expression of E-selectin by TNFalpha and attenuates tumor cell adhesion." FASEB J **18**(1): 140-142.

Order, S. E., S. Hellman, et al. (1968). "Improvement in quality of survival following whole-brain irradiation for brain metastasis." Radiology **91**(1): 149-153.

Otsuka, G., T. Nagaya, et al. (1999). "Inhibition of nuclear factor-kappaB activation confers sensitivity to tumor necrosis factor-alpha by impairment of cell cycle progression in human glioma cells." Cancer Res **59**(17): 4446-4452.

Packer, R. J., L. N. Sutton, et al. (1989). "A prospective study of cognitive function in children receiving whole-brain radiotherapy and chemotherapy: 2-year results." J Neurosurg **70**(5): 707-713.

Pan, G., K. O'Rourke, et al. (1997). "The receptor for the cytotoxic ligand TRAIL." Science **276**(5309): 111-113.

Park, C. M., M. J. Park, et al. (2006). "Induction of p53-mediated apoptosis and recovery of chemosensitivity through p53 transduction in human glioblastoma cells by cisplatin." Int J Oncol **28**(1): 119-125.

Perkins, N. D. (1997). "Achieving transcriptional specificity with NF-kappa B." Int J Biochem Cell Biol **29**(12): 1433-1448.

Pitti, R. M., S. A. Marsters, et al. (1996). "Induction of apoptosis by Apo-2 ligand, a new member of the tumor necrosis factor cytokine family." J Biol Chem **271**(22): 12687-12690.

Poulaki, V., N. Mitsiades, et al. (2001). "Fas-mediated apoptosis in neuroblastoma requires mitochondrial activation and is inhibited by FLICE inhibitor protein and Bcl-2." Cancer Res **61**(12): 4864-4872.

Rainov, N. G., K. Gorbatyuk, et al. (2008). "Clinical trials with intracerebral convection-enhanced delivery of targeted toxins in malignant glioma." Rev Recent Clin Trials **3**(1): 2-9.

Ravi, R., G. C. Bedi, et al. (2001). "Regulation of death receptor expression and TRAIL/Apo2L-induced apoptosis by NF-kappaB." Nat Cell Biol **3**(4): 409-416.

Reithmeier, T., E. Graf, et al. (2010). "BCNU for recurrent glioblastoma multiforme: efficacy, toxicity and prognostic factors." BMC Cancer **10**: 30.

Rieger, J., H. Ohgaki, et al. (1999). "Human astrocytic brain tumors express APO2L/TRAIL." Acta Neuropathol **97**(1): 1-4.

Roullin, V. G., M. Mege, et al. (2004). "Influence of 5-fluorouracil-loaded microsphere formulation on efficient rat glioma radiosensitization." Pharm Res **21**(9): 1558-1563.

Rozanov, D. V., A. Y. Savinov, et al. (2009). "Engineering a leucine zipper-TRAIL homotrimer with improved cytotoxicity in tumor cells." Mol Cancer Ther **8**(6): 1515-1525.

Russo, S. M., J. E. Tepper, et al. (2001). "Enhancement of radiosensitivity by proteasome inhibition: implications for a role of NF-kappaB." Int J Radiat Oncol Biol Phys **50**(1): 183-193.

Ryu, B. K., M. G. Lee, et al. (2001). "Increased expression of cFLIP(L) in colonic adenocarcinoma." J Pathol **194**(1): 15-19.

Salvati, M., A. D'Elia, et al. (2011). "Safety and feasibility of the adjunct of local chemotherapy with biodegradable carmustine (BCNU) wafers to the standard multimodal approach to high grade gliomas at first diagnosis." J Neurosurg Sci **55**(1): 1-6.

Salvesen, G. S. and C. S. Duckett (2002). "IAP proteins: blocking the road to death's door." Nat Rev Mol Cell Biol **3**(6): 401-410.

Secchiero, P., E. Melloni, et al. (2004). "TRAIL regulates normal erythroid maturation through an ERK-dependent pathway." Blood **103**(2): 517-522.

Sen, R. and D. Baltimore (1986). "Multiple nuclear factors interact with the immunoglobulin enhancer sequences." Cell **46**(5): 705-716.

Senger, D., J. G. Cairncross, et al. (2003). "Long-term survivors of glioblastoma: statistical aberration or important unrecognized molecular subtype?" Cancer J **9**(3): 214-221.

Shankar, S. and R. K. Srivastava (2004). "Enhancement of therapeutic potential of TRAIL by cancer chemotherapy and irradiation: mechanisms and clinical implications." Drug Resist Updat **7**(2): 139-156.

Sheridan, J. P., S. A. Marsters, et al. (1997). "Control of TRAIL-induced apoptosis by a family of signaling and decoy receptors." Science **277**(5327): 818-821.

Shi, L., J. Chen, et al. (2010). "MiR-21 protected human glioblastoma U87MG cells from chemotherapeutic drug temozolomide induced apoptosis by decreasing Bax/Bcl-2 ratio and caspase-3 activity." Brain Res **1352**: 255-264.

Shibata, M. A., Y. Ito, et al. (2004). "Lovastatin inhibits tumor growth and lung metastasis in mouse mammary carcinoma model: a p53-independent mitochondrial-mediated apoptotic mechanism." Carcinogenesis **25**(10): 1887-1898.

Shigeno, M., K. Nakao, et al. (2003). "Interferon-alpha sensitizes human hepatoma cells to TRAIL-induced apoptosis through DR5 upregulation and NF-kappa B inactivation." Oncogene **22**(11): 1653-1662.

Siegelin, M. D., T. Gaiser, et al. (2009). "Daidzein overcomes TRAIL-resistance in malignant glioma cells by modulating the expression of the intrinsic apoptotic inhibitor, bcl-2." Neurosci Lett **454**(3): 223-228.

Siegelin, M. D., T. Gaiser, et al. (2009). "Myricetin sensitizes malignant glioma cells to TRAIL-mediated apoptosis by down-regulation of the short isoform of FLIP and bcl-2." Cancer Lett **283**(2): 230-238.

Society, A. C. (2010). "I. Cancer Facts and Figures 2010."

Soderstrom, T. S., M. Poukkula, et al. (2002). "Mitogen-activated protein kinase/extracellular signal-regulated kinase signaling in activated T cells abrogates TRAIL-induced apoptosis upstream of the mitochondrial amplification loop and caspase-8." J Immunol **169**(6): 2851-2860.

Spierings, D. C., E. G. de Vries, et al. (2004). "Tissue distribution of the death ligand TRAIL and its receptors." J Histochem Cytochem **52**(6): 821-831.

Srivastava, R. K. (2001). "TRAIL/Apo-2L: mechanisms and clinical applications in cancer." Neoplasia **3**(6): 535-546.

Strater, J., U. Hinz, et al. (2002). "Expression of TRAIL and TRAIL receptors in colon carcinoma: TRAIL-R1 is an independent prognostic parameter." Clin Cancer Res **8**(12): 3734-3740.

Stummer, W., S. Stocker, et al. (1998). "In vitro and in vivo porphyrin accumulation by C6 glioma cells after exposure to 5-aminolevulinic acid." J Photochem Photobiol B **45**(2-3): 160-169.

Stummer, W., S. Stocker, et al. (1998). "Intraoperative detection of malignant gliomas by 5-aminolevulinic acid-induced porphyrin fluorescence." Neurosurgery **42**(3): 518-525; discussion 525-516.

Stupp, R., W. P. Mason, et al. (2005). "Radiotherapy plus concomitant and adjuvant temozolomide for glioblastoma." N Engl J Med **352**(10): 987-996.

Sun, A. Y., Y. L. Shen, et al. (2006). "Improvement of expression level and bioactivity of soluble tumor necrosis factor-related apoptosis-inducing ligand (Apo2L/TRAIL) by a novel zinc ion feeding strategy." Biotechnol Lett **28**(15): 1215-1219.

Sung, B., J. Ravindran, et al. (2010). "Gossypol induces death receptor-5 through activation of the ROS-ERK-CHOP pathway and sensitizes colon cancer cells to TRAIL." J Biol Chem **285**(46): 35418-35427.

Tapia-Perez, J. H., M. Sanchez-Aguilar, et al. (2010). "The role of statins in neurosurgery." Neurosurg Rev **33**(3): 259-270; discussion 270.

Theill, L. E., W. J. Boyle, et al. (2002). "RANK-L and RANK: T cells, bone loss, and mammalian evolution." Annu Rev Immunol **20**: 795-823.

Totzke, G., F. Essmann, et al. (2006). "A novel member of the IkappaB family, human IkappaB-zeta, inhibits transactivation of p65 and its DNA binding." J Biol Chem **281**(18): 12645-12654.

Tran, S. E., T. H. Holmstrom, et al. (2001). "MAPK/ERK overrides the apoptotic signaling from Fas, TNF, and TRAIL receptors." J Biol Chem **276**(19): 16484-16490.

Trarbach, T., M. Moehler, et al. (2010). "Phase II trial of mapatumumab, a fully human agonistic monoclonal antibody that targets and activates the tumour necrosis factor apoptosis-inducing ligand receptor-1 (TRAIL-R1), in patients with refractory colorectal cancer." Br J Cancer **102**(3): 506-512.

Troy, T., D. Jekic-McMullen, et al. (2004). "Quantitative comparison of the sensitivity of detection of fluorescent and bioluminescent reporters in animal models." Mol Imaging **3**(1): 9-23.

Tsurushima, H., X. Yuan, et al. (2007). "Radioresponsive tumor necrosis factor-related apoptosis-inducing ligand (TRAIL) gene therapy for malignant brain tumors." Cancer Gene Ther **14**(8): 706-716.

Turesson, C., L. T. Jacobsson, et al. (2008). "Cardiovascular co-morbidity in rheumatic diseases." Vasc Health Risk Manag **4**(3): 605-614.

Vaupel, P., F. Kallinowski, et al. (1989). "Blood flow, oxygen and nutrient supply, and metabolic microenvironment of human tumors: a review." Cancer Res **49**(23): 6449-6465.

Wahner, A. D., J. M. Bronstein, et al. (2008). "Statin use and the risk of Parkinson disease." Neurology **70**(16 Pt 2): 1418-1422.

Walczak, H., M. A. Degli-Esposti, et al. (1997). "TRAIL-R2: a novel apoptosis-mediating receptor for TRAIL." EMBO J **16**(17): 5386-5397.

Walczak, H., R. E. Miller, et al. (1999). "Tumoricidal activity of tumor necrosis factor-related apoptosis-inducing ligand in vivo." Nat Med **5**(2): 157-163.

Waldron, J. S., I. Yang, et al. (2010). "Implications for immunotherapy of tumor-mediated T-cell apoptosis associated with loss of the tumor suppressor PTEN in glioblastoma." J Clin Neurosci **17**(12): 1543-1547.

Wang, C. Y., P. Y. Liu, et al. (2008). "Pleiotropic effects of statin therapy: molecular mechanisms and clinical results." Trends Mol Med **14**(1): 37-44.

Wang, I. K., S. Y. Lin-Shiau, et al. (2000). "Suppression of invasion and MMP-9 expression in NIH 3T3 and v-H-Ras 3T3 fibroblasts by lovastatin through inhibition of ras isoprenylation." Oncology **59**(3): 245-254.

Wang, J., L. Zheng, et al. (1999). "Inherited human Caspase 10 mutations underlie defective lymphocyte and dendritic cell apoptosis in autoimmune lymphoproliferative syndrome type II." Cell **98**(1): 47-58.

Weaver, K. D., S. Yeyeodu, et al. (2003). "Potentiation of chemotherapeutic agents following antagonism of nuclear factor kappa B in human gliomas." J Neurooncol **61**(3): 187-196.

Wei, M. C., T. Lindsten, et al. (2000). "tBID, a membrane-targeted death ligand, oligomerizes BAK to release cytochrome c." Genes Dev **14**(16): 2060-2071.

Weis, M., C. Heeschen, et al. (2002). "Statins have biphasic effects on angiogenesis." Circulation **105**(6): 739-745.

Wejde, J., M. Hjertman, et al. (1998). "Dolichol-like lipids with stimulatory effect on DNA synthesis: substrates for protein dolichylation?" J Cell Biochem **71**(4): 502-514.

Weller, M. (2010). "Immunotherapy for glioblastoma: a long and winding road." Neuro Oncol **12**(4): 319.

Weller, M., P. Kleihues, et al. (1998). "CD95 ligand: lethal weapon against malignant glioma?" Brain Pathol **8**(2): 285-293.

Westphal, M., D. C. Hilt, et al. (2003). "A phase 3 trial of local chemotherapy with biodegradable carmustine (BCNU) wafers (Gliadel wafers) in patients with primary malignant glioma." Neuro Oncol **5**(2): 79-88.

Widhalm, G., S. Wolfsberger, et al. (2010). "5-Aminolevulinic acid is a promising marker for detection of anaplastic foci in diffusely infiltrating gliomas with nonsignificant contrast enhancement." Cancer **116**(6): 1545-1552.

Wiezorek, J., P. Holland, et al. (2010). "Death receptor agonists as a targeted therapy for cancer." Clin Cancer Res **16**(6): 1701-1708.

Wiley, S. R., K. Schooley, et al. (1995). "Identification and characterization of a new member of the TNF family that induces apoptosis." Immunity **3**(6): 673-682.

Willey, J. Z. and M. S. Elkind (2010). "3-Hydroxy-3-methylglutaryl-coenzyme A reductase inhibitors in the treatment of central nervous system diseases." Arch Neurol **67**(9): 1062-1067.

Wohlfahrt, M. E., B. C. Beard, et al. (2007). "A capsid-modified, conditionally replicating oncolytic adenovirus vector expressing TRAIL Leads to enhanced cancer cell killing in human glioblastoma models." Cancer Res **67**(18): 8783-8790.

Wolozin, B. (2002). "Cholesterol and Alzheimer's disease." Biochem Soc Trans **30**(4): 525-529.

Wrensch, M., M. L. Bondy, et al. (1993). "Environmental risk factors for primary malignant brain tumors: a review." J Neurooncol **17**(1): 47-64.

Wu, G. S. (2009). "TRAIL as a target in anti-cancer therapy." Cancer Lett **285**(1): 1-5.

Yin, S., S. Sethi, et al. (2010). "Protein kinase Cdelta and caspase-3 modulate TRAIL-induced apoptosis in breast tumor cells." J Cell Biochem **111**(4): 979-987.

Yong, R. L., N. Shinojima, et al. (2009). "Human bone marrow-derived mesenchymal stem cells for intravascular delivery of oncolytic adenovirus Delta24-RGD to human gliomas." Cancer Res **69**(23): 8932-8940.

Youle, R. J. and A. Strasser (2008). "The BCL-2 protein family: opposing activities that mediate cell death." Nat Rev Mol Cell Biol **9**(1): 47-59.

Zhang, L. and B. Fang (2005). "Mechanisms of resistance to TRAIL-induced apoptosis in cancer." Cancer Gene Ther **12**(3): 228-237.

Zhang, L., H. Zhu, et al. (2004). "Lack of p38 MAP kinase activation in TRAIL-resistant cells is not related to the resistance to TRAIL-mediated cell death." Cancer Biol Ther **3**(3): 296-301.

Zhang, X., A. C. Frank, et al. (2009). "Altered regulation of extrinsic apoptosis pathway in HCV-infected HCC cells enhances susceptibility to mapatumumab-induced apoptosis." Hepatol Res **39**(12): 1178-1189.

Zhu, C. J., Y. B. Li, et al. (2003). "Expression of antisense bcl-2 cDNA abolishes tumorigenicity and enhances chemosensitivity of human malignant glioma cells." J Neurosci Res **74**(1): 60-66.

Ziegler, D. S., J. Keating, et al. (2011). "A small-molecule IAP inhibitor overcomes resistance to cytotoxic therapies in malignant gliomas in vitro and in vivo." Neuro Oncol **13**(8): 820-829.

Zong, H., B. Yin, et al. (2009). "Over-expression of c-FLIP confers the resistance to TRAIL-induced apoptosis on gallbladder carcinoma." Tohoku J Exp Med **217**(3): 203-208.